Technical Report No. 32-31

Juno Final Report
Volume II

Juno II: Space Probes

Allen E. Wolfe

JET PROPULSION LABORATORY
CALIFORNIA INSTITUTE OF TECHNOLOGY
PASADENA, CALIFORINA

September 12, 1960

(NASA-CR-51639) JUNO 2: SPACE PROBES, VOLUME 2 Final Report (Jet Propulsion Lab.) 80 p

N75-75320

Unclas
00/98 23585

~~CONFIDENTIAL~~

Technical Report No. 32-31

Juno Final Report, Volume II.

Juno II: Space Probes

Allen E. Wolfe

John Small,
Juno Project Director

Copy No. HC 56
This document consists of covers and 46 leaves.

AVAILABLE TO U.S. GOVERNMENT AGENCIES ONLY

JET PROPULSION LABORATORY
CALIFORNIA INSTITUTE OF TECHNOLOGY
PASADENA, CALIFORINA

September 12, 1960

~~CONFIDENTIAL~~

PREFACE

Technical Report No. 32-31, which is prepared in 3 volumes, is a summary of Jet Propulsion Laboratory space-flight activities utilizing the *Juno I* and *Juno II* rocket-vehicle configurations.

Volume I described the *Juno I* Explorer satellite program.

This volume (Volume II) describes the *Juno II* rocket-vehicle and the program which led to the *Pioneer III* launching and culminated in the flight of *Pioneer IV*, the free-world's first successful lunar probe.

The general program presented in Volume I, and most of the work presented in Volume II, was conducted under sponsorship of the Department of the Army, Ordnance Corps, Contract No. DA-04-495-Ord 18. Shortly before the *Pioneer IV* flight, the program was transferred to the National Aeronautics and Space Administration, Contract No. NASw-6.

Volume III, which will be released next year, will be concerned with the *Juno II* earth-satellite flights.

CONTENTS

CONTENTS (Cont'd)

CONTENTS (Cont'd)

Part II Juno IIA' (Pioneer IV)

CONTENTS (Cont'd)

FIGURES

FIGURES (Cont'd)

FIGURES (Cont'd)

TABLES

ABSTRACT

The *Juno II* program was the result of a request to utilize the increased capabilities of the *Jupiter* booster and to prepare a space probe firing as part of the IGY. This combined effort by JPL and AMBA resulted in the launching of *Pioneer III* and *Pioneer IV*. Volume II discusses these probes in detail. The launching vehicle and probe (including experiments) for *Pioneer III* are first described. The tracking and communications network is discussed; system tests are noted. The performance of the *Pioneer III* probe is evaluated. System modifications for *Pioneer IV* are given. Preflight preparations and pad operations are examined. Finally the performance of the vehicle and probe is analyzed, along with the tracking network performance at each of the tracking stations.

I. INTRODUCTION

A. General

This Report represents Volume Two of the three report series covering the extent of the Jet Propulsion Laboratory (JPL) participation in early spaceflight activities. These activities were largely covered under the *Juno* program, although other programs [Orbiter, Reentry Test Vehicle (RTV), and Microlock (tracking and telemetering)] contributed much support, research information, and experience.

Juno was the name given to the general program for launching satellites and space probes utilizing a cluster of scale *Sergeant* solid-propellant motors for the upper stages of a vehicle in which the booster was either a modified *Redstone* (*Juno I*) or a modified *Jupiter* (*Juno II*).

Volume I of this series of reports covered the early history of the program, a detailed description of the high speed stages of the Microlock tracking and telemetry system, and all of the *Juno I* or early Explorer firings. Volume II covers the *Pioneer III* and *IV* space probes which represented the first two flights of the *Juno II* system. The third volume will be concerned with the use of the *Juno II* vehicle for earth satellites and will be published upon completion of the program in early 1961.

Volume II is further divided into two parts covering *Juno IIA* or *Pioneer III* and *Juno IIA'* or *Pioneer IV*. The description of those parts of the system that were the results of the *Juno I* program is relatively brief, and the reader is referred to Volume 1 for further details.

B. Objectives

With the unsuccessful firing of *Beacon* on 22 October 1958, the *Juno I* program was brought to completion. Even prior to the last firing, the major space effort of the Laboratory had shifted into the next phase, or *Juno II* program.

This effort was the result of a request in early 1958 for ABMA and JPL to utilize the increased capabilities of the *Jupiter* booster and to prepare a space probe firing as part of the US participation in the IGY. It was the responsibility of ABMA to provide the *Jupiter* booster and guidance system and of JPL to prepare the high-speed stages, the probe, and its associated ground tracking and telemetry equipment. This combined effort resulted in the successful launching of *Pioneer III* on 6 December 1958 and of *Pioneer IV* on 3 March 1959.

The basic objectives of this program were:

1. To establish the probe trajectory.
2. To measure cosmic-ray radiation during flight.
3. To test the communications to extended ranges.
4. To test engineering devices that would be useful in later flights.

The first objective, establishment of the trajectory of the probe, particularly in the vicinity of the Moon, had two phases. The first phase represented an in-flight checkout of a tracking system designed for use in a long-range space-exploration program. This tracking system involves the World Tracking Net of radio telescopes of

which the first component, the Goldstone tracking antenna, was in operation for this flight. The tracking system also involves the communications links connecting the tracking stations to the tracking computer. For this flight, communications were established between the Goldstone site, the launch site at Cape Canaveral, the Puerto Rico tracking site, and the JPL computing center. Additional communications were established to a standby computer at the RAND Corporation in Santa Monica. The tracking system also includes the tracking computer, which for this test was the JPL IBM 704 computer.

The second phase of the first objective was primarily scientific. It was desired to determine the distance of closest approach to the Moon, and the curvature of the trajectory near this point of closest approach. In principle, knowledge of these parameters will permit a determination of the mass of the Moon. If the trajectory is close enough to the Moon to cause a sizeable deviation of the flight path and if the tracking operation is sufficiently accurate, then it is possible that the accuracy of estimates of the Moon's mass could be improved beyond that now available. At the present time, the mass of the Moon is known to be within a few hundredths of 1%.

The second objective, that of measuring cosmic-ray radiation, was primarily for the purpose of further exploring the radiation belts around the Earth that were discovered during the flights of the early *Explorer* satellites. It was also the purpose of the test to measure the level of cosmic radiation at distances remote from both the magnetic field of the Earth and the magnetic field of the Moon, if such exists.

The third objective, that of testing the communication to extended ranges, was to be accomplished by making signal strength records and also by obtaining useful telemetry data out to ranges of several hundred thousand miles from Earth and then performing a reduction and analysis of the resulting data.

The fourth objective, the testing of probe components destined for use in future space probes, applied to the shutter-trigger mechanism and the despin mechanism. Both of these mechanisms would have application in future flights involving the photographing of the Moon.

C. Summary

Pioneer III was launched on 6 December 1958 at 05:44:52.3 GMT, four seconds later than the optimum launch time. Due to a premature cutoff of the booster and an angular dispersion in the upper stages, the probe failed to achieve escape velocity. A distance of 63,500 miles was achieved, however, and very good cosmic-ray data obtained. All other phases of the experiment were satisfactory with the exception of the engineering experiments which failed to function properly.

Pioneer IV was launched from the Atlantic Missile Range at 05:10:56.7 GMT on 3 March 1959. Vehicle performance was such that at injection the magnitude of the velocity vector was 86.9 m/sec below nominal, the pitch or elevation angle was low by 4.58 deg, and the azimuth dispersion 1.33 deg to the south. These errors resulted in the probe's closest approach to the Moon being 37,200 mi, 41½ hr after injection. Since the probe did obtain escape velocity it continued out into the solar system and established a heliocentric orbit. At the time probe contact was lost, the probe was approximately 407,000 miles from the Earth.

The objectives assigned to this operation were in nearly all cases satisfactorily achieved. Very good cosmic-radiation data were obtained during the periods when contact was established with the probe. Small regions near the peaks of the two radiation belts are missing due to an apparent malfunction of the highest speed scaler.

Of the engineering-evaluation experiments, the optical trigger device was not adjusted to operate at a miss distance of 37,000 miles and therefore a satisfactory test of the device could not be achieved. The probe despin device functioned satisfactorily and reduced the spin rate from 416 rpm to 11 rpm. Difficulties were encountered with the radio-frequency power monitor. Up to the time battery power began to fail, the signal level at the Goldstone site was sufficiently high to indicate the capacity for tracking this type of payload to a distance of more than 1,000,000 km, provided adequate battery lifetime was available.

PART I. JUNO IIA (PIONEER III)

II. *JUNO IIA* LAUNCHING VEHICLE

A. Introduction

The launching vehicle for the *Juno IIA* mission consisted of a modified *Jupiter* first stage, a guidance and instrumentation compartment, a rotational launcher for the high-speed stages, and three stages of scale *Sergeant* solid-propellant motors. The entire cluster of high-speed stages was covered by a large shroud that fastened to the instrument compartment.

The high-speed stages for the *Juno II* are similar in design to those used in the *Juno I* satellite launching vehicle. Their design is described more fully in Volume I. The launching tub which carries the stages on *Juno II* is also similar to that used in *Juno I*.

The flight plan required separation of the booster from the guidance and instrument compartment (with the high-speed stages attached) after burnout, shroud ejection during the early coast period, guidance compartment stabilization, and ignition of the high-speed stages.

B. First Stage

The modified *Jupiter* booster used in this experiment consisted of the main body section with its propulsion system and the instrument compartment which housed the guidance spatial attitude control, the events programmer, and the cluster drive motors.

The airframe used in this missile is a semi-monocoque cylindrical shell and is essentially the same as the air frame in a production-type missile except that the tank section has been elongated 36 in. for increased burning time. The power plant used is a NAAS-3D liquid-propellant engine which develops 150,000 lb sea-level thrust using RP 1 fuel and LOX (liquid oxygen). The engine is equipped with a gimbal mechanism operating in two planes to control the missile in pitch and yaw. Hinged turbine exhaust nozzles control roll.

C. Guidance System

After burnout, the main body section (thrust units and tanks) was separated from the rest of the vehicle. Figure 1 shows the main assemblies and the overall sequence of events. Separation was accomplished by firing the spring-loaded explosive bolts used to fasten the main body to the instrument compartment. Retrorockets located in the aft section of the main body were then fired to provide a substantial velocity difference between the two bodies and to preclude any possible bumping.

The shroud cap was then separated from the guidance compartment (by firing spring-loaded explosive bolts) and pushed out of the guidance compartment path (by firing a small rocket to exert a side force). During the

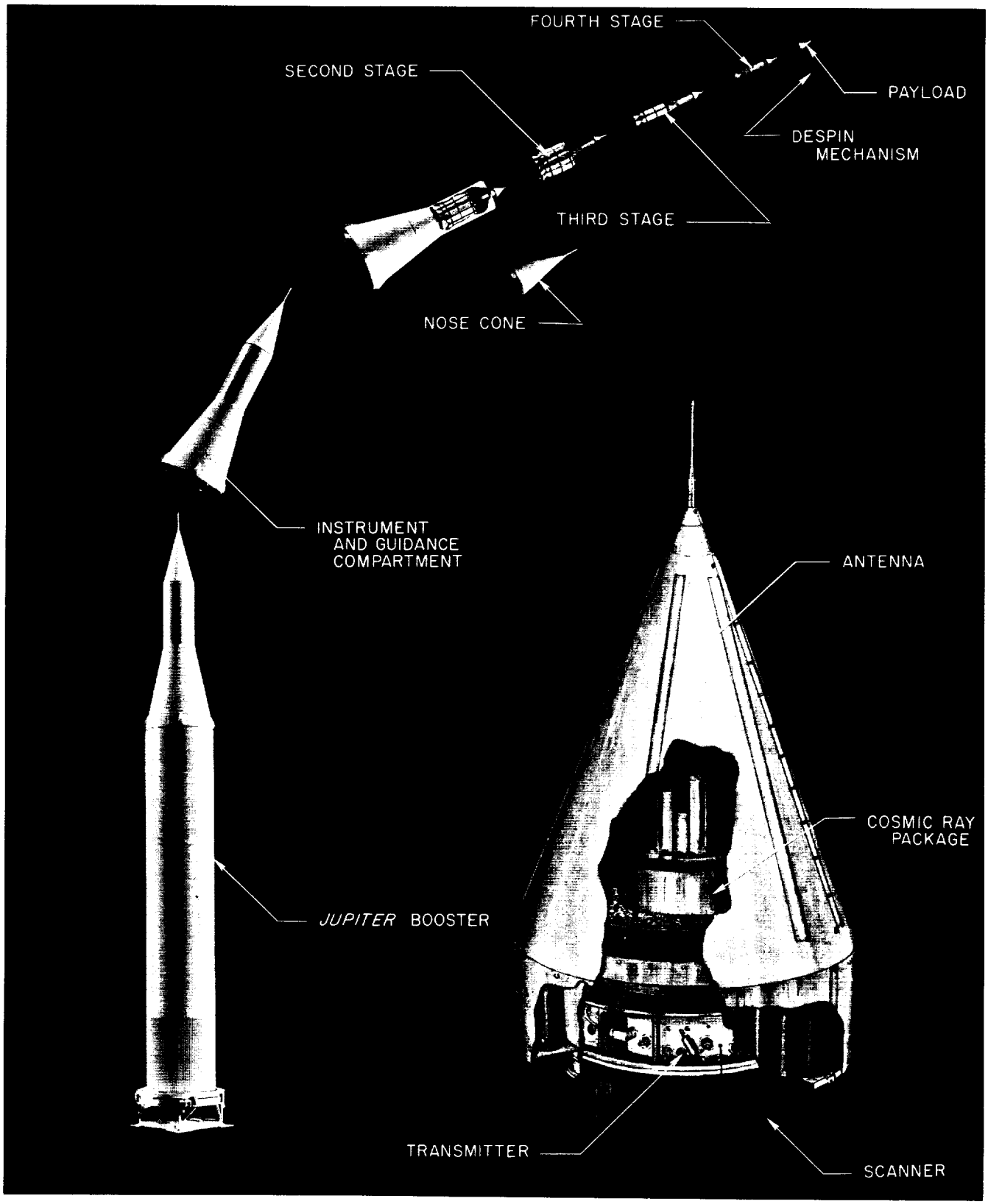

Figure 1. Separation Sequence of Juno II Space Probe Launch

remainder of the coasting period, a spatial-attitude control system positioned the instrument compartment so that the high-speed stages would be launched on the proper trajectory. This control system used compressed air nozzled through eight air jets, tangentially located on four finlike protuberances at the aft end of the instrument compartment.

D. Upper Stage Launcher

The upper stage launcher is permanently attached to the forward end of the instrument compartment. The launcher drive motors and their power supply were housed within the instrument compartment along with the launcher rpm control equipment. This control equipment was set to maintain a constant 250 rpm during the first 125 sec of flight, then to increase the rotational speed to 400 rpm and maintain that speed until stage 2 ignition. Calibration indicated that the speed of 400 rpm would be sufficient to insure spin stabilization and to minimize dispersion due to thrust malalignment.

E. Stage 2

The scaled-down *Sergeant* motors used in the second stage each contained approximately 50 lb of T17-E2 solid propellant composed of a polysulfide (rubber-type) fuel with an ammonium perchlorate oxidizer.

Each rocket motor contained an igniter, composed of two electric matches (DuPont type S-88) wired in parallel and a jelly-roll of metal oxidizer material encased in a plaster sheath.

Eleven of these rocket motors were arranged in an annular ring about a center tube and held in position radially by three transverse bulkheads. On the base of this center tube was a carefully machined ring which is mated to a similar ring at the base of the rotational launcher. The axial load was carried by the center tube, while transverse support for the cluster was provided by a ring on the forward section of the launching guides that engage mating surfaces on the forward bulkhead of stage 2.

Stage 2 receives its ignition current from batteries located in the instrument compartment, when a programmer in the instrument compartment reaches a preset time.

F. Stage 3

This stage also utilizes scaled-down *Sergeant* motors; however, the propellant is a higher performance polysulfide, JPL 136. The igniter is the same as that used in stage 2.

Stage 3 is formed by a bundle of three of these motors held by three transverse bulkheads with the motor cases carrying the axial loads. A cone-support structure is attached to the forward bulkhead on stage 3 to provide a support and launching structure for stage 4. The cone has exhaust holes cut in it so as to permit the exhaust gases of stage 4 to escape.

Ignition of stage 3 is controlled by a motor driven 20-sec timer located near the base of the stage 4 launch cone. The timer is started by the closure of either one of two pressure switches (mounted on two of the stage 2 motors) when stage 2 is ignited. Approximately 9 sec after the timer starts running, it completes a circuit that fires stage 3 (from batteries carried in the timer assembly).

G. Stage 4

The motor used for stage 4 is similar to those used in the other stages (except for external rings for mounting); however, the motor case was made from titanium rather than 410 steel. The propellant used in this motor is JPL 532A, a high-performance polyurethane propellant.

The ignition of stage 4 is provided by a battery, controlled by the same timer that fired stage 3. Ignition occurs approximately 9 sec after the ignition of stage 3. Immediately preceding the ignition of stage 4, the timer completes a circuit that fires a 15-sec delay train which controls the separation of stage 4 from the payload after stage 4 has completed burning.

III. PROBE

The *Juno IIA* probe was designed to achieve the following goals:

1. To aid in the establishment of the trajectory.
2. To measure the cosmic-ray radiation during the flight.
3. To test the communications for the extended range.
4. To test devices that could be useful in later flights.

The configuration is shown in Fig. 2, and the instrumentation block diagram in Fig. 3. The major divisions of the probe such as: transmitter and antenna, radiation experiment, shutter trigger, the power supply, timer and despin mechanism, and the structure are briefly described below. Table 1 summarizes the weight of the probe components.

A. Transmitter and Antenna

Figure 4 shows a block diagram of the transmitter. Semiconductor devices operating from 40 to 960 mc provide the RF signal that drives the vacuum-tube power amplifier. The oscillator is a grounded-base configuration with feedback from the collector to the emitter through a series resonant crystal. The frequency multiplier stages are also grounded-base configurations operating class C.

The general approach to obtaining stable performance at VHF frequencies was to design the transistor circuitry around a number of highly stable, passive coupling networks. These networks are critically coupled double-tuned transformers with sufficient loading so that variations in transistor characteristics with temperature, RF drive, and collector voltage produce relatively minor primary and secondary detuning. A low-pass LC filter is inserted between the transformer secondary and the emitter input in the frequency multipliers to reduce impedance reflections between the output and input circuits. Other stabilization techniques used are (1) Zener regulation of the oscillator collector-voltage (this stabilizes the transmitter drive and frequency); (2) direct grounding of collectors to chassis (this provides a good thermal path for collector heat dissipation); and (3) use of a specially developed transistor socket to provide stable mounting. The transistor socket consists of a relatively heavy, beryllium-copper spring mounted in a Kel-F base.

The X6 frequency multiplier unit contains a transistorized frequency doubler and a silicon-diode frequency tripler coupled to a 960 mc, high-Q cavity. Sufficient output (10-15 milliwatts) is generated to drive the following vacuum-tube amplifier class AB. Figure 5 shows the transmitter hardware and Table 2 gives the performance characteristics.

Table 1. Payload components

Component	Component weight, lb
Structure	1.04
Transmitter	1.35
Antenna	0.50
Batteries	7.17
Power Supply with VCO	0.88
Separation	1.76
Radiation Experiment	1.09
GM Tubes	
Counter Circuitry	
Shutter Trigger Experiment	0.36
Lens	
Photocells	
Amplifier and Coincidence Circuit	
Subcarrier (internal temperature)	
Despinning Device (incl. timer)	0.39
Balancing Weights	0.19
Total Weight	14.70

B. Antenna

The *Juno II* probe antenna is basically an unsymmetrically fed dipole built in the shape of a cone. The antenna cone is 12 in. high and 9⅜ in. in diameter with a 2¾ in. aluminum probe at its apex. The cone is fabricated of a cloth epoxy laminate 0.016 in. thick. Weight of the cone is 4.6 lb. Metallization of the cone is accomplished by depositing 0.0006-in. coating of silver and then plating with gold on the outside of the cone. Electrically, the antenna had a characteristic impedance of 50 ohms and a gain of 3 ± 0.5 db. Vibrational tests on the fiberglass cone at 20 g rms revealed several mechanical

Table 2. Performance characteristics

	Power, mw
Carrier	96 ± 7
Sub-carrier channel 1	14 ± 1.5
Sub-carrier channel 2	14 ± 1.5
Sub-carrier channel 3	36 ± 4
Distortion products	20
Total	180 ± 20

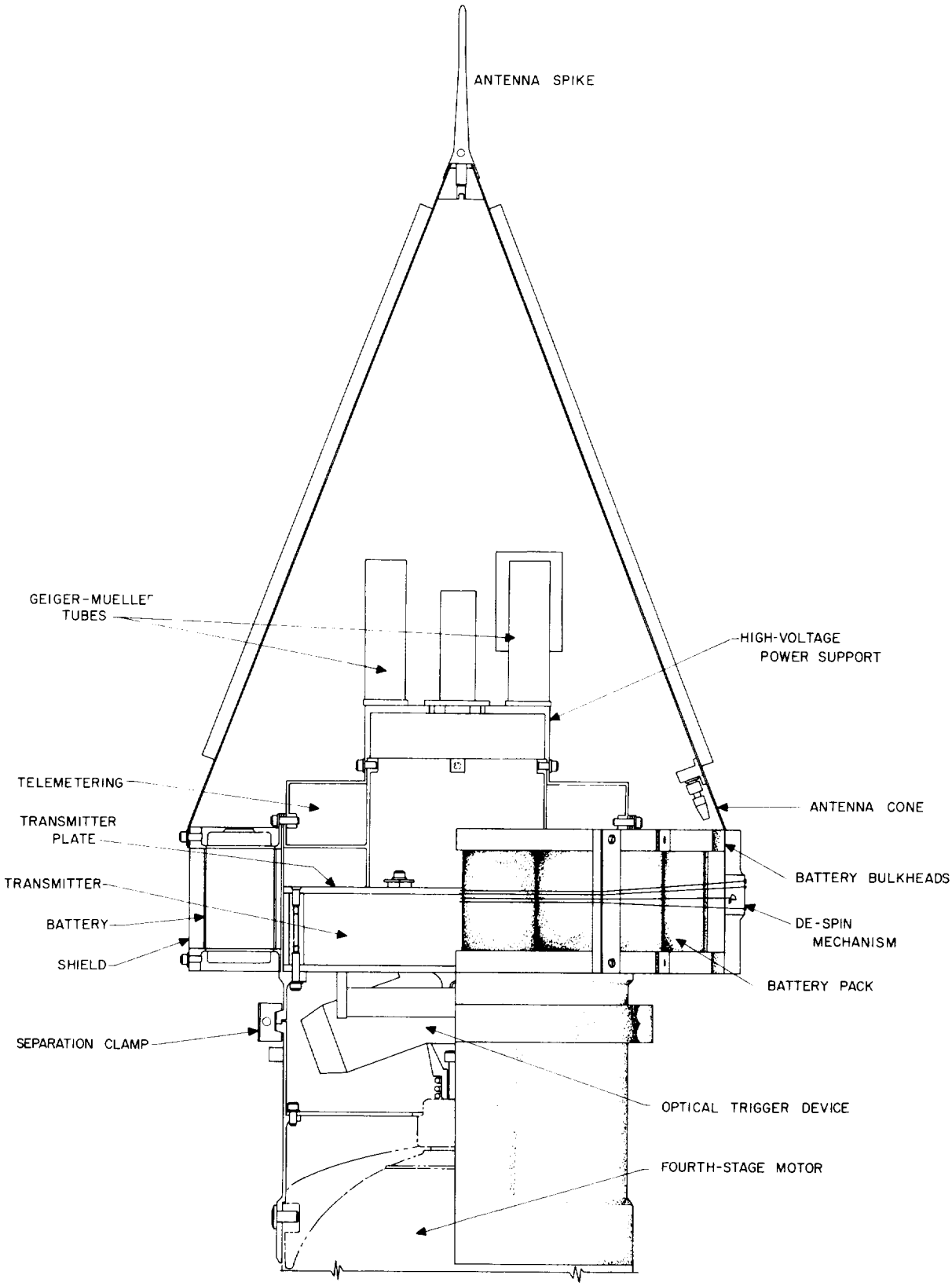

Figure 2. Payload Structure

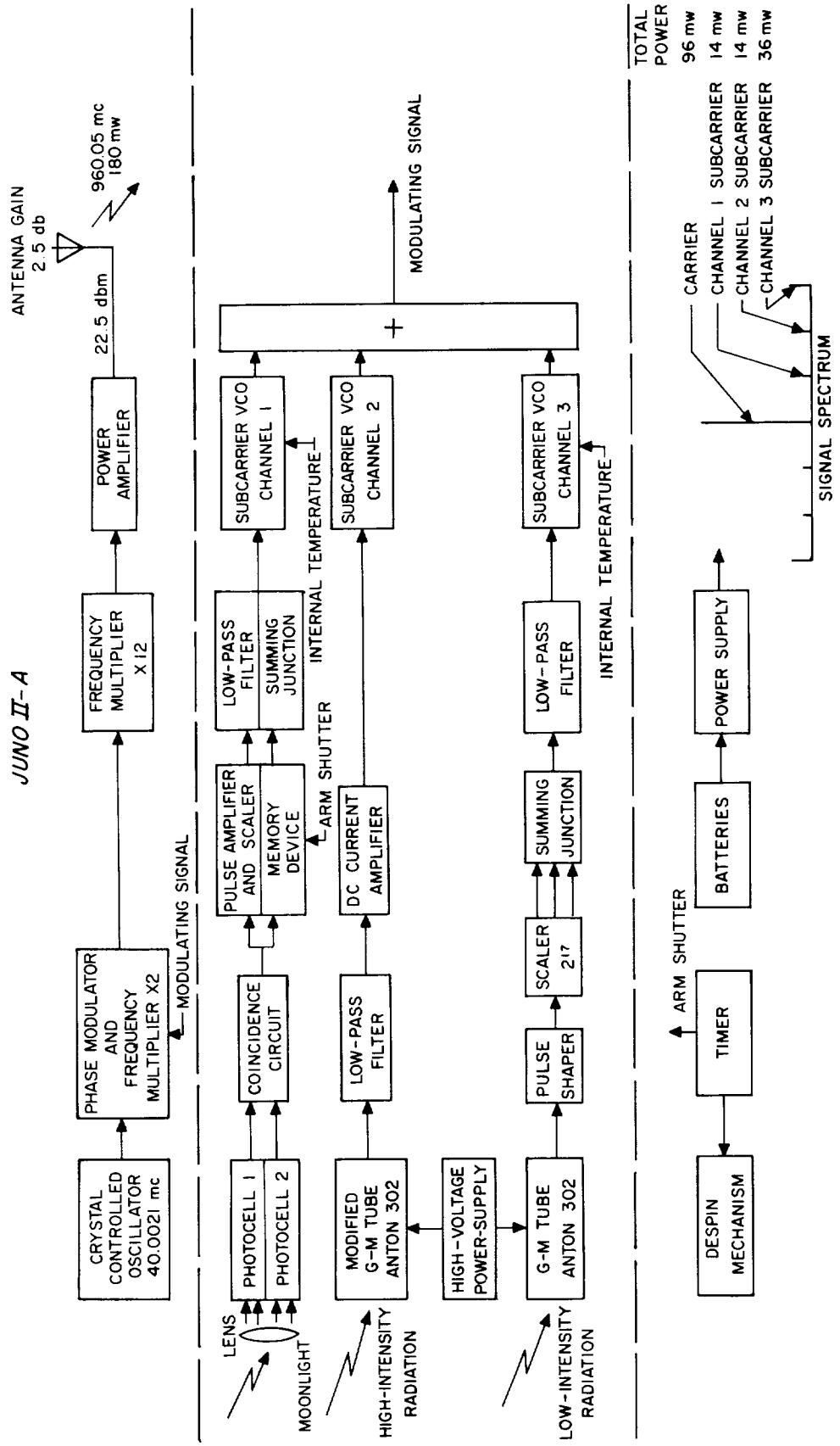

Figure 3. Probe Instrumentation

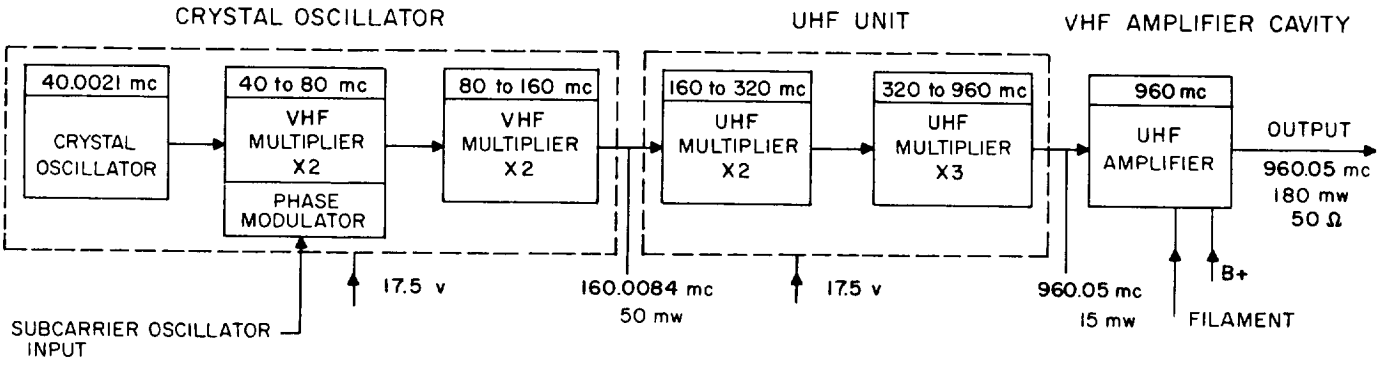

Figure 4. Block diagram of Juno II transmitter

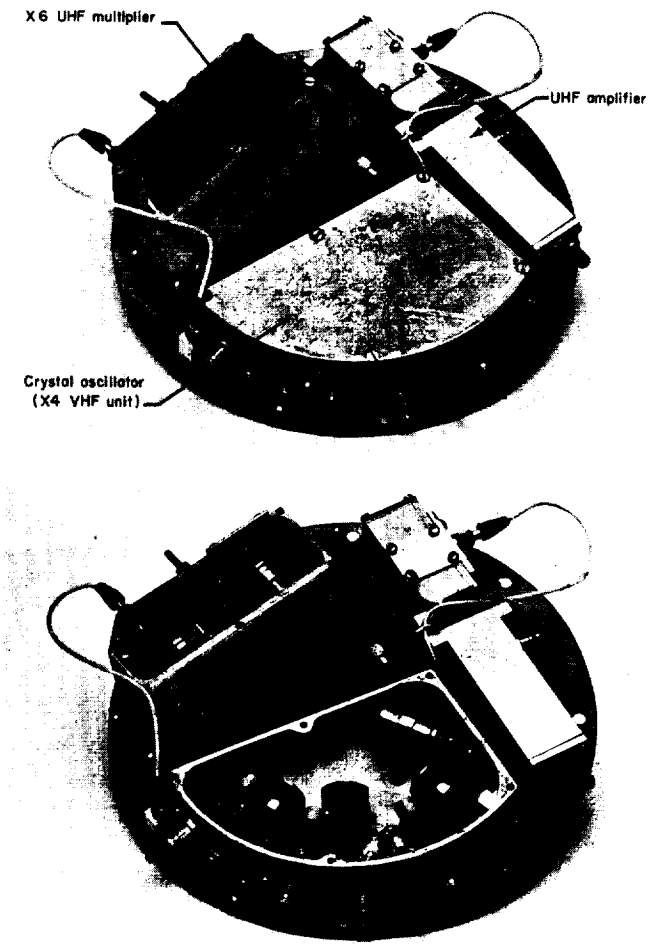

Figure 5. Developmental model of Juno II transmitter

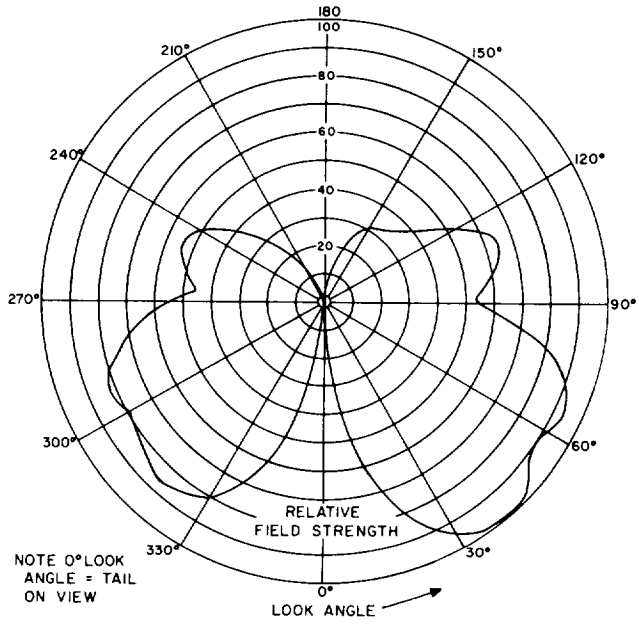

Figure 6. Antenna radiation pattern vs look angle

resonances. In order to provide the necessary mechanical rigidity, four longitudinal half-round external stiffeners and one internal bulkhead were added. Figure 6 shows the antenna radiation pattern versus look angle.

C. Description of Radiation Experiment

The general purpose of the *Juno IIA* radiation experiment was to measure radiation intensity along a prescribed payload trajectory, nominally between the Earth and the Moon and possibly beyond. The radiation detectors flown aboard *Pioneer III* were Anton Types 302 and 213 Geiger tubes used for counting and pulse integration purposes, respectively. Since both detectors were unshielded Geiger tubes, it was realized beforehand that the actual character of the measured radiation could only be surmised. The basic uncertainty that existed pertained to the precise nature and energy of the radiation being measured. These problems notwithstanding,

the quantitative space profile would be of considerable interest and value as measured with the proposed equipment.

D. Evolution of Experiment

As originally conceived by Dr. J. A. Van Allen of the State University of Iowa (SUI), the *Juno IIA* radiation package was to use two identical Geiger tubes (Type 302) to monitor both the gross and the high-energy penetrating portion of the space radiation. This system was to be similar to one of the radiation packages being assembled at SUI for *Explorer IV*. The Geiger tubes chosen for this experiment were tiny by comparison to the units used in the earlier *Explorers* before the high-intensity radiation belt was recognized. It was hoped that reduced counting-surface area on the *Explorer IV* detectors would permit the tubes to operate linearly through the radiation peak if, indeed, the peak were encountered. High-energy, or "hard," particles would be counted by a lead-shielded Geiger tube. Changes in the *Juno IIA* circuitry, which was being designed at JPL, would be contingent only upon certain results of the yet-untried *Explorer IV* radiation experiment, results that might adversely affect the dynamic range of radiation expected on the lunar shot. *Explorer IV* results were observed a few weeks before scheduled delivery of the first *Juno IIA* radiation subassembly to the JPL Payload Group. The radiation channel containing the unshielded "302" aboard *Explorer IV* had saturated with the peak nowhere in sight, and the lead in the "hard" channel reduced particle counts by only a modest 40%. In view of these results, Dr. Van Allen suggested a modification of the existing *Juno IIA* radiation package which would replace the "hard" detector and its associated counters with a detector capable of measuring high-intensity radiation. The dynamic-range requirements for this new detector was a subject of some concern since the peak space radiation levels were still a matter of conjecture.

The experiment flown aboard *Pioneer III* contained an unshielded 302 with its attendant counters as originally planned, and a Type 213 pulse-integrator followed by a stable d-c amplifier. The integrating Geiger tube was chosen in preference to the scientifically attractive ionization chamber because of its earlier availability.

E. Outline of Circuit Operation.

As shown in the block diagram of Fig. 7, pulses obtained from the Type 302 Geiger tube are processed through a trigger amplifier and then counted in a scaler from which three digital outputs are mixed and fed to a subcarrier oscillator. Maximum subcarrier variations due to each digital output are 5, 10, and 20 cps, respectively. Pulses obtained from the Type 213 Geiger tube are integrated in an RC filter and the average voltage thus formed is fed to a second subcarrier oscillator through a unity voltage gain power amplifier. Frequency limits for the subcarrier were 530 and 590 cps. The circuitry just described is contained in the subassembly of Fig. 8 and illustrated schematically in Fig. 9.

F. High-Voltage Power Supply

The high-voltage power supply for the Geiger tubes contains a saturable-core oscillator supplying square-wave power to a rectifier and voltage-doubler circuit (see Fig. 9). Regulation of dc is accomplished with a 700-v Corona regulator that idles at about 80 μa under no-load conditions. Idling current has been adjusted to a value larger than the largest expected combined Geiger-tube currents plus the minimum Corona-tube operating current. An initial idling current appreciably larger than the load demands permits the regulator to handle these load demands at the end of the experiment when battery voltage is low and idling current has been significantly reduced. The regulated outputs of the supply are 730 and 650 v for the 302 and 213 tubes, respectively.

G. Pulse-Forming Circuit

The circuitry connected to the shell of the 302 tube consists of a current-limiting resistor and an R-C network coupled to the trigger amplifier. The trigger amplifier standardizes pulse amplitude and coarsely regulates pulse width.

H. Counter Circuit

1. Scaler Chain

The basic flip-flop (see Fig. 9) is a saturating device capable of operation up to 100 kcps under standard amplitude triggers. The flip-flop performs with "semi-starved" collector currents at a power dissipation of 1.4 mw per stage. The entire chain of 17 flip-flops plus the two auxiliary stages have been demonstrated to operate reliably between the relatively wide supply-voltage limits of 2 and 20 v at room temperature. Similar performance was obtained between 5 and 10 v between ambient temperature extremes of $-15°C$ and $+75°C$.

2. Coding

To improve the readability of the scaler output caused by a pulse input having a widely varying counting rate,

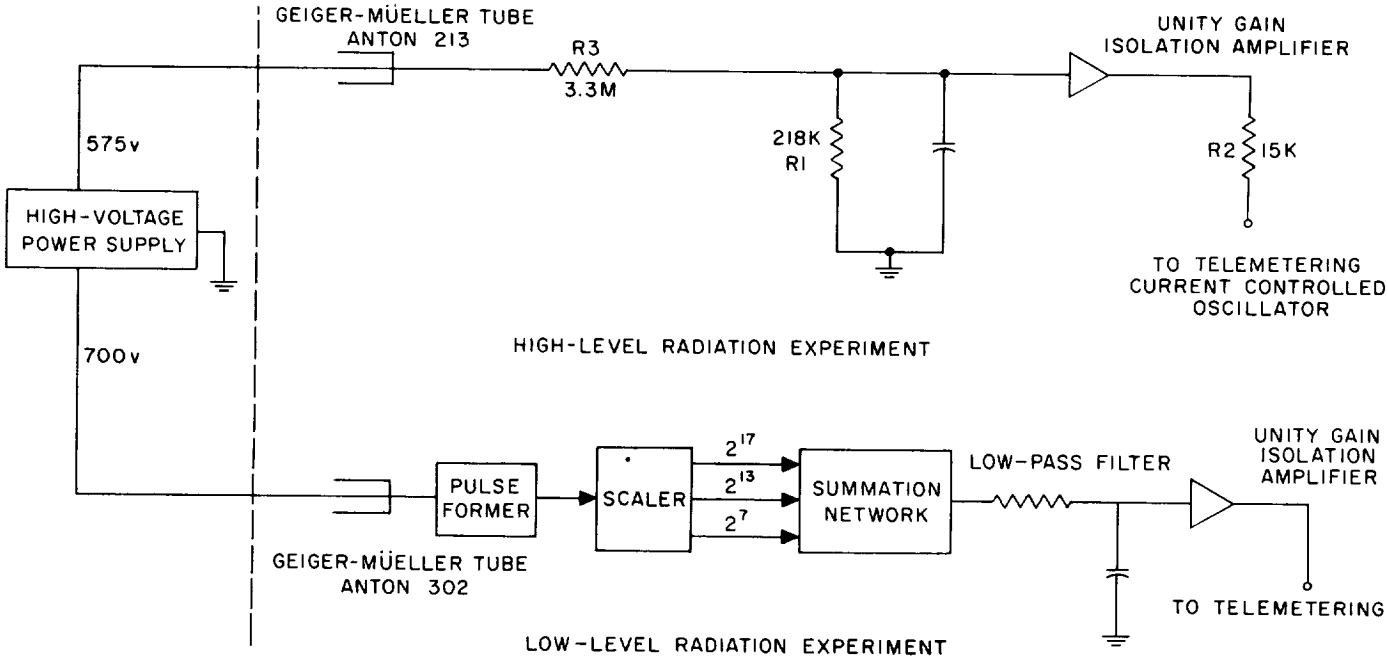

Figure 7. Radiation Experiment

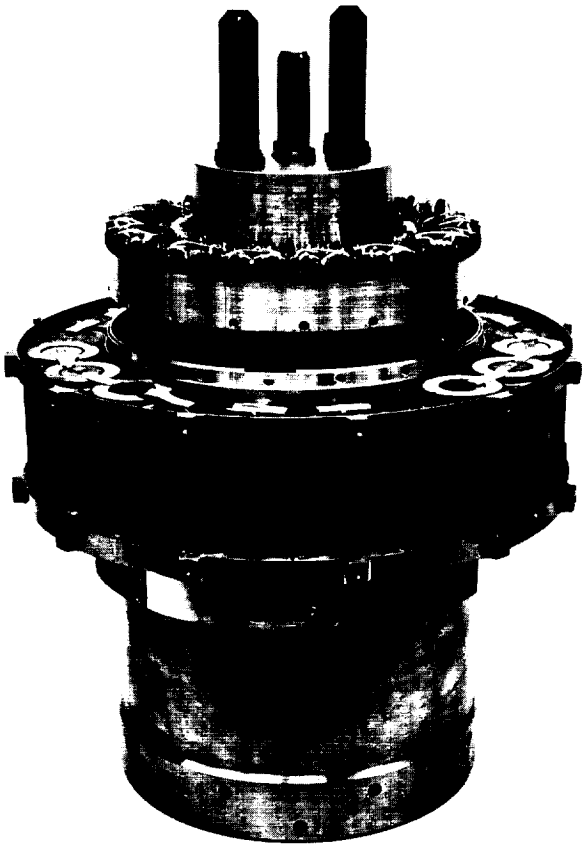

Figure 8. Radiation deck

three outputs have been selected at four-stage intervals. These signals are mixed in the ratio of 1:2:4 for the first, second, and last tap, respectively. The result is the consolidation of information that might ordinarily require three subcarriers into one subcarrier. Reading speeds of slow counting rates are thereby improved by as much as 256:1 over that obtained from a single tap at the end of an identical number of counter stages. The unfiltered composite output waveform is shown in Fig. 10. The uncompensated mixed waveform produces a large voltage step once every 217 pulses or once every major scaler cycle. To preclude the occurrence of correspondingly large step changes in frequency at the output of the subcarrier oscillator, an auxiliary flip-flop (stage 18, Fig. 9) provides step reduction at the critical point. Similar compensation is performed on the subcycle by stage 19. The step reduction mechanism permits minimization of the output shaping-filter time constant for given values of VCO band swing.

3. Scaler Length

The scaler chain was made long enough to prevent the fastest expected output signal appearing at the last stage from being severely attenuated by the shaping filter in the mixer circuit. By shaping the output square-waves into exponentially rising and falling edges, steady-state signal phase error occurring in the receiver phaselocked loop can be fixed at a tolerable maximum. In broad terms, the scaler length is indirectly determined

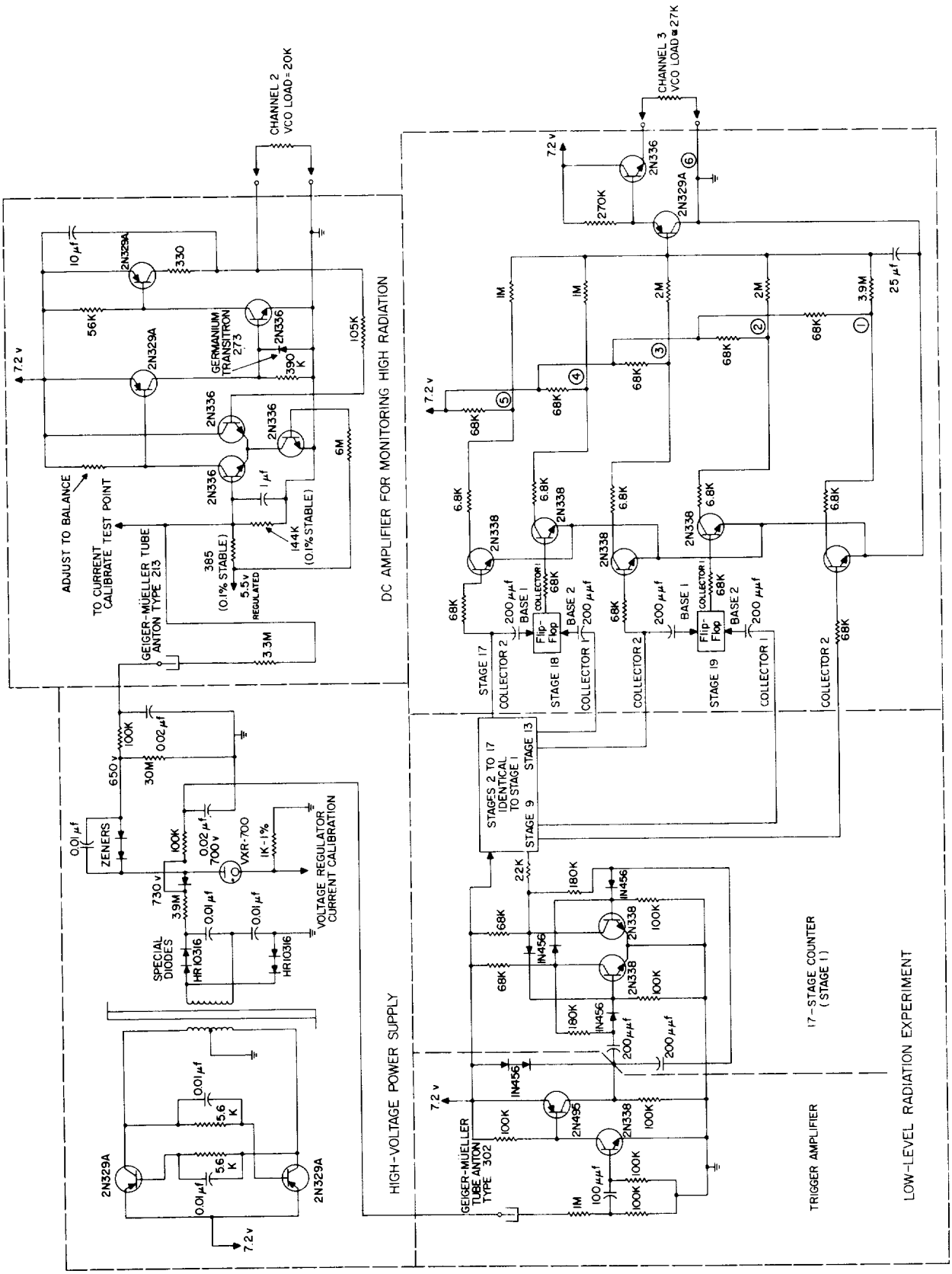

Figure 9. Cosmic ray experiment

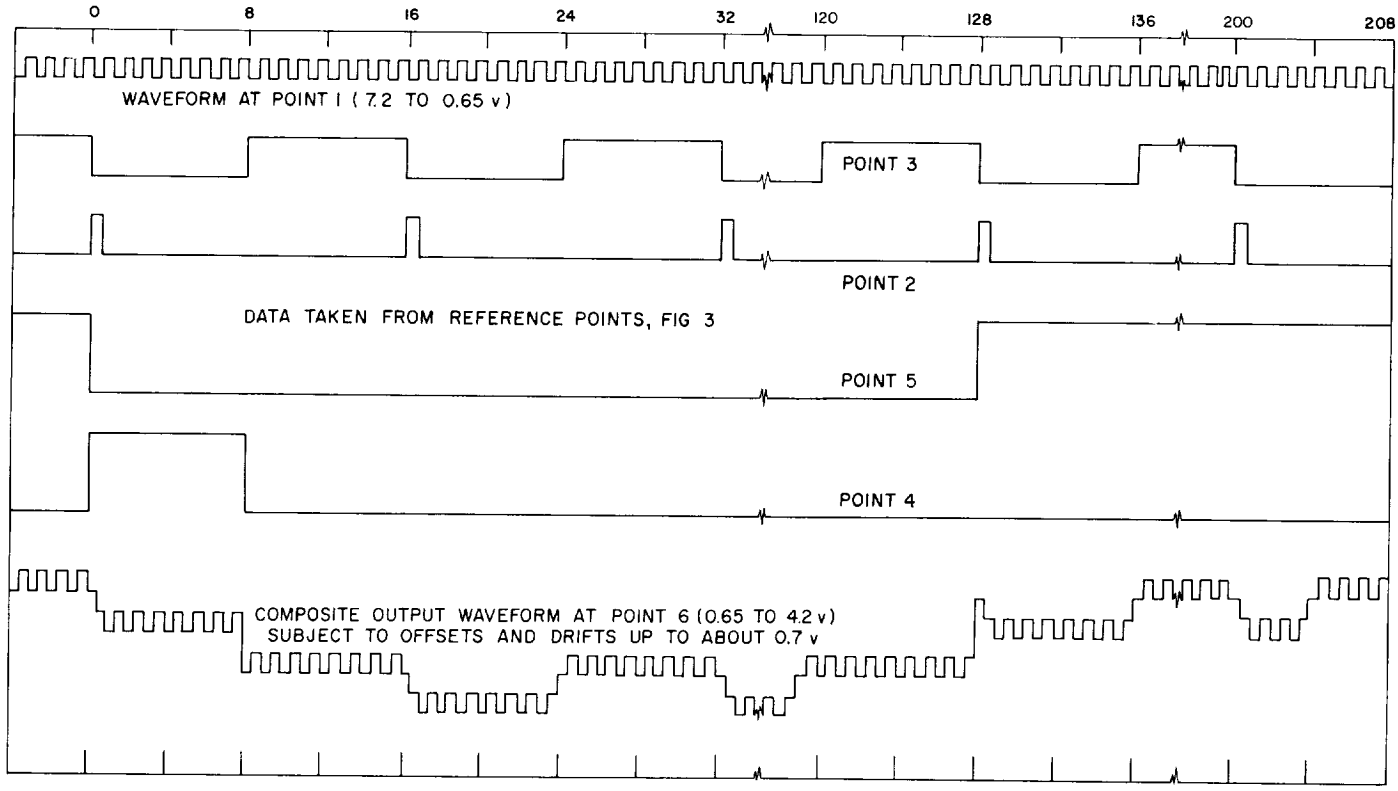

Figure 10. Scaler and timing waveforms

by such interrelated items as sideband power, receiver loop-bandwidth, and signal-to-noise ratios at threshold distances.

I. DC Amplifier

The amplifier used with the 213 Geiger tube converts average tube currents in the order of 20 to 40 μa into output currents having magnitudes large enough to supply signal current requirements for the associated subcarrier oscillator (300 μa input current for full-band deflection). The transfer characteristic of the amplifier is 0.1 v/μa and its representative drift coefficient is 1 mv/°C at 40°C.

J. Counting Range

The maximum rate at which the 302 will count as determined by tube dead time is about 16,000 to 18,000 cps. The recovery effect is sketched in Fig. 11. When particle counting rates are far in excess of the maximum counting ability of the tube, an increasing percentage of the particles will either not be counted or will produce ionizations occurring at intervals slightly larger than the dead time. Peak-to-peak amplitude of the closely spaced pulses will be sharply attenuated, resulting in a smaller percentage of the pulses being large enough to trigger the input stage of the scaler. The reduced pulse amplitude has the effect of producing a double-valued calibration curve. This characteristic, in some respects, is superior to one which remains saturated, providing little or no change in scaler counting rate for large changes in radiation intensity. The pulse integrator circuit used as a high-intensity monitor can also resolve ambiguities in the 302 channel caused by the double-valued nature of its response. Maximum average count rate obtainable in the *Pioneer III* experiment was 11.5 kcps.

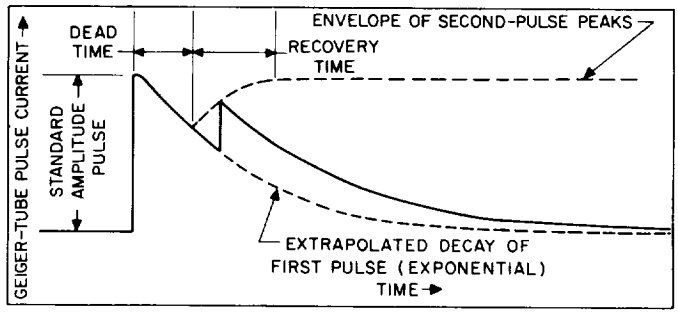

Figure 11. Reduction in amplitude caused by recovery-time effects

K. Optical Trigger Unit

A prototype trigger unit of the type which is to be used to trigger a camera shutter was flown on the first flight in order to test its operation. Two types of signals are transmitted on the same telemetering channel: (1) a memory-type signal which indicates only that the trigger unit and coincidence circuits functioned, and (2) a superimposed pulsing signal which transmits a pulse each time the optical sensor sees a large light source. A photograph of the flight-type unit is shown in Fig. 12.

When a large light source enters the field of view of the shutter trigger lens, the image is large enough to activate both photocells simultaneously, and a pulse is generated by the coincidence circuit. The first pulse generated after the shutter trigger circuit is armed operates the memory device which establishes a new permanent center frequency for the channel 1 VCO. The scale-of-four counter cycles the VCO about the new center frequency, causing it to deviate once for each two revolutions of the payload. The low-pass filter is included to reduce the rate of change of the voltage output of the counter, thereby preventing high rates of change of the VCO.

L. Power Supply

The purpose of the payload power supply is to distribute required power to all payload circuitry at the impedance levels and regulation desired. Approximately 85% of the available power is required by the transmitter oscillator, frequency multiplying, and output circuits. The remaining 15% is utilized by the subcarrier oscillators, the radiation and shutter experiments, the timer, and the despin mechanism.

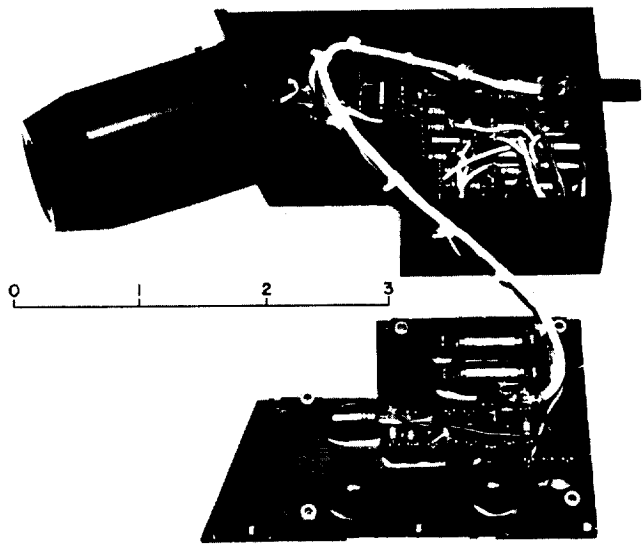

Figure 12. Trigger unit for camera shutter

Figure 13 shows a block diagram of the complete power supply. The battery pack consists of 18 Mallory RM 42-R mercury cells arranged series-parallel to give a nominal 7.2 v output with a 42 amp/hr capacity which provides approximately 90 hr operating time. The batteries weigh 6.6 lb and occupy a volume of 52.2 cubic in.

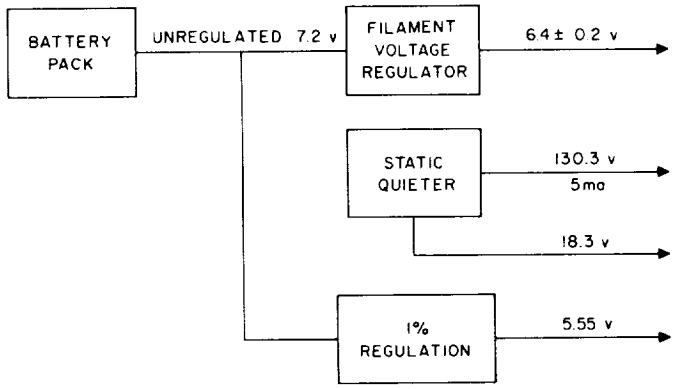

Figure 13. Block diagram of power supply

The filament voltage regulator is essentially a switch, the duty cycle of which is varied to maintain the regulated output constant at 6.4 v dc. Control of the output voltage is accomplished by driving the switching transistor according to the switching cycle of a voltage-controlled multivibrator. The switching cycle of the multivibrator is determined by an error voltage which is obtained by comparing the regulator output with a standard voltage. Working laboratory models have been constructed which are 89% efficient. This efficiency was obtained utilizing a system which was not completely optimized and may be expected to improve. The design goal is a regulator of 95% efficiency, weighing no more than 75 grams and occupying no more than 6 cubic in.

The static inverter is the conventional Royer circuit or RL coupled multivibrator. The battery voltage is chopped and transformed to the voltage levels required by the transmitter and driver circuitry. The frequency of operation is 2000 cps, since this relatively high frequency permits use of small cores and filter capacitors. The upper frequency limit is set by allowable core loss (which increases with frequency) and the minority carrier storage effects in the switching transistors. To achieve high efficiencies, tape-wound cores of low coercitivity are used with minimum thickness tapes.

M. Timer

Early in the program there was made known the need for rugged, lightweight timing devices capable of performing one or more of the following functions.

1. Delayed arming of the shutter trigger.
2. Delayed operation of the payload despin mechanism.

The operating temperature range is sufficiently restricted and the accuracy requirements are not too stringent, so that a very rugged, reliable device can be constructed using the principles of fluid flow. Accordingly, development of a hydraulic timer was undertaken.

Because of the small flow rates involved and in order to minimize error due to temperature variations, Dow Corning No. 200 silicone fluid in a 12,500 centistokes viscosity grade was selected as the operating fluid. Early in the investigation, the use of needle valves to control flow rate was abandoned because of the prohibitively small valve clearances necessary to achieve the combination of flow rate and piston load desired. Instead, it was decided to use a length of hypodermic tubing to control the flow; fine adjustment of the flow rate can be accomplished by a slight crimping of the tube.

A prototype model of the hydraulic timer is shown in Figs. 14 and 15. The timer is completely filled with silicone fluid except for the captive air chamber in the top cap which allows for thermal expansion. A check valve in the piston permits rapid cocking of the device by pulling outward on the knob; the device then runs down, under the influence of the spring load on the piston, oil flowing around the piston via the external time-controlling tube. The tube shown in the photograph has a bore diameter of 0.042 in. and gives ½ in. of travel in approximately 30 min; times up to several days could be accommodated with reasonable lengths of 0.020-in.-diameter capillary tubing. The timer was manually started by removing the shaft lock screw which extended through the probe support shell. The timer was adjusted to give delay times of 11 hr 50 min for despin and 19 hr 50 min for trigger arming at 35°C.

N. Despin Mechanism

The *Juno IIA* despin mechanism is shown schematically in Fig. 16. (See Ref. 1 for a description of the principle of operation of the mechanism.) It consists of two weights, each with a 5-ft. length of cable attached. The free end of each cable is tied to an eyelet which fits

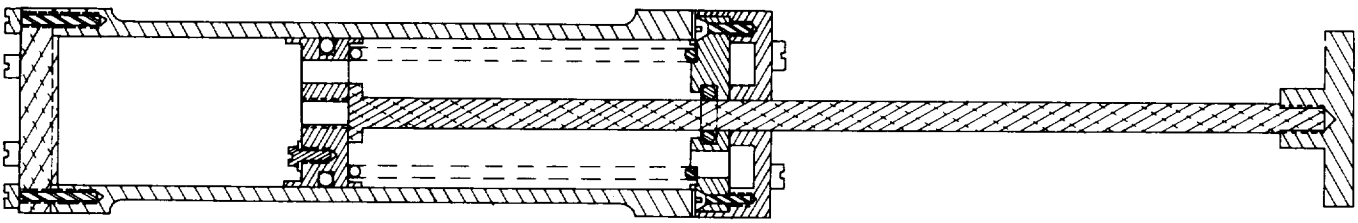

Figure 14. Hydraulic timer

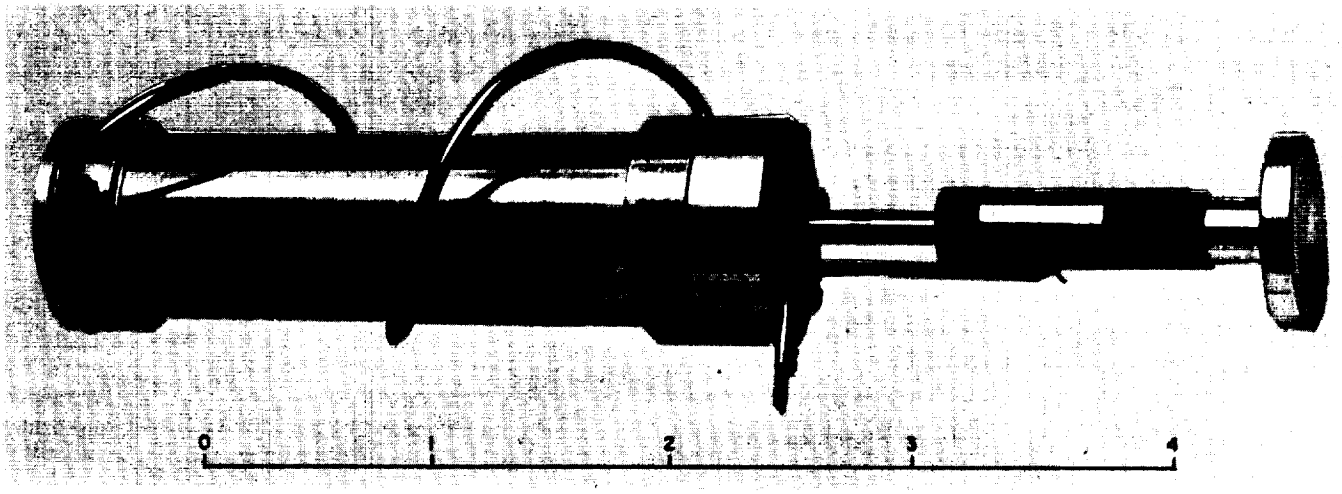

Figure 15. Prototype hydraulic timer

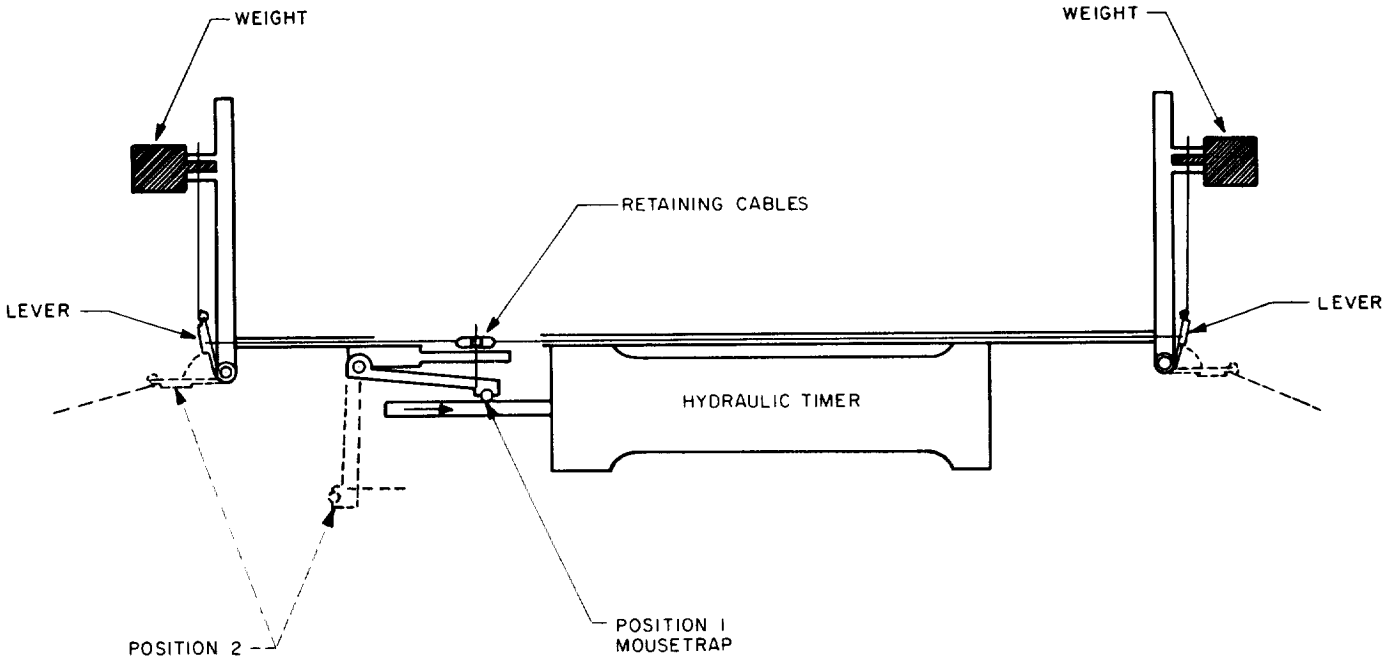

Figure 16. Despin mechanism

over a hook on the periphery of the payload. Each cable is wound around the payload in a manner opposite to that in which the payload spins. The weights are secured to the payload by pins.

The despin process is initiated by motion of the hydraulic timer shaft. This shaft holds the mouse trap in position 1. As time progresses, the timer shaft moves to the right. When the end of the shaft clears the mouse trap roller, the following sequence of events takes place:

1. The mouse trap assumes position 2 and in doing so pulls a pin which releases the retaining cables that hold the spring-loaded levers in the cocked position (position 1).
2. The levers assume position 2, thus pulling the pins which hold the weights to the payload.
3. When the weights are released, they fly outward due to centrifugal force causing the cables to unwind. This results in a transfer of energy and angular momentum from the payload to the weights and cables, thus slowing down the payload spin rate.
4. The hook and eyelet system is so designed that the cables are released when they arrive at a radial position. The payload retains the reduced spin rate it has when the cables are released.

The theoretical formula for radial release is

$$\frac{W_F}{W_I} = \frac{\bar{I}}{A}\left(1 - \sqrt{\frac{\frac{A}{\bar{I}} - 1}{\frac{AC}{B^2} - 1}}\right)$$

$$A = I + m\,(l + a)^2 + pl\,(al + a^2 + 1/3\,l^2)$$

$$B = ml\,(l + a) + pl^2\,(1/3\,l + 1/2\,a)$$

$$C = l^2\,(m + 1/3\,pl)$$

where W_F is the final spin, W_I the initial spin, $\bar{I}$ is the moment of inertia of the payload with the wire wrapped around, I is the moment of the payload alone, m is the total mass of both small weights, $P/2$ is the linear density of the wire, a is the distance from the payload axis to the point where the wire pivots as its swings into the radial position, and l is the length of wire from the pivot point to the small weight center of mass. In practice W_F/W_I is adjusted by varying m. The theoretical value for the ratio of the final spin rate to the initial spin rate as a function of the mass of the weights is shown in Fig. 17.

The despin mechanism has been subjected to environmental test levels in excess of those specified for the payload and found to perform quite satisfactorily. Several additional tests were performed, and it was estab-

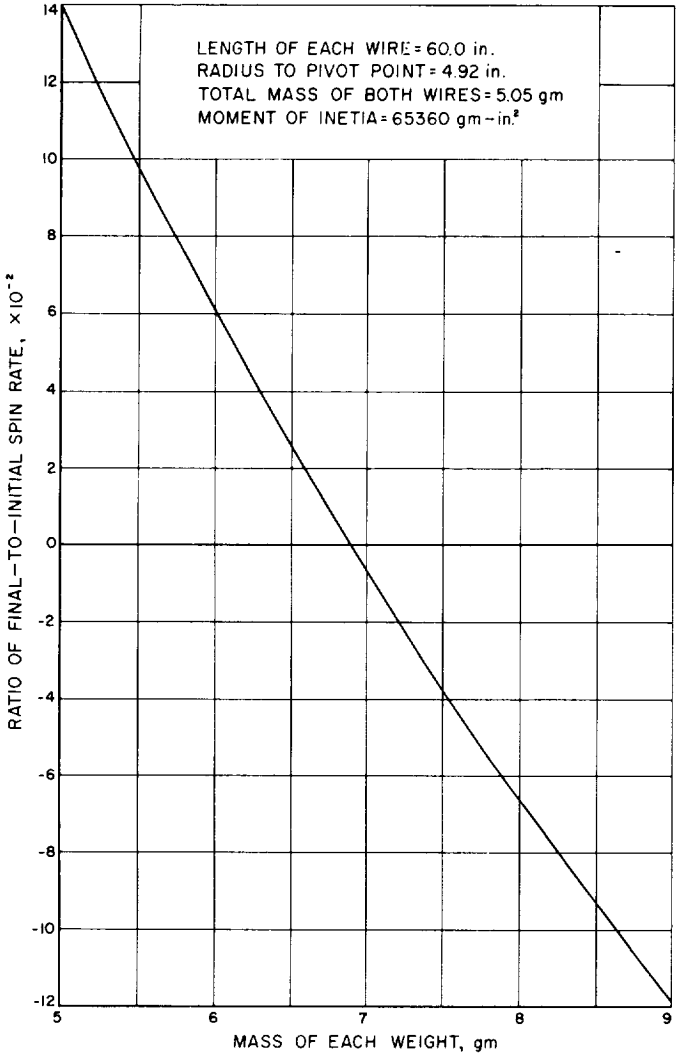

Figure 17. Spin rate

lished that the repeatability of the despin mechanism and process is within the required accuracies of the system. Ratios of final-to-initial spin rates were determined and compared with the theoretical values. The experimental ratios deviated from the theoretical, since these tests were performed in air and not in vacuum. A careful study revealed that the deviations could be explained by the aerodynamic drag effects on the weights and cables.

O. *Structures*

In order to meet the weight requirement, it was necessary to tailor the structure closely to the overall electrical and mechanical needs. This "optimization" of structure exacted a penalty by minimizing the versatility of the unit.

The basic shape of the payload was dictated by the following major needs:

1. The Geiger-Mueller tubes should not be excessively "shadowed" by the payload structure.
2. The optical equipment should have an unimpaired view.
3. The inertia about the roll axis must exceed the inertia about the pitch axis.
4. The electronic components must be accessible for adjustment and repair.
5. The antenna pattern must meet the needs of the communications system.
6. The weight must not exceed 15 lb.

It is believed that all of the aforementioned needs were satisfied.

The probe structure forward of the separation joint consists of a primary structure (which is the load-carrying member from the probe adapter), the probe proper, and a secondary structure which provides the mounting of probe subassemblies and component parts.

The primary structure is composed of a cylindrical aluminum support shell and a battery assembly consisting of two support bulkheads and 18 RM42 RT mercury batteries. The batteries were modified in the following manner: (1) strips of thermo-setting glass-cloth electrical tape (¼ in. in width) are attached at each end of the batteries and (2) a split micarta sleeve having a $\frac{1}{32}$-in. wall and cut to a length equal to the spacing between bulkheads is then bonded to the battery cases.

This structure is shown in Fig. 18. It has been subjected to 25 g of sine wave vibration from 20 to 2000 cps

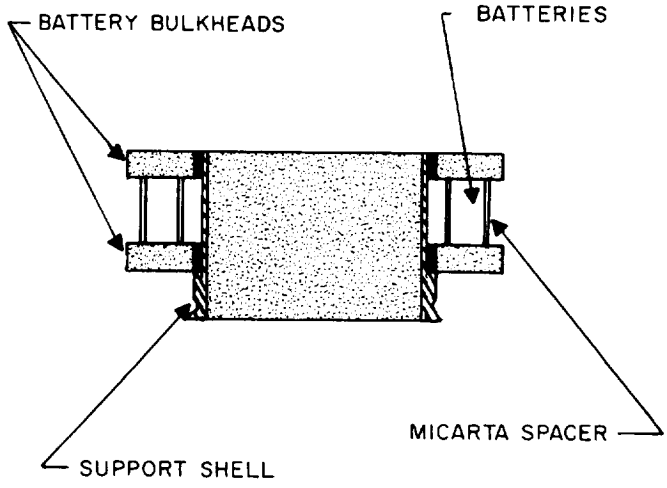

Figure 18. Payload prime structure

and 35 g rms of noise band limited from 20 to 1500 cps. The structure was loaded and successfully withstood the equivalent of 300 g of static acceleration.

The secondary structure consists of four aluminum alloy substructures: (1) transmitter platform, (2) transmitter plate, (3) timer support, and (4) high-voltage and cosmic ray support. These four substructures are bolted together and in turn are bolted to the primary structure. The antenna cone completes the structure.

The assembled prime and secondary structures have been subjected to 25 g of sine wave vibration from 20 to 2000 cps and 35 g rms of noise band limited from 20 to 1500 cps. The structure has also been tested to a spin environment of 1450 rpm.

P. Internal Temperature Control

In order to assure that the probe subassemblies are maintained at a reasonable operating temperature, the absorptivity and emissivity ratios of the probe surface were controlled by providing a special surface treatment or coating to the entire probe as shown in Fig. 19. The internal temperatures were expected to vary with the angle of incidence between the probe and the sun. With the coatings as shown above the internal temperature should be approximately 36°C when the probe incident angle is 45 deg and 47°C when the incident angle is 60 deg.

INSTRUMENTATION SECTION

AREA I. GOLD-PLATED ALUMINUM-FOIL SHIELD 15% (11.02 square in.) PAINTED 1 COAT ZINC CHROMATE, 2 COATS *SERGEANT* BLACK MIL E-10687A.

AREA II. GOLD-PLATED ALUMINUM-FOIL SHIELD MICARTA-SILVER PLATED WITH A GOLD WASH.

AREA III. REMAINDER OF VISIBLE INSTRUMENT SECTION. 100% PAINTED 2 COATS OF ALUMINUM PAINT KEPCO NO. 25.

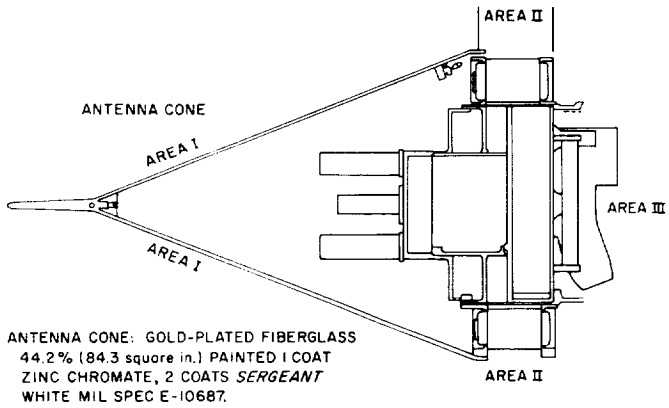

ANTENNA CONE: GOLD-PLATED FIBERGLASS 44.2% (84.3 square in.) PAINTED 1 COAT ZINC CHROMATE, 2 COATS *SERGEANT* WHITE MIL SPEC E-10687.

Figure 19. Nose cone, showing surface coating

IV. THE TRACKING AND COMMUNICATIONS NETWORK FOR *JUNO II*

A. Introduction

The tracking net utilized for the *Juno II* lunar probe flights was designed with the primary objective of satisfying the mission requirements for those flights. A secondary design objective was that the concepts of the system and the basic hardware elements involved could be utilized in the evolution of a deep space network which would meet the tracking and communications requirements of future more sophisticated deep space experiments.

To illustrate the logic of the tracking and communications network configuration used with the *Juno IIA* vehicle experiment, it is necessary to consider the experiment objectives as described previously in this Report, i.e., (1) determination of probe trajectory, (2) continuous measurement of cosmic-ray intensity from near the Earth to beyond the known radiation belts and, at least intermittently, from beyond the radiation belts to the distance of the Moon, (3) evaluation of payload hardware and techniques utilized for temperature control to aid development of future space probe payloads. These requirements dictate a network which provides continuous reception of telemetry signals from the probe from launch through the first several hours of flight and intermittently thereafter at least to the distance of the Moon, plus a highly reliable system for measurement of vehicle coordinates and the associated computation on those data to determine the vehicle path.

B. The Network Configuration

The configuration which was selected to satisfy the basic tracking and communication requirements consisted of a minimum receiving station at the Cape Canaveral launching site, a medium capability tracking station at Mayaguez, Puerto Rico, and a high capability station installed at Goldstone Lake on the Camp Irwin military reservation near Barstow, California (approximately 100 miles air distance NE of Pasadena). All of these stations were connected together by a telephone and teletype communication network with a control and orbital computing center located at the Jet Propulsion Laboratory in Pasadena (Fig. 20).

The function of the launch site station was to provide pre-flight checkout of the payload radio equipment prior to launch, and telemetry reception and one-way Doppler

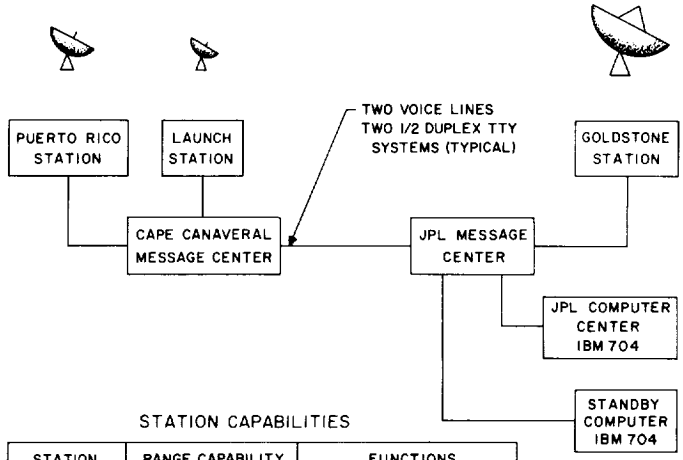

STATION CAPABILITIES

STATION	RANGE CAPABILITY (FOR 200 mw)	FUNCTIONS
LAUNCH	10^6 km	TELEMETRY, DOPPLER
PUERTO RICO	1.6×10^5 km	TELEMETRY, DOPPLER ANGLES 0.1 - 1° ACCURACY
GOLDSTONE	1.8×10^6 km	TELEMETRY, DOPPLER ANGLES .01 - .1 ACCURACY

Figure 20. Tracking and communications network

during the first 10 to 15 min of flight. This station utilized a narrow-band, phase-locked receiver with a manually directed, relatively broad-beam antenna. For a normal trajectory, the vehicle would disappear below the launch station horizon 10 to 15 min after launching. Shortly before the time of loss at the launch site (approximately 6 min after lift-off), the vehicle would appear on the NW horizon at the Puerto Rico station, and that station would acquire the signal.

The Puerto Rico station has a narrow-band, phase-locked receiver which is used in conjunction with a 10-ft.-diameter automatic tracking antenna mounted on a modified Nike AZ-EL antenna pedestal (Fig. 21). Data provided by the station include vehicle coordinates (AZ-EL), one-way Doppler, and telemetry. As the probe continues in its flight toward the Moon, its apparent easterly motion is arrested due to the rotation of the earth. After approximately 5 hr of track by the Puerto Rico station, the vehicle will appear to rise on the SE horizon at Goldstone and that station will acquire the signal (Fig. 22). At this time the probe is approximately 50,000 miles from the Earth, still high in the sky at Puerto Rico and providing a signal several db above the Puerto Rico station receiver threshold.

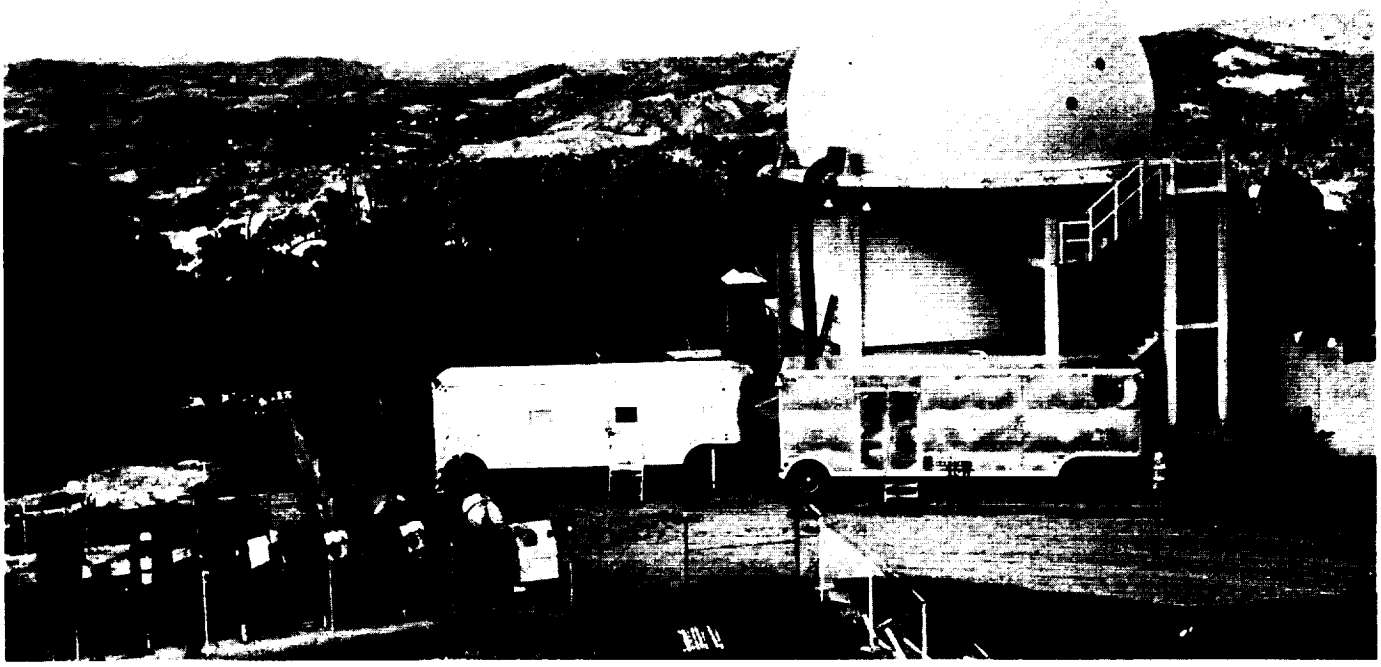

Figure 21. Puerto Rico tracking station

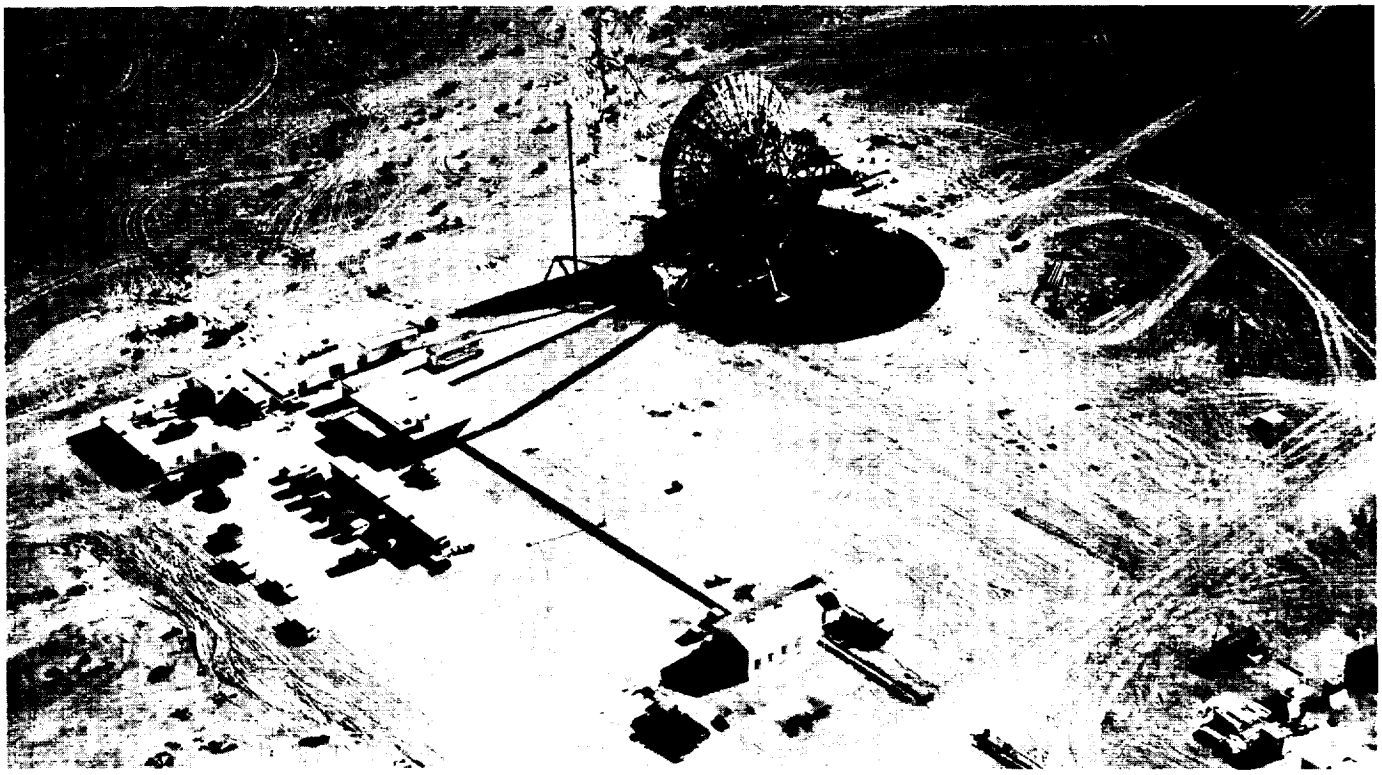

Figure 22. Goldstone tracking station

The Goldstone station has a phase-locked receiver used in conjunction with an 85-ft-diameter polar-mounted tracking antenna. Basic data provided by the Goldstone installation are the same as for Puerto Rico: angular position, one-way Doppler, and telemetry. The Goldstone station tracks the probe from horizon to horizon, a period of about 9 hr. After the probe sets in the west at Goldstone it is not visible again by that station for about 15 hr, after which time it would again be acquired and tracked for another 9-hr period.

During the sequence of tracking by the various stations, the IBM 704 computer at the JPL computing center calculates the vehicle orbit based on an initial predicted orbit and data received from launch phase instrumentation and the network tracking station. As quickly as possible after launch, predictions of the future position of the vehicle and the signal frequency are made by the computer and sent to the Puerto Rico tracking station to assist in acquisition and, if necessary, reacquisition of the vehicle by the tracking antenna and phase-locked receiver. Approximately 1 hr prior to the expected acquisition at Goldstone, position and signal frequency predictions are furnished by the computer. As an independent back-up method for generating acquisition coordinates at the Goldstone station, azimuth and elevation readings are sent directly from Puerto Rico, and these readings (time labeled) are graphically converted to pointing angles at Goldstone.

C. Launch Station System Description

The main purpose of the launch station was to provide doppler and telemetering data throughout the period from missile launch until acquisition was accomplished by the downrange tracking station. It was also used as a payload checkout facility prior to the firing. In order to fulfill these requirements, the station, built in a single trailer, was mechanized with a narrow-band radio receiver, a telemetering recording system, and data-handling facility. Each of the three classes of equipment was designed by separate groups and integrated in an existing Microlock trailer. Essentially, the trailer was laid out in three separate sections. The aft section as shown in Fig. 23 contained the telemetering and record-

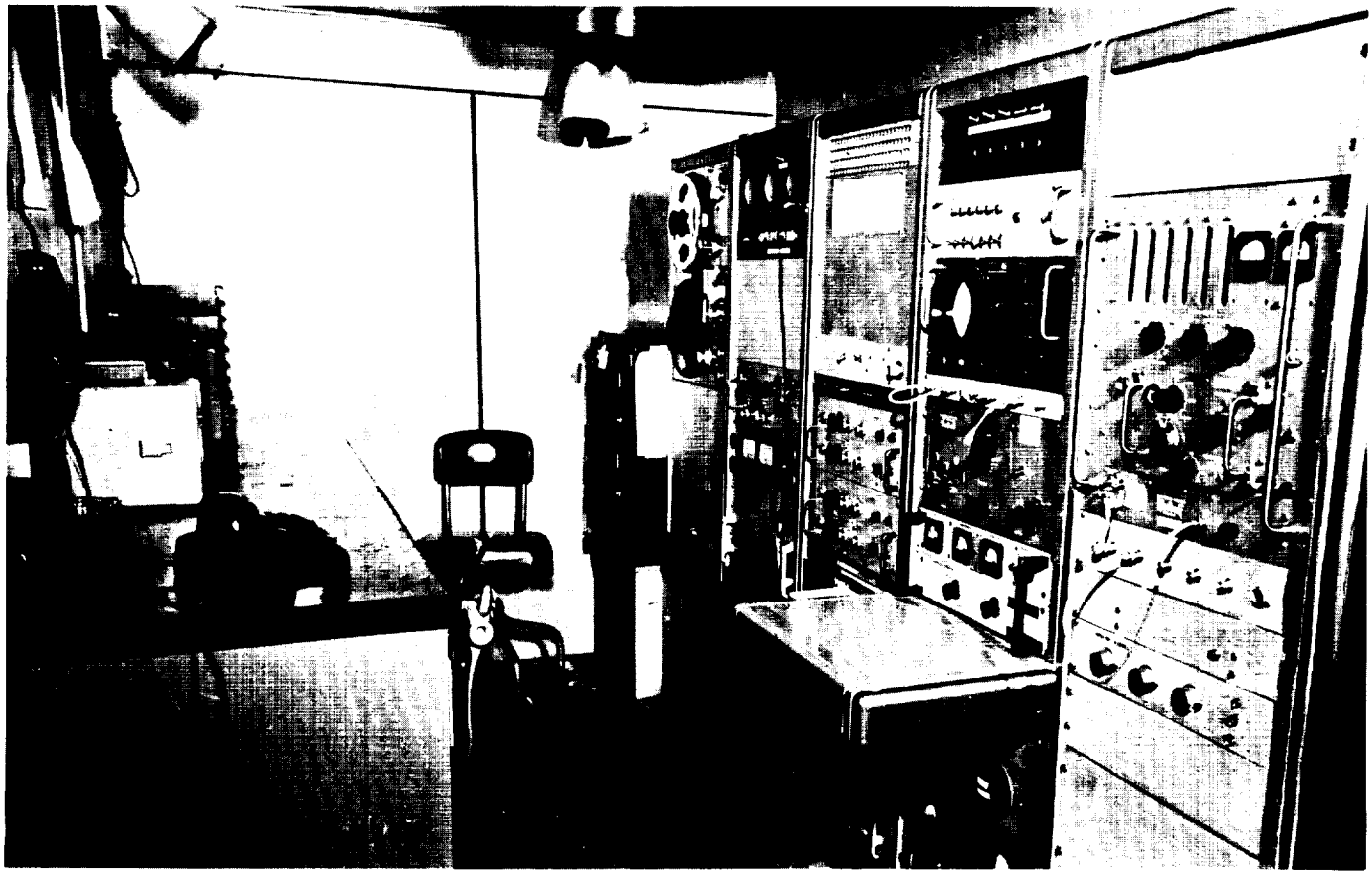

Figure 23. Microlock trailer

ing equipment, a workbench, and a locked file. The center section (Fig. 24) comprised the main operation control console. Located in this section were the RF radio receiver equipment, the necessary operator controls and meters, the main power switches, the communications equipment and controls, a signal generator, and an oscilloscope. The data-handling facility was located in the section immediately forward of the control console, as shown in Fig. 25.

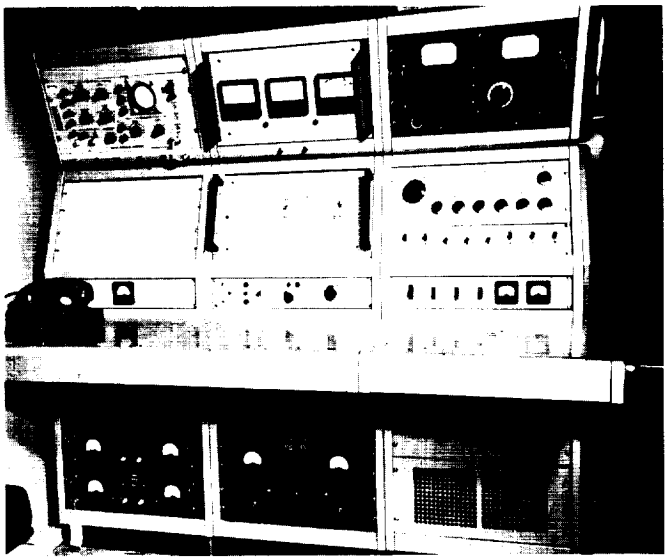

Figure 24. Operation control console

Figure 25. Data-handling facility

1. Radio Receiver

The radio receiving system consisted of an extremely sensitive, narrow-band 960.05-mc receiver preceded by a 6-ft circularly polarized parabolic antenna. The antenna which was illuminated with a four-turn helical feed (Fig. 26) was mounted on a vertical column and was manually positioned, using coarse cursors for determining the antenna pointing direction. The antenna possessed a 12-deg beamwidth and gain figures of 16.4 db for vertical polarization and 17.5 db for horizontal polarization.

The receiver as shown in block diagram form in Fig. 27 is basically similar to the Puerto Rico receiver with the exception that it does not possess the two-angle measuring channels. It consisted of a REL model S-1566 RF converter in conjunction with a Microlock receiver modified to operate at 960.05 mc. This form of mechanization was chosen because the converter was easily adaptable to this type of system, rather inexpensive and readily available.

A complete technical description of the receiver appeared in Ref. 2 through 4, the only major difference being in the use of a coherent AGC system. The system was mechanized with two RF loop bandwidth positions. The wide bandwidth position (2_{B_L}=60 cps) was used during takeoff and throughout the burning of the high-speed stages. This was necessary to track the expected doppler rates. The narrow bandwidth position (2_{B_L}=20 cps) was used after injection occurred and throughout the remainder of the flight. Under this condition the receiver possessed a threshold sensitivity of −153 dbm.

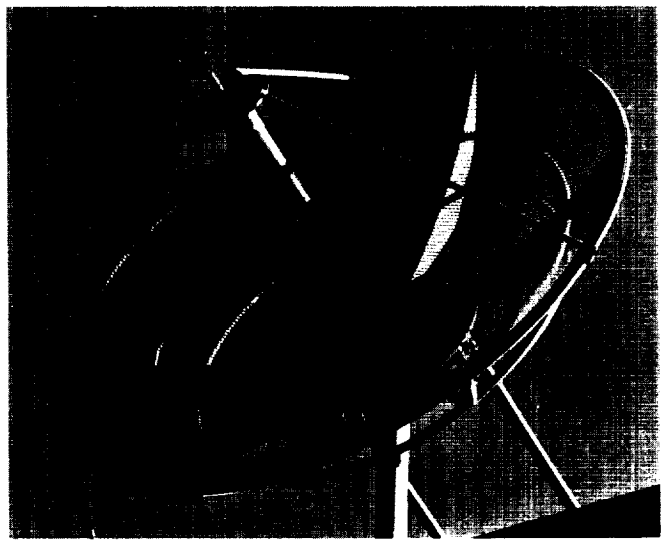

Figure 26. Four-turn helical feed antenna

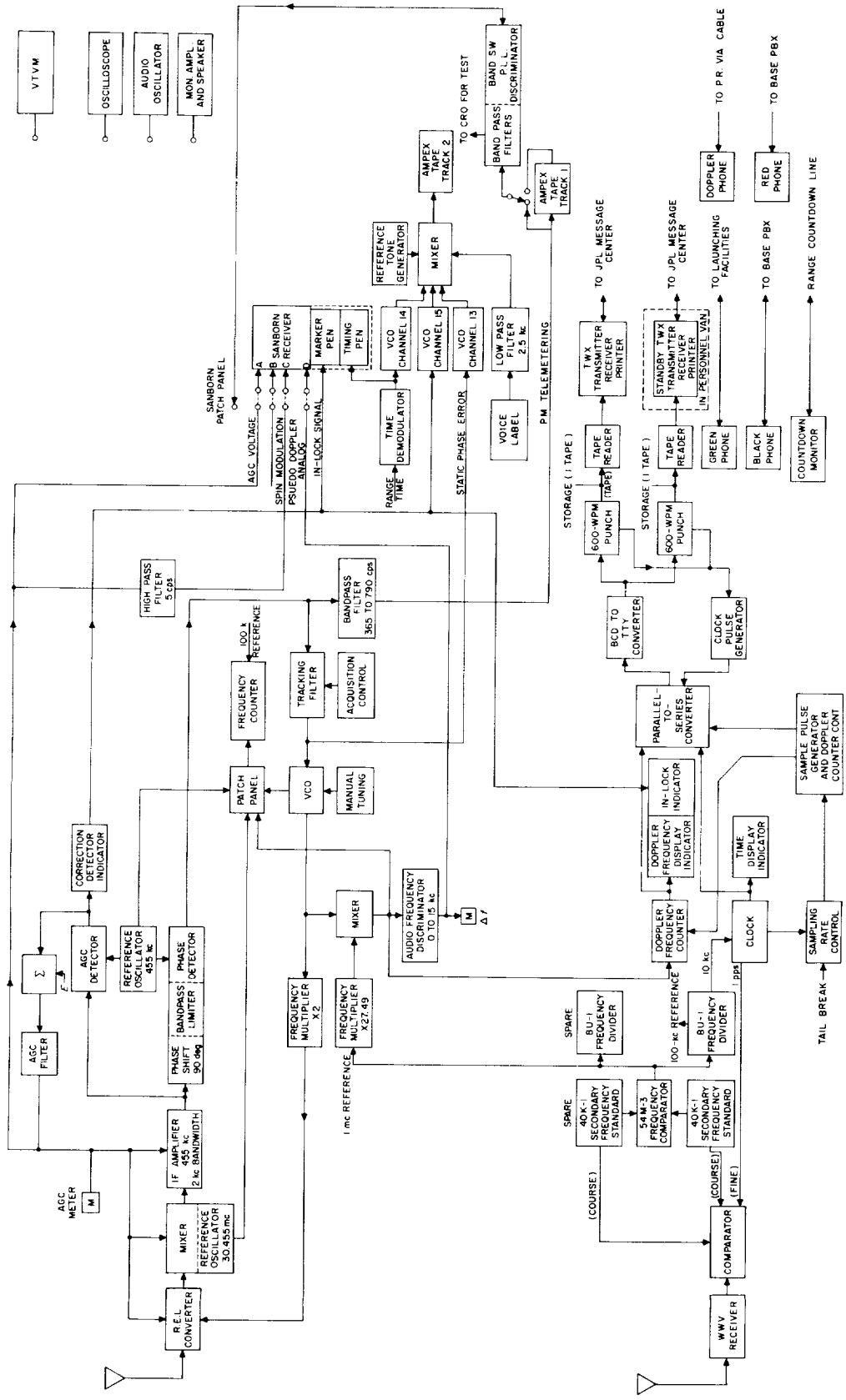

Figure 27. Telemetering recording system

2. Telemetering Recording System

The telemetering recording system was designed and built using equipment that was available in the Laboratory. The resulting system (Fig. 27) consists basically of a dual-track magnetic tape recorder, a band-switching phase-lock discriminator, and a four-channel direct-writing oscillograph. In addition to these major equipments, the system includes voltage-controlled oscillators, vacuum tube mixer, wow and flutter compensation tone generator, range timing unit, and station test equipment. This system was tied together in a central patch panel which had normal through patches to make the interconnections necessary for flight recording.

The following signals were recorded by this system.
Payload telemetering:

1. The composite signal, consisting of RDB channels 1, 2, and 3, was recorded on track 1 of the magnetic tape recorder.
2. Channel 3 was discriminated and recorded in real time on trace 2 of the oscillograph.
3. The discriminator voltage-controlled-oscillator frequency was mixed with other signals and recorded on track 2 of the magnetic tape recorder.

Receiver data signals:

1. Doppler frequency was discriminated in the receiver portion of the launch station. The dc output of this discriminator was recorded in real time on trace 4 of the oscillographs.
2. Spin modulation was recorded on trace 3 of the oscillograph.
3. Receiver signal level was recorded on trace 1 of the oscillograph.
4. Receiver "in-lock," "out-of-lock" signal was recorded on the events trace of the oscillograph. This voltage was also used to frequency modulate channel 12 voltage-controlled-oscillator which was mixed and recorded on track 2 of the magnetic tape recorder.
5. Static phase error was used to frequency modulate channel 13 voltage-controlled-oscillator which was mixed with other signals and recorded on track 2 of the magnetic tape recorder.

Timing and controls signals:

1. Range time, 1 pulse/sec, modulated channel 11 voltage-controlled-oscillator which was mixed with other signals and recorded on track two of the magnetic tape recorder. The range time signal was also recorded on the timing trace of the oscillograph.
2. Voice labels were recorded on track 2 of the magnetic recorder. During voice recording it was necessary to turn off the discriminator tracking VCO (730 cps).

3. Facility

The data-handling section consists of two frequency standards, WWV receiver, a frequency multiplier, a digital clock, doppler counter, sample rate controller, parallel-to-serial converter, two high speed TTY paper tape punches, two remote TD's, and two TTY machines.

1. The frequency standards are two Collins Radio Model 40K1 oscillators, 8U1 frequency dividers, and a 54M1 frequency comparator. The units are interchangeable with one acting as the main frequency source and the other acting as the backup. The outputs were 1 mc to the frequency multiplier, 100 kc to the HP frequency counter, and 10 kc to the digital clock.
2. The WWV receiver is a Collins Radio Model 51J4. The frequency of the frequency standard is calibrated against WWV by measuring the local time (digital clock) vs WWV time at two times and calculating the frequency difference from the drift.
3. The frequency multiplier is a Gertch FM-6 frequency meter (modified). It takes 1 mc and multiplies it to 27.49 mc for the doppler frequency mixer. This provides the doppler frequency on a 10-kc frequency bias. The accuracy of the frequency multiplier output is the accuracy of the 1-mc frequency standard.
4. The digital clock counts the 10 kc from the frequency standard to provide time in hours, minutes, and seconds. It has a 1 pulse/sec output and a binary coded decimal (BCD) output for each digit of the time (i.e., hours, minutes, seconds).
5. The sample rate controller allows the operator to select different sample rates. It provides the doppler counter time base and the commands which start the sampling operation.
6. The parallel-to-serial converter converts the parallel BCD data into serial TTY five-bit code data, forms the TTY format, and drives the high-speed TTY punches.
7. The high-speed punches punch the serial TTY data into paper tape for permanent storage and for transmission on the communication system. The punches operate at 600 wpm for each sample operation. There is a primary punch and a parallel operated backup punch.

8. There is a remote paper tape reader (TD) associated with each punch which reads the tape at 60 wpm and sends out the data on the teletype system. Each TD is connected into a teletype machine.
9. There are two TTY lines into the Launch Doppler Station with a parallel phone (red phone) for teletype control. Each TTY line has a TTY machine. The machines are used for entering the data from the remote TD into the communication system, as a means of general communication and to supply a printed readout of the data being sent.

D. Puerto Rico Station

The downrange tracking station, located at Mayaguez, Puerto Rico, was to accomplish the following objectives: (1) to receive and record telemetered cosmic-ray data from the space probe from the time of injection to Goldstone acquisition, (2) to provide information on the trajectory of the space probe, and (3) to increase the probability of acquisition of the space probe by the Goldstone tracking station by providing information by means of the IBM 704 as to its position based on Goldstone site coordinates.

Design of the system is such that angular position and radial velocity data will be transmitted to the JPL message center as it is generated by the radio system. Figure 28 illustrates the functional operation of the station. The system consists of a radio receiver of the phase-locked-loop type; a servo-driven tracking antenna pedestal on which is mounted a circularly polarized simultaneous-lobing antenna; a data recording facility; and a data-handling and transmission facility.

The radio receiver was assembled from existing CODORAC components by the Collins Radio Company. This system consists of a main receiver and two coherent angle-error detector receivers. One angle-error detector provides the error signal to drive the azimuth servo system and the other provides the error signal to drive the elevation servo system. The main receiver has an RF tracking loop that generates a phase coherent 31-mc signal with doppler information. The reference frequency for the doppler detector is generated in the data-handling van. A 30.455-mc and a 455-kc reference oscillator are used in detecting the RF and angle-tracking errors and in generating a coherent AGC voltage. Within the RF tracking loop the telemetry subcarriers are recovered and passed on to the audio discriminators in the telemetry van to provide the measured data. Refer to Fig. 30 for the block diagram of the radio system.

The noise bandwidth of the RF loop may be set to either 20 or 60 cps by switching the time constant of the post detection tracking filter. The wide bandwidth is used during the acquisition phase and approximately the first hour of tracking because at that time the doppler rate and signal strength are high. From then on the narrow bandwidth is used, so as to take advantage of the maximum receiver sensitivity. With the low bandwidth, the theoretical receiver threshold is −153.5 dbm. The original radio system design parameters and final measured performance are shown in Table 3.

The components which comprise the receiver are located both in the antenna pedestal and in the radio control van. The three 960-mc preselectors and balanced mixers and 30-mc IF preamplifiers are located directly behind the antenna. The high-frequency portion of the local oscillator chain and associated power supplies are located in the base of the antenna pedestal. RF signals from the elevation axis bypass the sliprings and pass through the cable wrap-up. The remainder of the receiver is located in rack 5 of the radio control van. The equipment is mounted on three hinged plates attached to a frame which pulls out on drawer slides for accessibility. The top plate contains the RF tracking receiver; the center plate contains the reference oscillators and the low frequency portion of the local oscillator, and the bottom plate contains the azimuth receiver on the front and the elevation receiver on the rear. (Refer to Fig. 30 and 31.) Rack 6 contains equipment for testing and adjusting the receiver, along with a frequency meter and the required power supplies.

Figures 32 and 33 are views of the interior of the radio-control van and the operating console, respectively. The left rack of the console contains a counter for measuring the frequency of the reference oscillators and the RF voltage-controlled oscillator. The 100-kc standard for this counter is generated in the data-handling van. The center rack has a 30-mc spectrum analyzer, oscilloscope, and receiver control panel. The right rack has a digital readout of Greenwich Mean Time, a count-down clock, monitor meters, and the servo control panel.

The antenna is a simultaneous lobing system designed to receive circularly polarized radio waves. The antenna provides simultaneously and continuously three distinct radiation patterns: a reference pattern or single on axis lobe, an elevation error pattern, and an azimuth error pattern. The error patterns consist of two fan-shaped beams at an angle from the antenna axis, the resulting valley between the fan beams passing perpendicularly through the antenna axis and perpendicular to the plane described by the movement of the antenna in the angu-

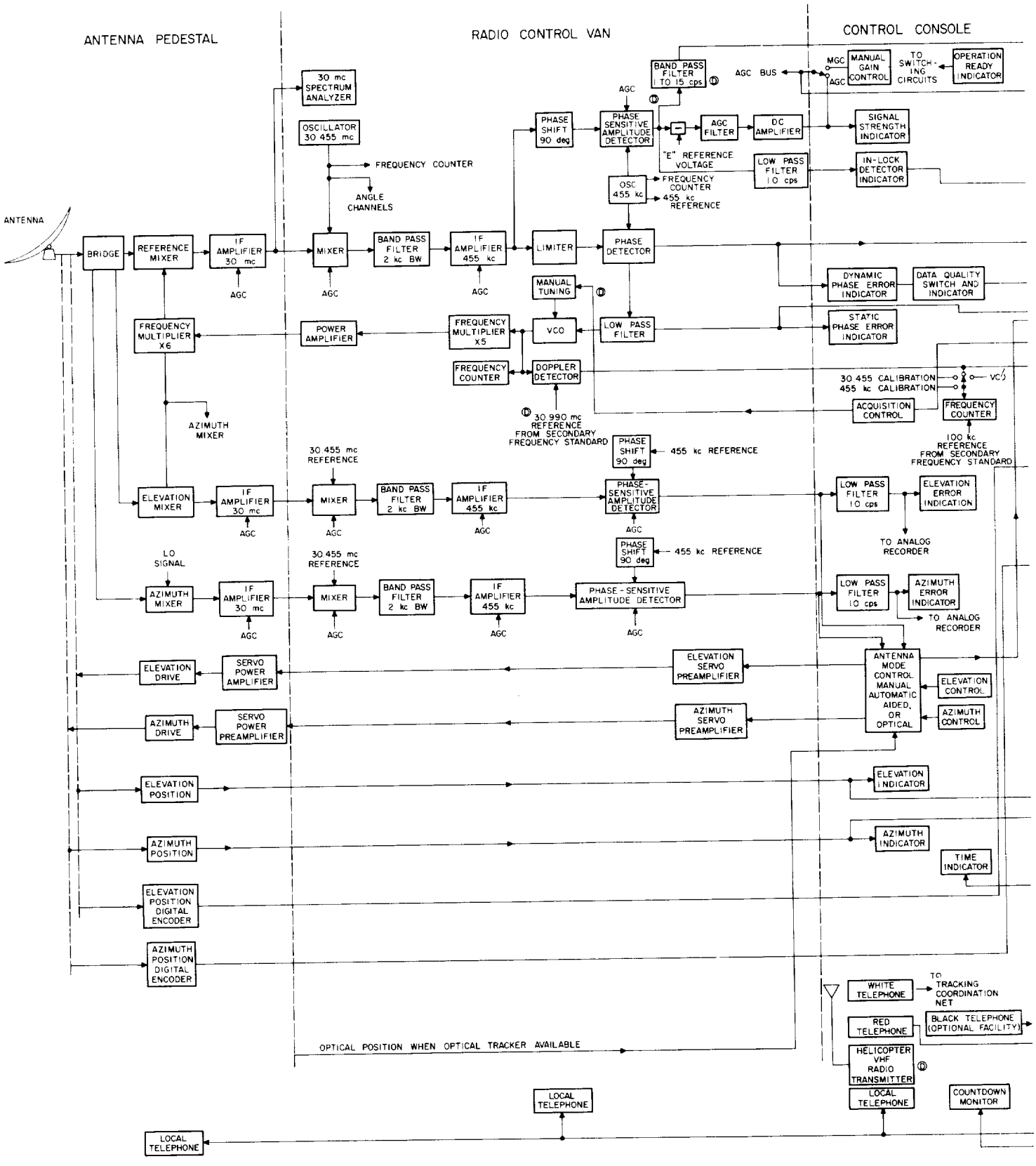
ANTENNA PEDESTAL
RADIO CONTROL VAN
CONTROL CONSOLE
ANTENNA
BRIDGE
REFERENCE MIXER
IF AMPLIFIER 30 mc
AGC
30 mc SPECTRUM ANALYZER
OSCILLATOR 30.455 mc
FREQUENCY COUNTER
ANGLE CHANNELS
MIXER
BAND PASS FILTER 2 kc BW
IF AMPLIFIER 455 kc
LIMITER
PHASE DETECTOR
PHASE SHIFT 90 deg
PHASE SENSITIVE AMPLITUDE DETECTOR
BAND PASS FILTER 1 TO 15 cps
AGC BUS
MGC
MANUAL GAIN CONTROL
TO SWITCHING CIRCUITS
OPERATION READY INDICATOR
AGC FILTER
DC AMPLIFIER
SIGNAL STRENGTH INDICATOR
"E" REFERENCE VOLTAGE
LOW PASS FILTER 10 cps
IN-LOCK DETECTOR INDICATOR
OSC 455 kc
FREQUENCY COUNTER
455 kc REFERENCE
MANUAL TUNING
VCO
LOW PASS FILTER
DYNAMIC PHASE ERROR INDICATOR
DATA QUALITY SWITCH AND INDICATOR
STATIC PHASE ERROR INDICATOR
FREQUENCY MULTIPLIER X6
POWER AMPLIFIER
FREQUENCY MULTIPLIER X5
FREQUENCY COUNTER
DOPPLER DETECTOR
30.455 CALIBRATION
455 kc CALIBRATION
VCO
ACQUISITION CONTROL
FREQUENCY COUNTER
100 kc REFERENCE FROM SECONDARY FREQUENCY STANDARD
30.990 mc REFERENCE FROM SECONDARY FREQUENCY STANDARD
AZIMUTH MIXER
30.455 mc REFERENCE
PHASE SHIFT 90 deg
455 kc REFERENCE
ELEVATION MIXER
IF AMPLIFIER 30 mc
MIXER
BAND PASS FILTER 2 kc BW
IF AMPLIFIER 455 kc
PHASE-SENSITIVE AMPLITUDE DETECTOR
LOW PASS FILTER 10 cps
ELEVATION ERROR INDICATION
TO ANALOG RECORDER
LO SIGNAL
AZIMUTH MIXER
IF AMPLIFIER 30 mc
MIXER
BAND PASS FILTER 2 kc BW
IF AMPLIFIER 455 kc
PHASE-SENSITIVE AMPLITUDE DETECTOR
LOW PASS FILTER 10 cps
AZIMUTH ERROR INDICATOR
TO ANALOG RECORDER
ELEVATION DRIVE
SERVO POWER AMPLIFIER
ELEVATION SERVO PREAMPLIFIER
ANTENNA MODE CONTROL MANUAL AUTOMATIC AIDED, OR OPTICAL
ELEVATION CONTROL
AZIMUTH CONTROL
AZIMUTH DRIVE
SERVO POWER PREAMPLIFIER
AZIMUTH SERVO PREAMPLIFIER
ELEVATION POSITION
ELEVATION INDICATOR
AZIMUTH POSITION
AZIMUTH INDICATOR
TIME INDICATOR
ELEVATION POSITION DIGITAL ENCODER
AZIMUTH POSITION DIGITAL ENCODER
WHITE TELEPHONE
TO TRACKING COORDINATION NET
RED TELEPHONE
BLACK TELEPHONE (OPTIONAL FACILITY)
HELICOPTER VHF RADIO TRANSMITTER
LOCAL TELEPHONE
COUNTDOWN MONITOR
OPTICAL POSITION WHEN OPTICAL TRACKER AVAILABLE
LOCAL TELEPHONE

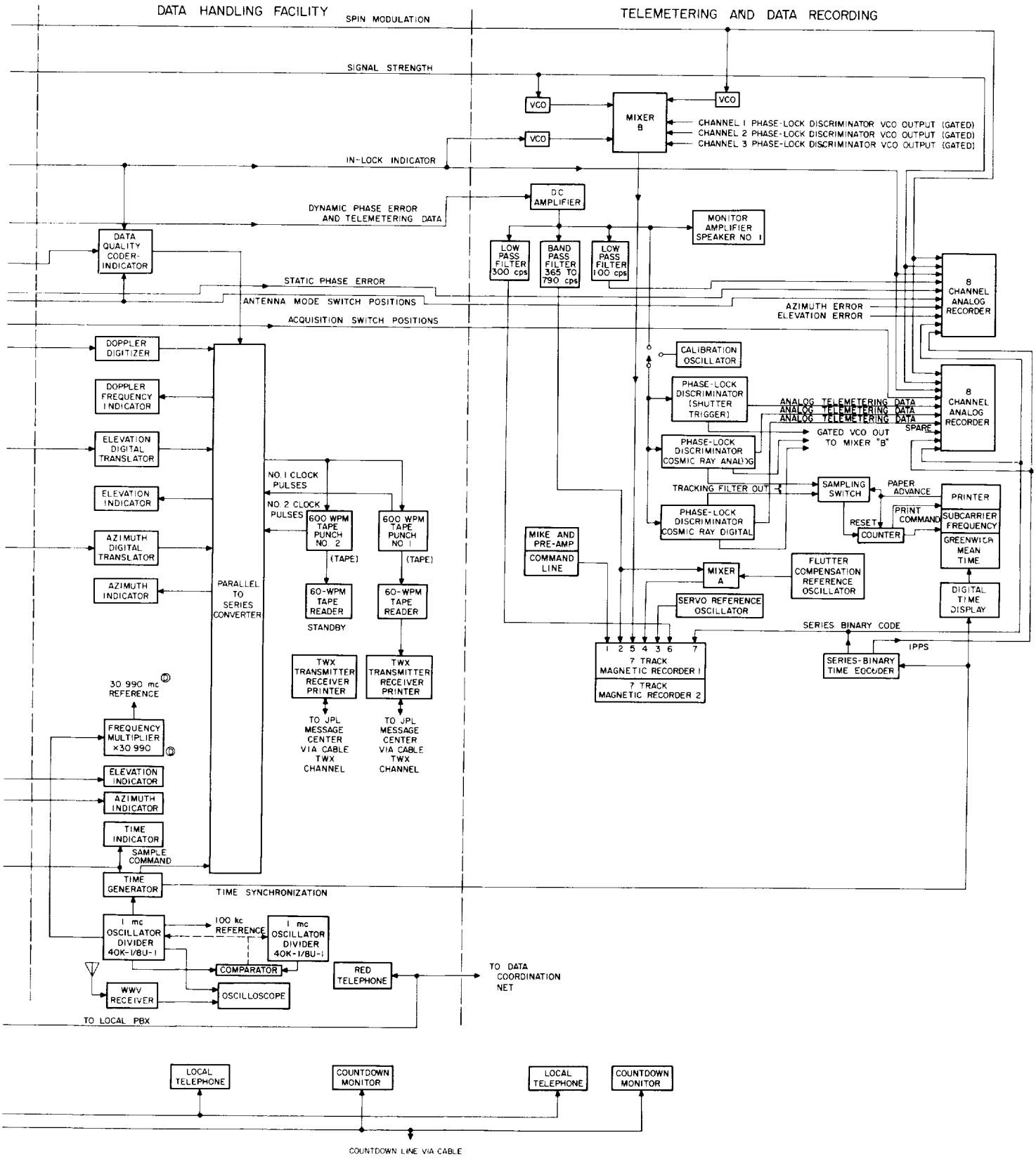

Figure 28. Functional block diagram of radio system

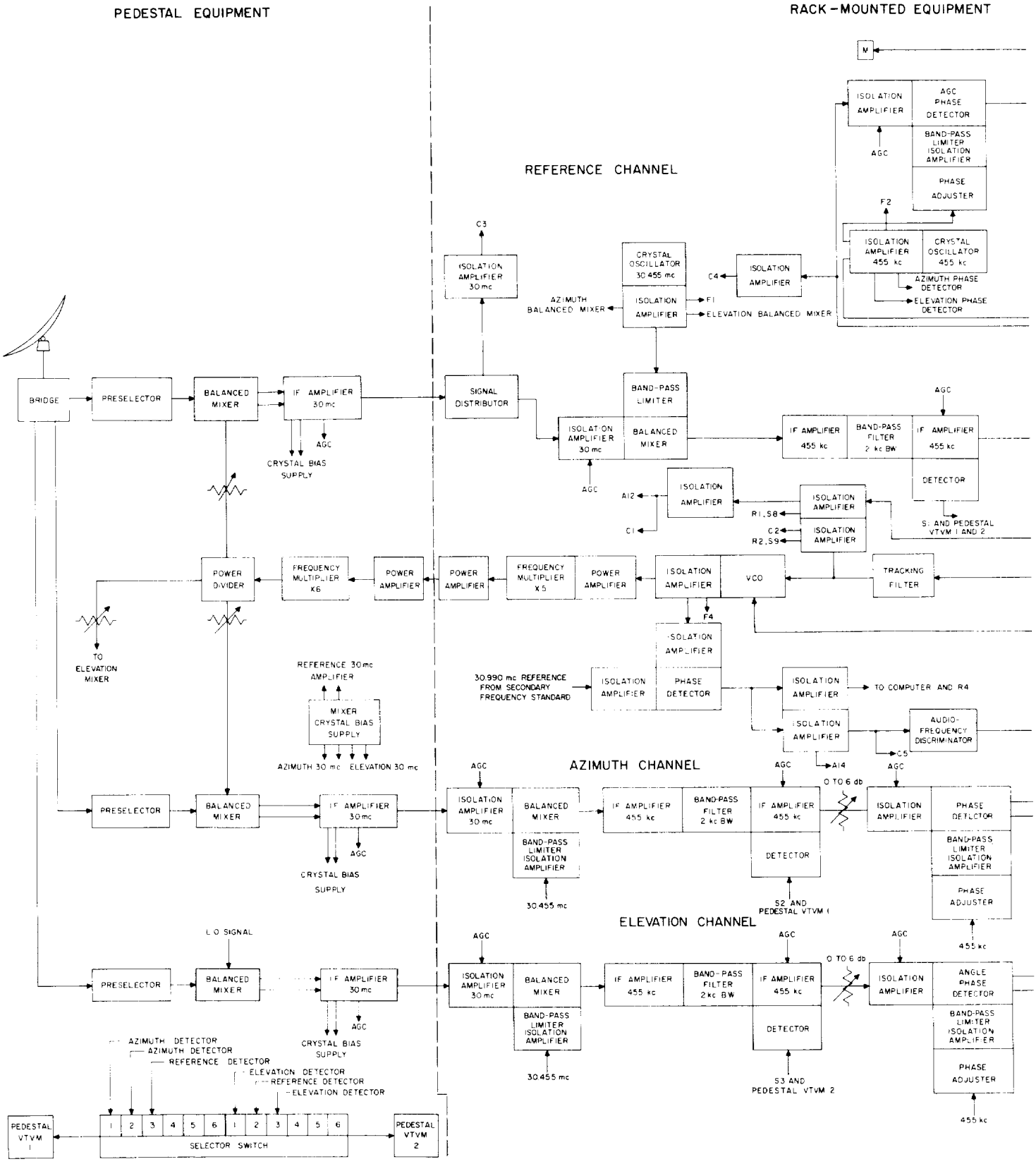
PEDESTAL EQUIPMENT
RACK-MOUNTED EQUIPMENT
REFERENCE CHANNEL
AZIMUTH CHANNEL
ELEVATION CHANNEL
BRIDGE
PRESELECTOR
BALANCED MIXER
IF AMPLIFIER 30 mc
CRYSTAL BIAS SUPPLY
AGC
SIGNAL DISTRIBUTOR
ISOLATION AMPLIFIER 30 mc
BAND-PASS LIMITER
BALANCED MIXER
IF AMPLIFIER 455 kc
BAND-PASS FILTER 2 kc BW
DETECTOR
S1 AND PEDESTAL VTVM 1 AND 2
ISOLATION AMPLIFIER
CRYSTAL OSCILLATOR 30.455 mc
AZIMUTH BALANCED MIXER
ELEVATION BALANCED MIXER
CRYSTAL OSCILLATOR 455 kc
AZIMUTH PHASE DETECTOR
ELEVATION PHASE DETECTOR
AGC PHASE DETECTOR
BAND-PASS LIMITER ISOLATION AMPLIFIER
PHASE ADJUSTER
POWER DIVIDER
FREQUENCY MULTIPLIER X6
FREQUENCY MULTIPLIER X5
POWER AMPLIFIER
VCO
TRACKING FILTER
TO ELEVATION MIXER
REFERENCE 30 mc AMPLIFIER
MIXER CRYSTAL BIAS SUPPLY
AZIMUTH 30 mc
ELEVATION 30 mc
30.990 mc REFERENCE FROM SECONDARY FREQUENCY STANDARD
PHASE DETECTOR
TO COMPUTER AND R4
AUDIO-FREQUENCY DISCRIMINATOR
0 TO 6 db
S2 AND PEDESTAL VTVM 1
S3 AND PEDESTAL VTVM 2
30.455 mc
455 kc
L.O. SIGNAL
ANGLE PHASE DETECTOR
AZIMUTH DETECTOR
REFERENCE DETECTOR
ELEVATION DETECTOR
PEDESTAL VTVM 1
PEDESTAL VTVM 2
SELECTOR SWITCH

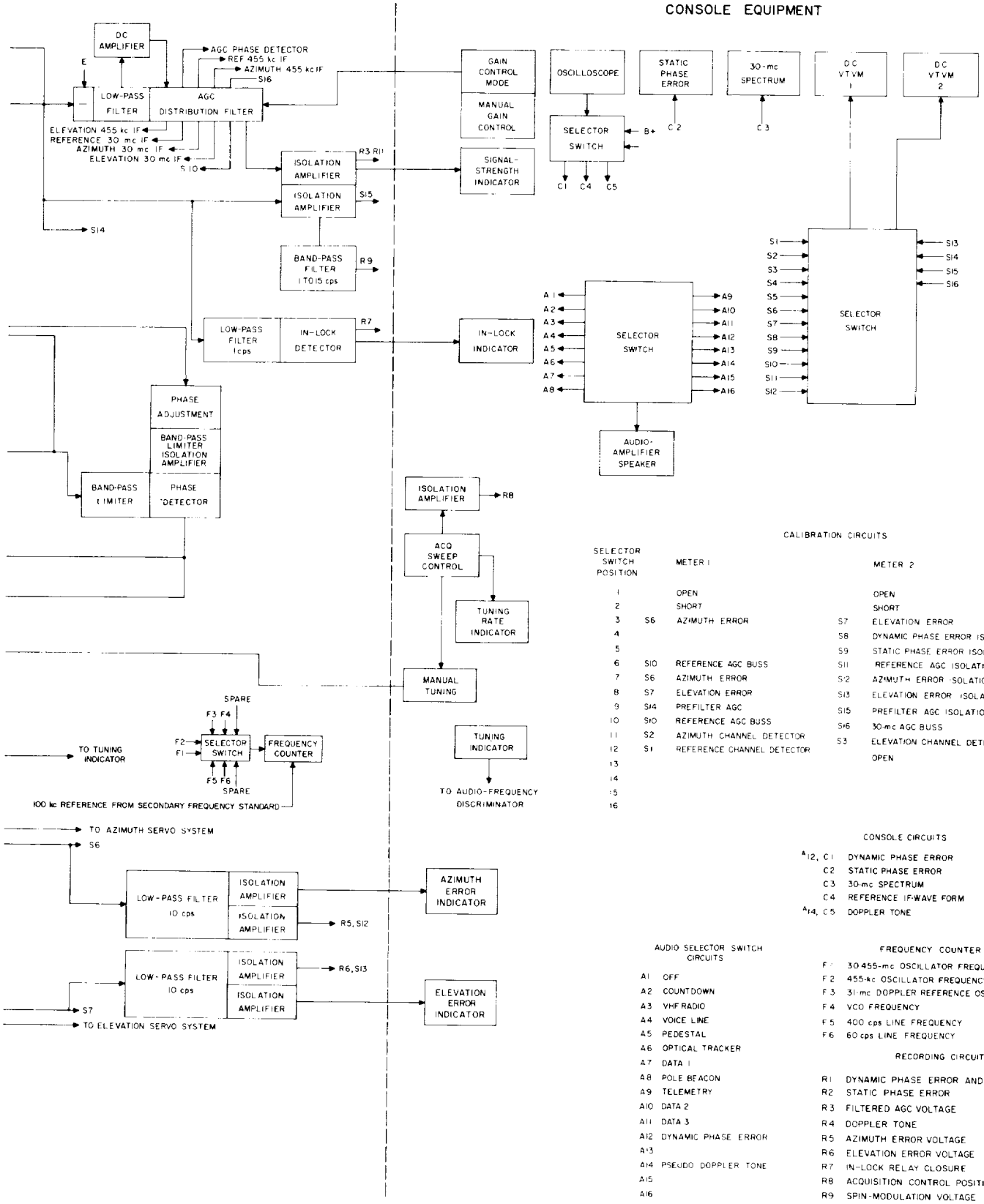

CALIBRATION CIRCUITS

SELECTOR SWITCH POSITION	METER 1		METER 2	
1		OPEN		OPEN
2		SHORT		SHORT
3	S6	AZIMUTH ERROR	S7	ELEVATION ERROR
4			S8	DYNAMIC PHASE ERROR ISOLATION AMPLIFIER
5			S9	STATIC PHASE ERROR ISOLATION AMPLIFIER
6	S10	REFERENCE AGC BUSS	S11	REFERENCE AGC ISOLATION AMPLIFIER
7	S6	AZIMUTH ERROR	S12	AZIMUTH ERROR ISOLATION AMPLIFIER
8	S7	ELEVATION ERROR	S13	ELEVATION ERROR ISOLATION AMPLIFIER
9	S14	PREFILTER AGC	S15	PREFILTER AGC ISOLATION AMPLIFIER
10	S10	REFERENCE AGC BUSS	S16	30-mc AGC BUSS
11	S2	AZIMUTH CHANNEL DETECTOR	S3	ELEVATION CHANNEL DETECTOR
12	S1	REFERENCE CHANNEL DETECTOR		OPEN
13				
14				
15				
16				

CONSOLE CIRCUITS

A12, C1	DYNAMIC PHASE ERROR
C2	STATIC PHASE ERROR
C3	30-mc SPECTRUM
C4	REFERENCE IF-WAVE FORM
A14, C5	DOPPLER TONE

AUDIO SELECTOR SWITCH CIRCUITS

A1	OFF
A2	COUNTDOWN
A3	VHF RADIO
A4	VOICE LINE
A5	PEDESTAL
A6	OPTICAL TRACKER
A7	DATA 1
A8	POLE BEACON
A9	TELEMETRY
A10	DATA 2
A11	DATA 3
A12	DYNAMIC PHASE ERROR
A13	
A14	PSEUDO DOPPLER TONE
A15	
A16	

FREQUENCY COUNTER CIRCUITS

F1	30.455-mc OSCILLATOR FREQUENCY
F2	455-kc OSCILLATOR FREQUENCY
F3	31-mc DOPPLER REFERENCE OSCILLATOR FREQUENCY
F4	VCO FREQUENCY
F5	400 cps LINE FREQUENCY
F6	60 cps LINE FREQUENCY

RECORDING CIRCUITS

R1	DYNAMIC PHASE ERROR AND TELEMETERING
R2	STATIC PHASE ERROR
R3	FILTERED AGC VOLTAGE
R4	DOPPLER TONE
R5	AZIMUTH ERROR VOLTAGE
R6	ELEVATION ERROR VOLTAGE
R7	IN-LOCK RELAY CLOSURE
R8	ACQUISITION CONTROL POSITION
R9	SPIN-MODULATION VOLTAGE

Figure 29. Block diagram of downrange radio system

lar direction associated with the corresponding error pattern.

The antenna (Fig. 34) consists of a 10-ft-diameter parabolic aluminum spinning $^3/_{16}$-in. thick with a feed assembly located at the focus (5.4 ft from the base of the antenna) and supported by a tapered central column. The feed assembly consists of four turnstile antennas mounted symmetrically on a 20-in.-diameter ground plane

Table 3. Downrange tracking station radio system parameters

Parameter	Design Value	Measured Value	Parameter	Design Value	Measured Value
Receiver noise temperature, °K (noise figure, db)	1340 (7.5)	2010 (9.0)	Receiver RF channel maximum gain (+8v AGC voltage), db	157	157
Antenna noise temperature, °K (estimated)	100 (max)	—	Dynamic signal level range, db	123	123
Receiver RF loop noise bandwidths at threshold ($2B_L$), cps			Receiver AGC loop noise bandwidths at threshold ($2B_L$), cps		
Wide bandwidth	60	73.0	Wide bandwidths	31.4	30.0[a]
Narrow bandwidth	20	15.5	Narrow bandwidths	0.2	0.2[a]
Receiver IF bandwidth (6db), kc	2.0	2.13	Receiver AGC minimum open loop gain	26.8	19.0
Receiver RF threshold signal level, dbm			Receiver AGC filter time constant, sec	0.4	0.44[a]
Wide bandwidth	−149.2	−147.0	Wide bandwidths	67	66[a]
Narrow bandwidth	−153.5	−152.0	Narrow bandwidths		
Signal-to-noise ratio in IF passband at RF threshold, db			Receiver AGC gain error for −100 dbm to −152 dbm signal level variation, db	1.0	1.12
Wide bandwidth	−15.2	−14.9	Receiver AGC signal to noise ratio at RF threshold (narrow bandwidth), db	20	20[a]
Narrow bandwidth	−19.5	−19.9	Receiver AGC reference voltage, v	−3.9	−4.1
Receiver Signal suppression factor at RF threshold			Antenna error lobe separation, deg		
Wide bandwidth	0.156	—	Azimuth	8	9.5
Narrow bandwidth	0.0936	—	Elevation	8	8.6
Receiver RF minimum open loop gain	2.96×10^5 sec	2.91×10^5 sec^{-1}	Receiver angle error gain, v/deg		
Receiver RF wide bandwidth tracking filter constants			Azimuth	1.53	1.0
$R_0 + R_1$	1.07×10^6 ohm	1.0×10^6 ohms	Elevation	1.53	1.2
R_2	750 ohms	750 ohms	Spin modulation channel noise bandwidth, cps	20	20
C	100 μf	99 μf	Carrier signal level at spin modulation thresholds (3db mod.), dbm	−135.2	−133.0[b]
Receiver RF narrow bandwidth tracking filter constants			Carrier signal level at telemetry thresholds, dbm		
$R_0 + R_1$	9.67×10^6 ohm	9.1×10^6 ohms	Channel 1	−151.2	−150.7
R_2	250 ohms	250 ohms	Channel 2	−151.2	−150.5
C	100 μf	99 μf	Channel 3	−149.2	−148.8
Reference channel antenna gain, db	+21.5	+22.0			
Maximum RF tracking range (a) +19 dbm transmitter power (b) +2.5 db transmitter antenna gain	1.78×10^5 km	1.68×10^5 km[a]			

[a]Value computed from other listed parameters.
[b]Estimated from direct-writing oscillograph record; this value may be improved upon by reducing the noise bandwidth during the data-reduction process.

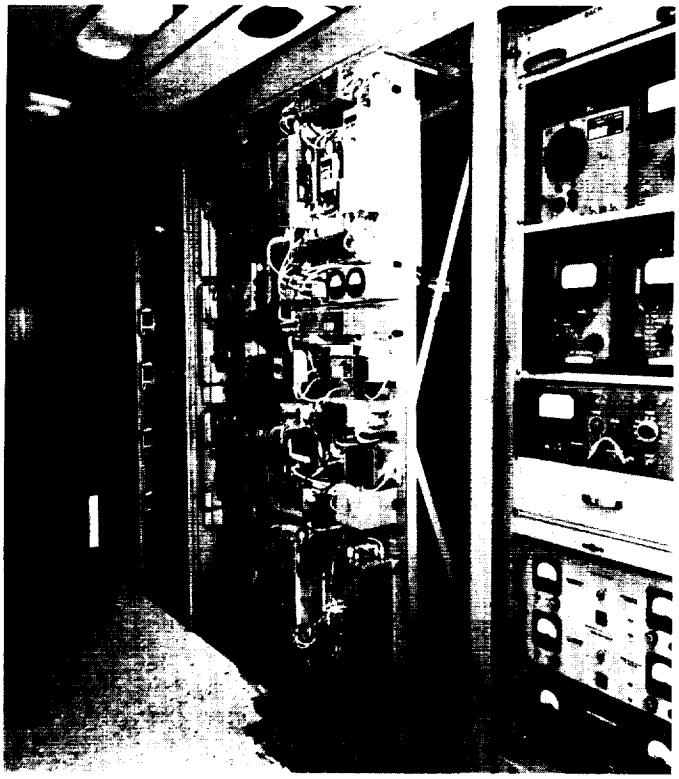

Figure 30. Front view of radio receiver plate

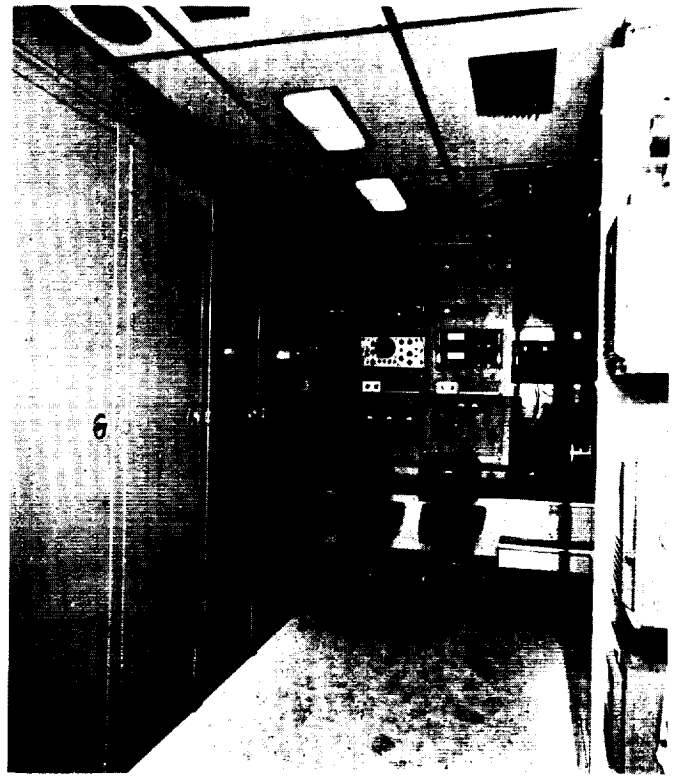

Figure 32. Interior of radio control van

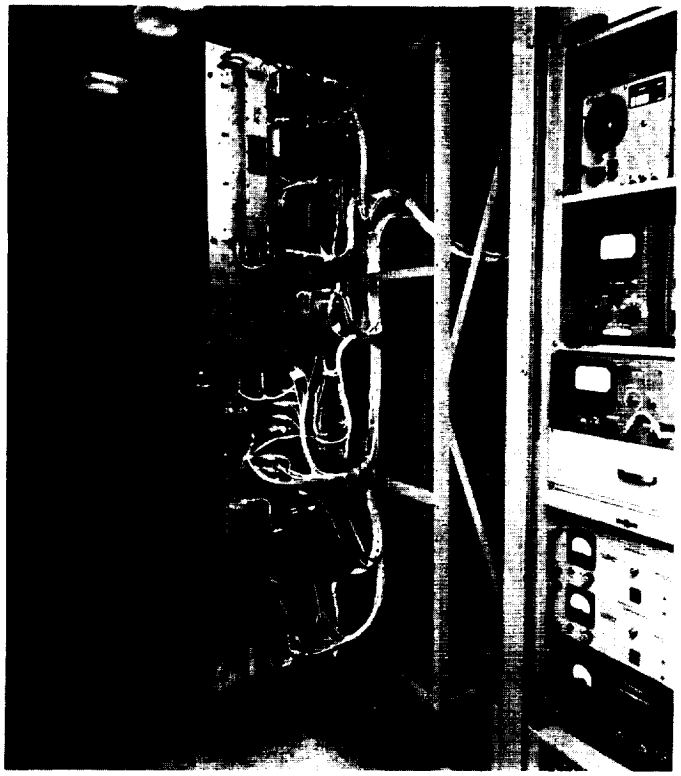

Figure 31. Rear view of radio receiver plate

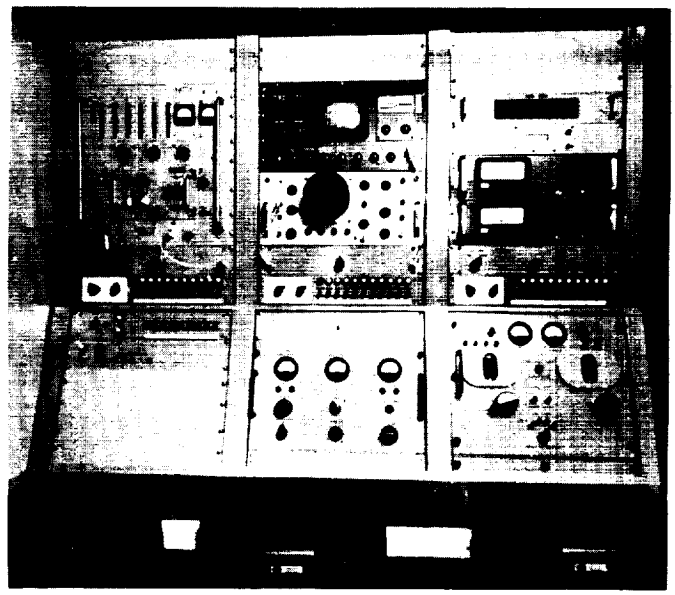

Figure 33. Control console

(Fig. 35). The turnstiles, located approximately ¼ wavelength from the ground plane, feed a coaxial rat-race bridge (Fig. 36) which produces the various pattern configurations mentioned above. The coaxial transmission

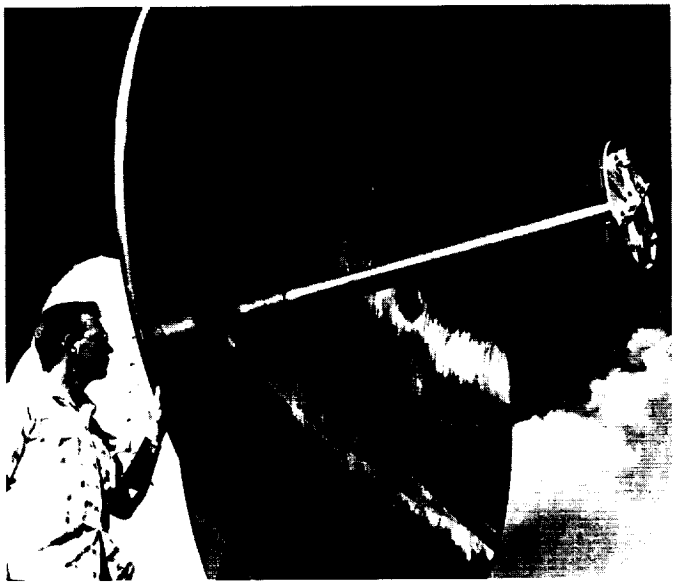

Figure 34. Downrange tracking station antenna

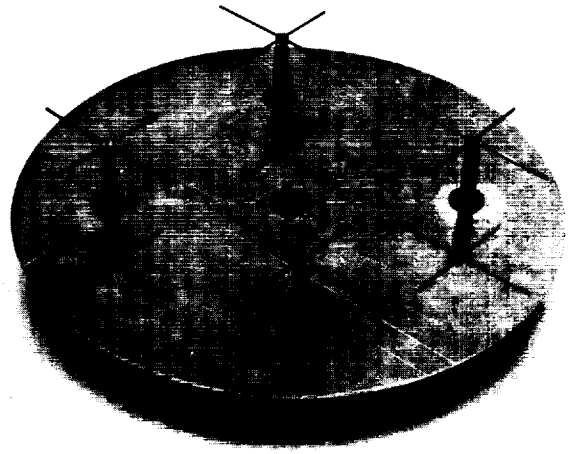

Figure 35. Prototype turnstile antenna and ground plane

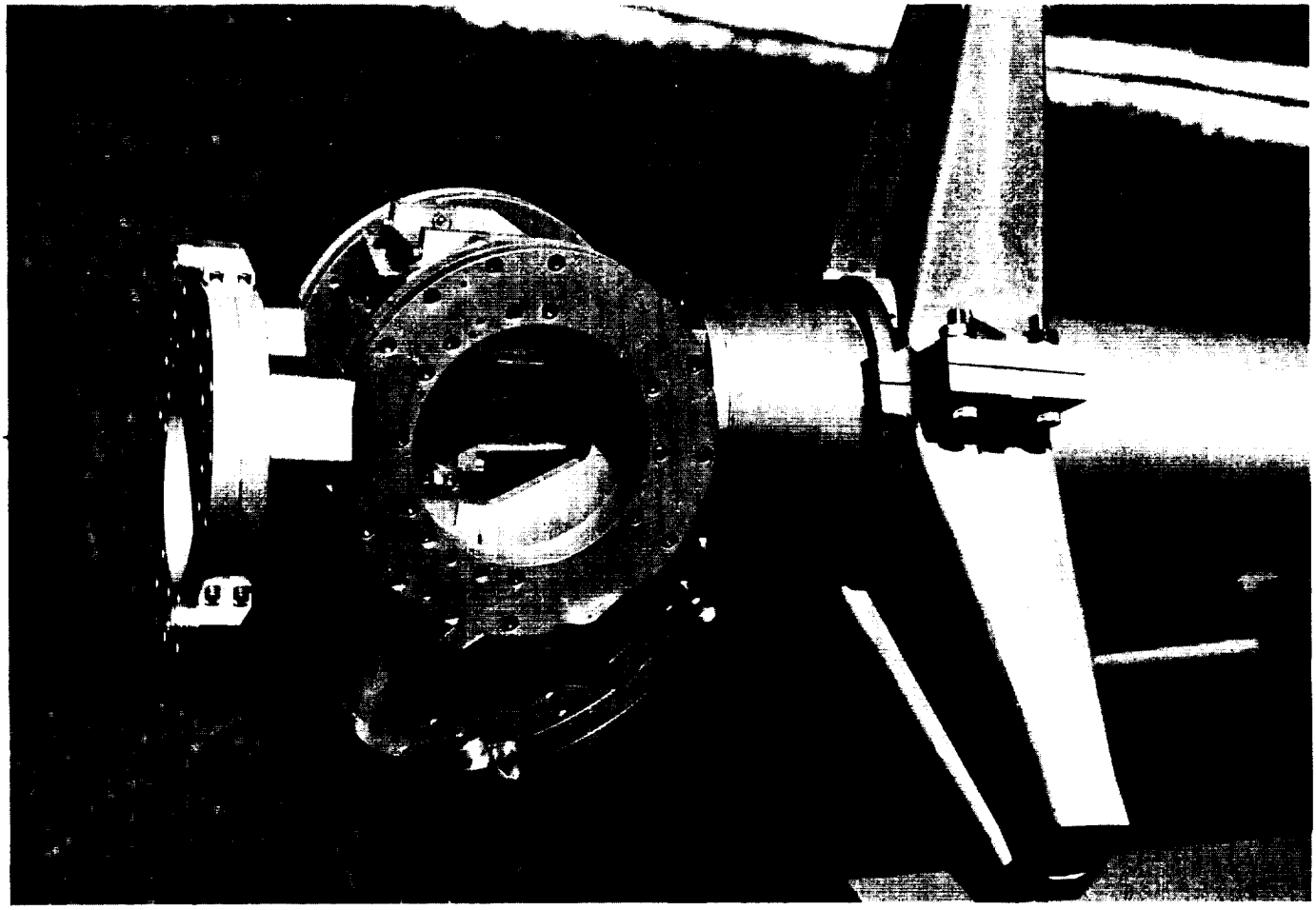

Figure 36. Coaxial ratrace bridge

lines from the turnstiles pass through the center of the support column to the bridge assembly mounted behind the antenna reflector. The bridge, supporting column, and feed were designed as an integral unit to facilitate focusing and alignment of the antenna system. Thus, rigid coaxial lines were run between the bridge and the feed elements in order to minimize the possibility of phase errors occurring between the incoming signals in the four coaxial lines.

For boresighting, evaluation of the tracking antenna, and providing an RF source for the ground station, a 78-ft portable tower with an attached 6-ft-diameter linearly polarized parabolic reflector and optical target is provided. (See Fig. 37)

To prevent excessive torques applied to the tracking antenna pedestal by winds, a protective radome enclosed the antenna and pedestal. This radome is a low-boresight shift structure fabricated from 0.018-in.-thick nylon fabric coated with hypalon, a highly abrasive-resistant, weather-sealing material. The spherical radome was 34 ft in diameter with its equator 4 ft above the floor level. This is not the optimum condition electrically, as the equatorial plane should include the antenna pedestal elevation axis. However, the smaller radome was more readily available and presented a reasonable compromise. The shape of the radome is maintained with a static pressure of 3 in. of water provided by a continuously running fan. The pressure control unit will automatically start a second fan under emergency conditions such as a damaged radome which requires extra air volume or when high winds occur and added air pressure is necessary (6 in. of water) to maintain the contour within 1 in. The radome is entered through an air lock to prevent excessive air leakage. The radome is air conditioned to maintain an inside air temperature of 75°F. and a relative humidity of 50%. To permit visual observations of the boresight target and the azimuth alignment target, several 12-in.-diameter windows of 0.005-inch-thick Mylar are placed in the radome. These windows produced no distortions; however they did reduce the resolution of the boresight optical target. This was not a serious problem as the reference telescope contained a calibrated reticle.

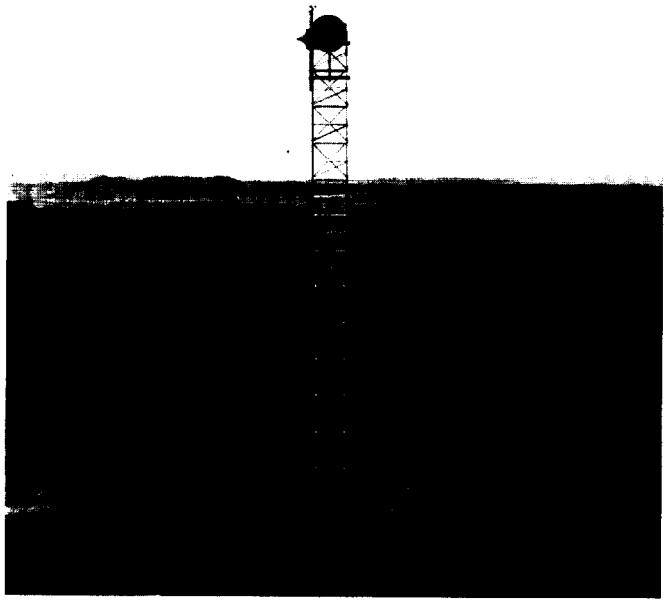

Figure 37. Portable boresight tower

Ground reflections were considered a serious problem due to the broad-beam widths and the high side lobe levels of the antenna and because of the low elevation tracking angles that were expected. Calculations indicated that without any control, a boresight shift of 0.5 deg could result with an elevation angle of 5 deg. Control of the ground reflection was only necessary in the easterly direction at the downrange site, as there was a large stand of trees to the north, and the trajectory elevation angles were large toward the southeast.

This ground-reflection control was obtained by using a series of fences, the separation of which was calculated to intercept all incoming RF energy before it could be reflected into the antenna. The fences were 8 ft high and consisted of chicken wire (which appeared as a solid ground plane at the operating frequency) topped by a foam absorber to eliminate any RF diffraction from the top edge of the fence. A 6-ft wainscotting of RF absorber was used inside the radome to help control large angle reflections in all directions. In addition, precautions were taken to locate all vans close to the building and to locate the generators, fuel tanks, and boresight tower in a nontracking zone.

The antenna pedestal was similar to that developed by the Laboratory for the CODORAC feasibility program. It consisted of a modified *Nike Ajax* antenna pedestal with a redesigned antenna reflector. The *Nike* servo system was modified to provide five modes of operation. These are automatic track, manual control, aided track, remote control, and optical track. The optical-track mode-control circuits have been incorporated in the antenna pedestal and radio-control van, but the optical tracker itself was not required for the initial series of tests.

As the signal strength from the airborne transmitter will be low at space probe ranges in excess of 20,000 miles, it was desirable to use as large an antenna reflector as possible. The results of an investigation indicated that an 8-ft-diameter reflector could be depressed to the local horizontal (a system requirement), while a 10-ft-diameter reflector would depress to approximately 9 deg. However, the system antenna gain requirements dictated that a 10-ft-diameter reflector was mandatory. This resulted in a configuration where the elevation axis was moved vertically 11 in., as shown in Fig. 38. The disadvantage of this arrangement is that the antenna reflector can be rotated through an elevation angle of only 150 deg. This prevents plunging the antenna pedestal during azimuth orientation, reference telescope orthogonalization and antenna boresighting operations.

A cable wrap-up system was incorporated so that the RF and angle-encoder signals could bypass the slip rings to eliminate any noise problem. It consists of a large circular pan attached to the base of the antenna pedestal in which is coiled the signal cables. A spring tensioning device winds the cables and switches limit the travel of the yoke to plus and minus one and a half revolutions.

A major share of the servo components are mounted in two racks located in the radio control van (Fig. 39). The rack to the left contains the required power supplies and regulators, oscilloscopes and test panel which monitors the dc voltages in the racks. The servo control rack located on the right has the azimuth and elevation mode controller plates and the miscellaneous control plate. All wires entering these racks come through a terminal drawer located at the top. Each rack has a blower at the base for cooling, the air flow being controlled by adjustable distribution baffles located on the sides.

The standard *Nike* data unit was extensively modified for use in the downrange tracking antenna pedestal. The sine-cosine potentiometer was completely removed, and an encoder was added. The potentiometer cams and switches were removed and the azimuth cable wrap-up limit switches installed. The cursor dials were re-engraved and the gear train redesigned to read in degrees rather than Army mils. An evaluation test using

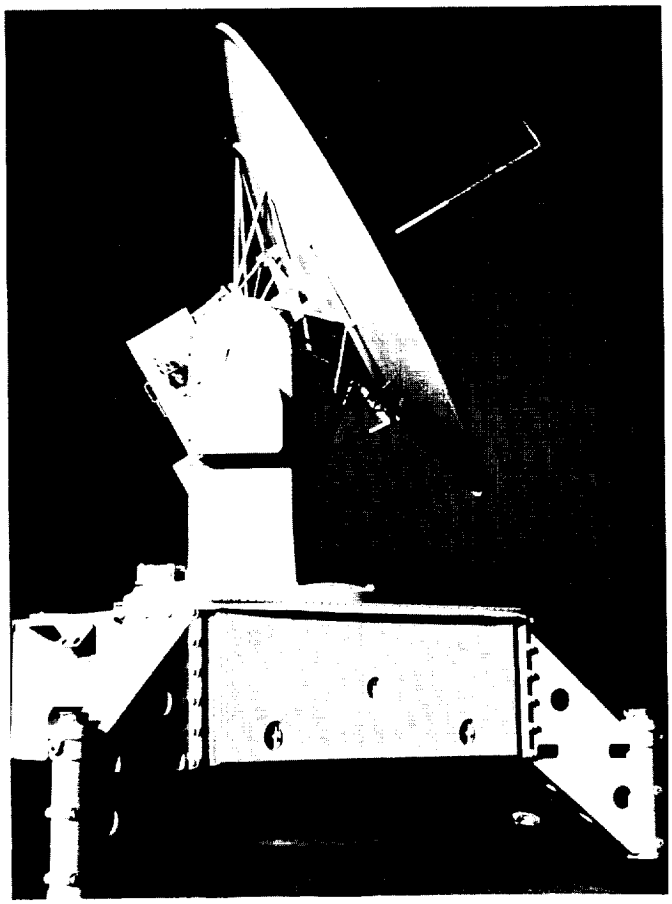

Figure 38. Downrange tracking station antenna pedestal

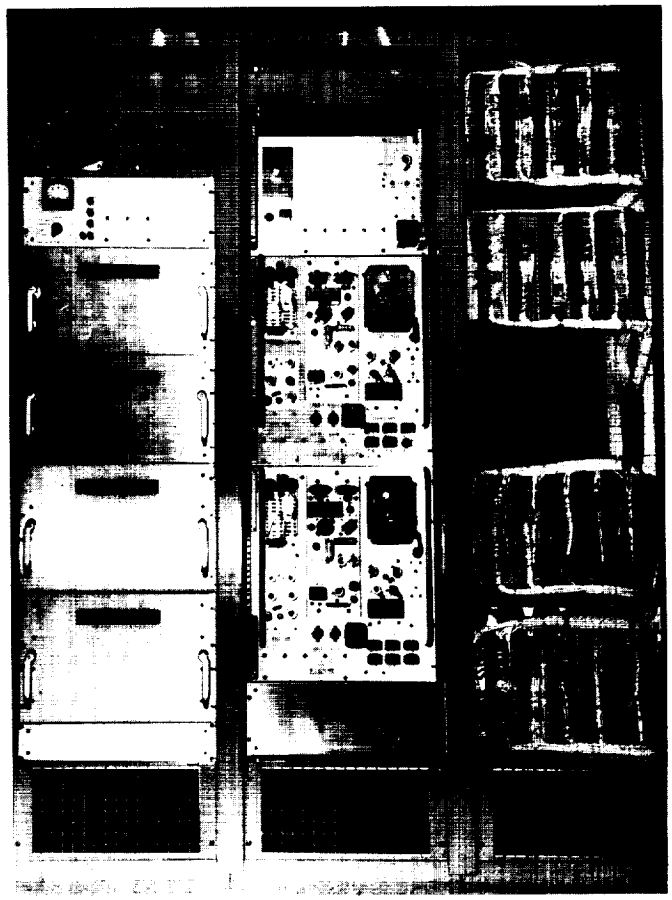

Figure 39. Servo control racks

a T-2 theodolite indicated an average bias of +0.001 deg and an rms error of 0.0037 deg in the azimuth cursor, and an average bias of +0.004 deg and an rms error of 0.0053 deg in the elevation cursor. The cursor locking clutch was also modified to insure a more positive locking action.

A new technique was used to orthogonalize the reference telescope, since the antenna pedestal cannot be plunged. A front surface mirror was attached to the elevation axis and a bracket was attached to the antenna pedestal yoke on which is mounted a Wild T-2 theodolite with an integral autocollimator attachment. Using this equipment, the reference telescope can be orthogonalized by sighting a special target which was located some distance from the antenna pedestal (Fig. 40.)

The data-handling system consists of data recording and real-time tagged transmission of angular and doppler data necessary for Goldstone acquisition. The heart of this system is a parallel-to-serial converter called a shift register. Upon a sampling command emanating from the timing system, digitalized data from several sources (Table 4) is read into the shift register. This data is in binary coded decimal (BCD) form. Each of the above words (groups of digits) is serially shifted out digit by digit into a converter matrix. The matrix converts the 4-bit BCD data to 5-bit teletype code. A high-speed punch stores the data by punching a tape at an information rate of 60 characters/sec. Clock pulses

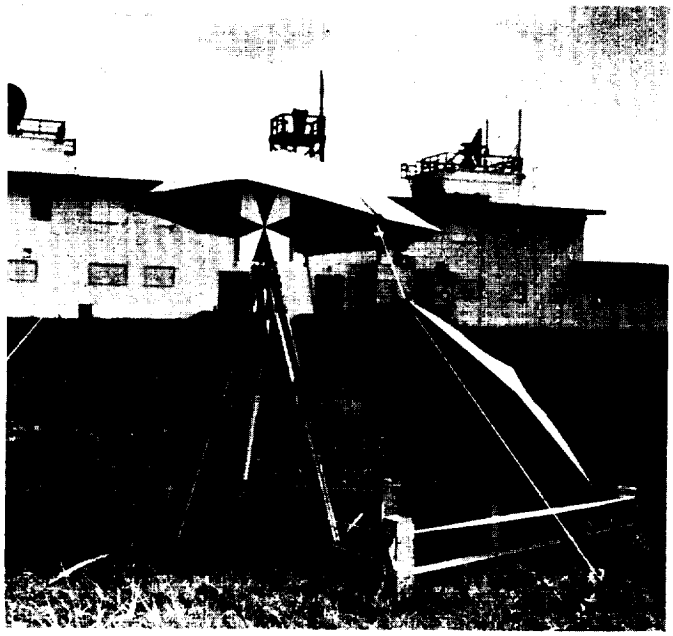

Figure 40. Orthogonalization target

Table 4. Digital data

Data	Number of Digits	Units
Station identification	1	—
Data condition	1	—
Time	6	hr-min-sec
Azimuth angle	6	decimal deg
Elevation angle	6	decimal deg
Doppler	5	cycles

generated by the high-speed punch determine the rate at which the data is serialized out of the shift register. This ensures synchronism between the electronic data readout and the punch actuation.

The data-condition indication is derived from a weighted binary code and indicates the conditions in the following tabulation:

RF lock ..... in or out
Tracking mode ..... auto or other
Good-bad switch position ..... good or bad data

The good-bad switch is manually operated to provide human judgment when data is questionable, such as intermittent RF lock between sample commands.

A 1-mc oscillator, which has a long time stability of 1 part in 10^8 per 24 hrs is used to generate time information. A working standby oscillator, periodically adjusted by means of a frequency comparator to the frequency of the oscillator in use, is available as a secondary timing source. Daily adjustments are made on the oscillator in use with WWV as a reference. The oscillator output with appropriate counters is used to provide the binary coded time in hours, minutes, and seconds which is read into the shift register.

Angular encoding is achieved with photoengraved discs geared to the antenna pedestal axes. Stationary brushes riding over conducting and nonconducting segments of the discs resolve the disc into 2000 quanta or counts. With a 45:1 gear increase, the resolution is increased to 90,000 quanta. Another disc (similar to coarse-fine synchros) keeps track of the revolutions of the 2000 count disc. Assuming perfect gearing, the encoder accuracy is ±1 count per 90,000 counts or ±0.004 deg out of 360 deg.

A doppler counter counts the number of cycles of received doppler for a period of 1 sec. Counting begins ½ sec before time and angular information is sampled and therefore can be considered an average doppler

frequency. The 1-mc oscillator frequency is multiplied to 30.99 mc by a modified Gertsch frequency multiplier to obtain a doppler reference which transmitted to the radio van. This doppler reference is 10,000 cps below the frequency associated with the zero radial velocity vector and eliminates the requirement of polarity sensing by the doppler counter. The inherent inaccuracy of the doppler is ± 1 count, which could be minimized by increasing the frequency at which doppler information is compared with the doppler reference.

As mentioned previously, the serialized output of the shift register is stored on punched tape. A transmitter distributor, commonly referred to as a reader, converts the punched tape to electric signals for transmission. The punch tape information is read at 6 characters/sec or at $^1/_{10}$ the maximum punch rate. By proper patching, the output of the reader may be sent on hard lines to distant teletype equipment and/or monitored by the local teletype machines (Fig. 41). The output of the code converter in the shift register is channeled in parallel to two punches (far right rack in Fig. 42), reader and teletype equipment combinations, one acting as the backup for the other.

Figure 41. Data handling van teletype communication machines

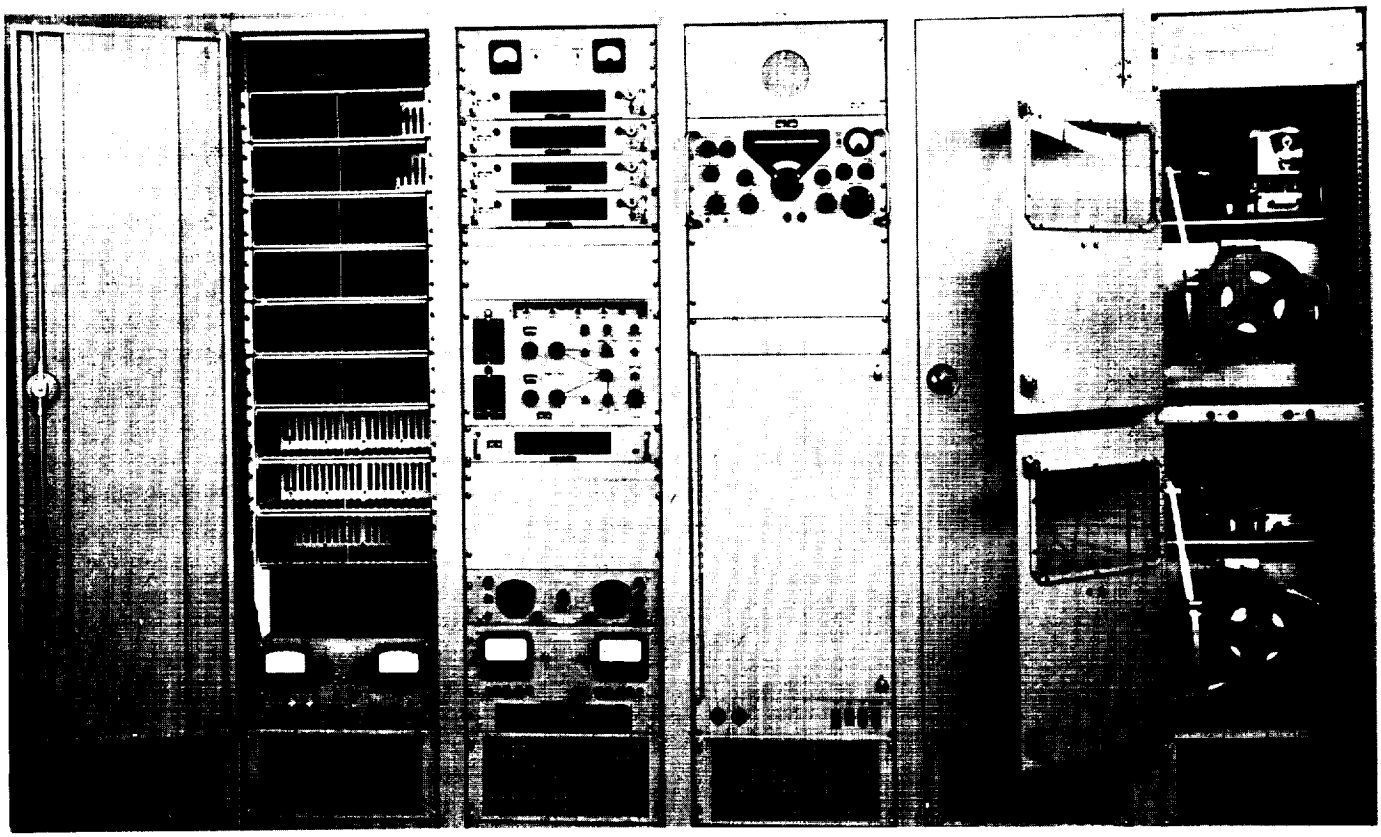

Figure 42. Data handling van equipment racks

The teletype system is used to transmit data to the computer and to receive prediction data in return; the teletype system is also being used for administrative communication. During the actual tracking operation a telephone system tying all stations together is referred to as the "red net" and serves as a backup for data transmission.

Visual displays receive inputs from the storage portions of the shift register and display in decimal form the following information:

1. Time in hours, minutes, and seconds, with the presentation changing every second.
2. Angular position of the antenna in increments of 0.004 deg.
3. Doppler count in increments of 1 cps.

The angular position and doppler-count information is held between samples such that it is associated with the previous sample.

The telemetering and data-recording portion of the downrange tracking station is mounted entirely in nine standard relay racks housed in a van (Fig. 43). All input signals are routed through a centrally located patch bay which permits monitoring and/or switching of all data channels. The system includes 14 tracks of magnetic tape recording, 16 traces of oscillographic analog recording, 3 channels of phase-locked-loop discriminators, and a provision for timed digital sampling of analog measurements.

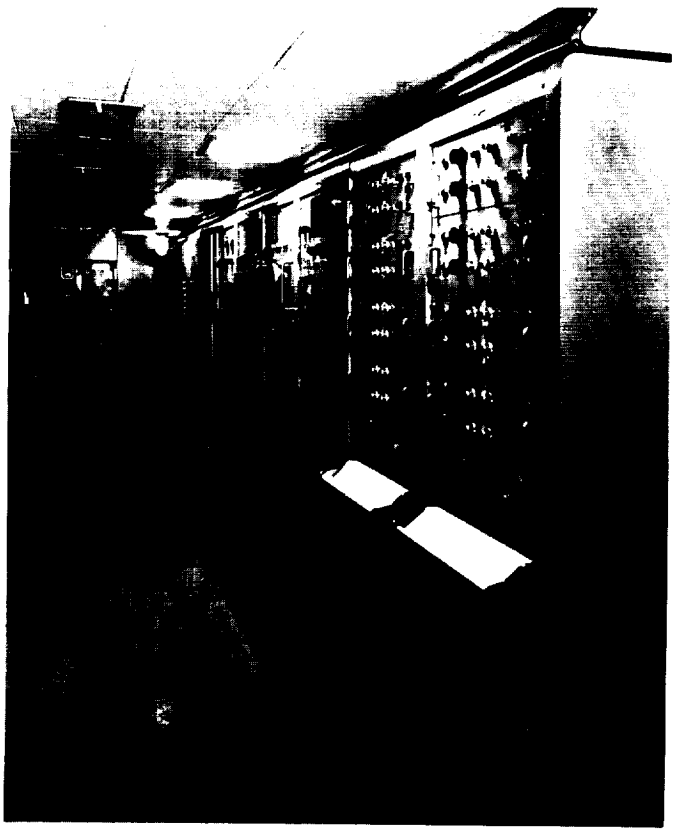

Figure 43. Interior of telemetering van

The two Ampex magnetic tape recorders are normally operated with parallel inputs. The tape speed is 1⅞ in./sec (with an accuracy of ±0.25%) which permits recording continuously for 8.5 hr. The average cumulative flutter (nominal) is 0.8% peak-to-peak. There are five direct record tracks having the characteristics as listed in the following tabulation:

Dynamic range	50 db
Optimum input level	1.0 volt rms
Input impedance	100,000 ohms (unbalanced to ground)
Frequency response	30 to 3500 cps
Output level	1 v rms nominal (across 10,000 ohm load)
Output impedance	125 ohms (unbalanced to ground)

In addition, there are two frequency-modulated tracks having the characteristics as listed in the following tabulation:

Input range	± 1.4 volts peak
Input impedance	100,000 ohms (unbalanced to ground)
Frequency response	0 to 312 cps
Output level	±1.4 volts peak
Output impedance	125 ohms (unbalanced to ground)

The two direct-writing oscillographic recording systems consist of an 8-channel Sanborn recorder with dc amplifiers. The 16 in.-wide paper has a speed of 1 mm/sec, thereby permitting recording continuously for 16½ hr. The input sensitivity is 0.1 to 100 v/cm with a frequency range of 0 to 50 cps. The stability is good; drift after warmup is less than 0.5 mm/hr.

The magnetic tape channel assignments are listed in Table 5, while those of the Sanborn recorder are shown in Table 6.

Digital data recording equipment incorporates a Hewlett-Packard digital printer and electronic counter and an 8-position sampling switch. Sampling rate and switch advance rate are coupled and can be varied from a 5 per sec readout 0.1 sec count period to a 3 per min 10 sec count period. The digital printer presentation includes Greenwich Mean Time in seconds and data

Table 5. Magnetic tape track assignments

Track No.	Type	Assignment
1	direct record	voice signals, local command line, countdown, and voice labeling
2	direct record	composite telemetering signal
3	direct record	playback servo reference signal
4	direct record	mixed composite telemetering signal and flutter compensation reference oscillator signal
5	direct record	mixed VCO signals (a) gated channel 1 telemetering discriminator tracking VCO output (b) gated channel 2 telemetering discriminator tracking VCO output (c) gated channel 3 telemetering discriminator tracking VCO output (d) RDB* channel 4 voltage-controlled oscillator modulated by receiver acquisition in-lock indicator (e) RDB channel 5 voltage-controlled oscillator modulated by signal strength (f) RDB channel 6 voltage-controlled oscillator modulated by the spin-modulation signal
6	frequency modulation	receiver dynamic phase error
7	frequency modulation	encoded Greenwich Mean Time

*Research and Development Board.

Table 6. Oscillograph trace assignments

Trace No.	Assignment
A1	Receiver acquisition in-lock indicator
A2	channel 1 telemetering analog data
A3	channel 2 telemetering analog data
A4	channel 3 telemetering analog data
A5	receiver signal strength
A6	spin modulation
A7	acquisition-switch position
A8	unused
Dynamic 1A	encoded Greenwich Mean Time
Dynamic 2A	1 pulse/sec
B1	receiver signal strength
B2	spin modulation
B3	acquisition in-lock indicator
B4	static phase error
B5	mode selector switch position
B6	azimuth servo error
B7	elevation servo error
B8	dynamic phase error
Dynamic 1B	encoded Greenwich Mean Time
Dynamic 2B	1 pulse/sec

frequency count to four significant places of telemetering channels 1 and 2.

All time signals used in the recording van are derived from the 1 pulse/sec signal from the precision time standard located in the data-handling van. This signal operates a sensitive relay to key the 1 pulse/sec dynamic reference trace on the Sanborn recorder. Time recorded on the digital printer is provided by an UED digital clock. Encoded time used for magnetic tape recording and time labeling of the oscillographic records is provided by a serial reading pulse width time encoder designed and fabricated by Collins Radio Company.

Data conditioning equipment includes filters, isolation and balancing (biasing) circuits, and balanced line to single-ended input circuits necessary to feed signals to the recording equipment.

Three Hallamore discriminators have been modified by the Laboratory for use as phase-locked-loop subcarrier discriminators. These discriminators have the characteristics listed in Table 7. In addition, each discriminator can be switched to operate at 0.5, 2, 4, or 8 times this bandwidth. Each discriminator has an input impedance of 20,000 ohms, a power consumption of approximately 60 watts, and a sensitivity (minimum signal plus noise) of 50 mv peak-to-peak. The output capability (for +7.5% deviation) is ±6.6 to ±30 v with a linearity of better than 0.5% of full bandwidth. The out-of-lock indication is a small amplitude 60-cps signal superimposed on the dc output level. A manual sweep over the entire bandwidth is used for acquisition. The static phase error is monitored on the meter panel for a null adjust with the acquisition voltage.

E. Design Philosophy of a Deep Space Station

The configuration of the tracking and communications network derived from the *Juno IIA* mission requirements has been discussed in the preceding sections. It is evident that one of the stations in the network (the Goldstone station) must be capable of receiving and tracking the output of a low-power transmitter to a considerable

Table 7. Phase-locked-loop subcarrier discriminator characteristics

Item	Channel		
	1	2	3
Center frequency, cps	400	560	730
Channel (limiter) bandwidth, cps	60	84	110
Loop noise bandwidth ($2B_L$) at threshold, cps	4	4	8
Noise-to-signal (N/S) ratio in channel bandwidth at threshold	6 (7.8 db)	8.4 (9.2 db)	5.5 (7.4 db)
Limiter suppression factor at threshold	0.340	0.292	0.353
Minimum signal-to-noise (S/N) ratio at discriminator output at threshold, db	20	20	20

distance, by conventional standards, and it should therefore be designed as a sensible step toward a true deep space tracking and communication station. This brings the discussion back to what was described in the introduction to this Section as the secondary design objective of the tracking network. As in other phases of the *Juno II* program, it was desired to build experience and facilities in the tracking and communications areas which would be a proper basis for further, more advanced space probe experiments. In order to pursue this objective to the extent of the means at our disposal, consideration was given to the extrapolated capabilities of the system design which was evolving for the *Juno II* network.

The two major questions which must be answered in the design of a communications system for extreme range applications are the following: What is the operating frequency? What is the size of the ground antenna? Because the electronic equipment and antenna installations can be quite expensive, it is well worth while to delineate the assumptions and technical limitations which determine the communication system that should be used.

1. Received Power

The transmitter in the space vehicle produces a signal power P_t limited by the efficiency of the transmitter and the weight of the vehicle electrical power supply. This power can be beamed in the direction of the earth receiver, the beaming action resulting in an effective concentration or gain, G_t, of the signal power relative to radiation uniformly into space. If the vehicle's attitude cannot be controlled or if the vehicle's antenna cannot be pointed accurately enough, the amount of possible beaming is limited. For example, if the vehicle might tumble and roll violently, it is necessary to radiate uniformly into space, and hence, G_t is close to unity. The early satellites were in this category, i.e., the vehicle antennas were said to be gain limited.

Within a short time, however, space vehicles will be considerably different. Satellites will be controlled to have one side facing the surface of the earth, and lunar and interplanetary vehicles will certainly have sufficient stabilization to keep antennas pointed roughly in the direction of the earth (several degrees pointing accuracy). Such is already the case in the spin-stabilized lunar probes (two axes stabilization). Stabilization accurate to a few degrees about three axes will soon be achieved; antenna beamwidths of a few square degrees solid angle could thus be utilized. Such narrow beamwidths are produced practically only by using significant physical antenna area. Under these conditions, it is preferable to talk in terms of effective antenna size or area, A_t, rather than in terms of gain. The relation between gain and area is given by the identity:

$$G = 4\pi A/\lambda^2$$

where λ is the wavelength of the transmitted signal. It is evident that if the wavelength is too great (the frequency too low), it will be very difficult to achieve appreciable gain (a factor of 100, for example) without building a very sizeable antenna. For frequencies of interest and for vehicles available for some years to come, the area of the vehicle antenna is considered to be the principal limiting factor in achieving signal beaming.

If the beamed signal power is intercepted at a distance r with an earth antenna of area A_r, the received power is given by

$$P_r = G_t P_t A_r/4\pi r^2$$

The maximum effective area of the earth antenna, however, is limited by manufacturing tolerances which must be of the order of a small fraction of a wavelength of the received signal. Antennas for extreme sensitivity applications are built as large as manufacturing tolerances (i.e., reasonable expense) will permit. The 200-in. astronomical telescope at Mount Palomar is about as large as optical tolerances will permit; a larger size large as optical tolerances will permit; a large size would not produce stronger images but might even pro-

duce differential cancellation. Radio telescopes are faced with the same problem but scaled in frequency. The diameter of the earth antenna is directly proportional to the wavelength of the received signal: by using manufacturing tolerances of 1:4000 an 85-ft parabola may be used for frequencies up to about 1500 mc; a 250-ft parabola with the same fractional tolerance may be used to about 500 mc. The earth antenna, therefore, is gain limited, whereas the vehicle antenna, for the time being at least, is area limited. Using the same relation between gain and area for the earth antenna as was used for the vehicle antenna, the received power is therefore given by:

$$P_r = A_t P_t G_r / 4\pi r^2$$

The conclusions are perhaps unexpected:

1. The received power is not a function of frequency, to first order.
2. The received power is not a function of the size of the ground antenna, only of antenna gain; hence, a smaller antenna operating at a higher frequency is equivalent to a larger antenna at a lower frequency.
3. Evidently both frequency and earth antenna size must be determined from other considerations.
4. The received power is a direct function of the size of the vehicle antenna.

2. Propagation Effects

The previous section on received power resulted in an open choice of frequency. The choice can be narrowed somewhat by choosing frequencies which are not seriously affected by the ionosphere (above 100 mc) nor by the atmosphere (below about 10,000 mc).

3. Interference

Virtually every known source of radio interference decreases with increasing frequency. Manmade interference decreases because of less usage of the higher frequencies, greater difficulty of generation of power at higher frequencies, greater propagation loss at higher frequencies if line-of-sight is denied and greater beaming of high-frequency energy tending to permit much better control of interference by site selection.

Of particular importance to space communications is the decrease in brightness temperature of the galaxy with frequency. As low-noise solid-state amplifiers come into use and reduce the effects of internal receiver noise, the principal limitation becomes the antenna temperature which in turn is determined by galactic noise and by the Earth's black body radiation into the antenna side lobes. An effective receiver temperature of 40°K may well be achievable at a frequency of 1500 mc. The pronounced increase in interference below 500 mc will seriously limit the growth potential of any space communication technique using lower frequencies.

Galactic interference is not uniformly distributed across the heavens. By far the largest source of interference lies along the Milky Way or galactic center in a band approximately 15 deg wide lying near the possible destinations and orbits of space vehicles. To reject this interference, two steps are possible: use antennas of beamwidths of a few degrees at most, and use the highest frequencies that are practical. By coincidence, a fraction of a degree also represents the minimum beamwidth that can be achieved without expensive manufacturing techniques. In other words, a gain-limited Earth antenna is a practical solution to the problem of rejecting galactic noise.

4. Practical Electronics

At the time that satellites were first planned, practical electronics considerations restricted the choice of frequency to below 200 mc. The satellites were very low-weight devices, power was at a premuim, and the only highly efficient transmitters were transistorized. At that time, transistor transmitters above 200 mc were not available. In addition, receivers of low noise figure were not available at frequencies beyond a few hundred megacycles.

The changes in practical electronics since 1954 are noteworthy. An efficient transmitter at 1000 mc is being used in the *Juno II* lunar probe; transistor techniques are used in all but the last stage, which the state-of-the-art will shortly transistorize as well. Extremely low-noise-figure receivers of the parametric and solid-state maser variety are making possible sensitive reception at UHF and microwave frequencies. Solar energy converters are being developed which will make possible transmitters with 10 to 100 watt capability at UHF and microwave frequencies. These new devices are pushing the state-of-the-art at the present time; by the time that interplanetary vehicles are launched, the devices will be nearly commercial. Another development of signficance in space communications is the technique of phase-locked receivers for extreme sensitivity and narrow bandwidth reception at frequencies from 100 to 20,000 mc. The technique, used by JPL in the Microlock (108 mc) and the CODORAC (10,000 mc), permits use of receiver bandwidths significantly smaller than the doppler shift expected from space vehicles.

Under the present severe weight and power limitations, it is difficult to generate stable signal power effi-

ciently at frequencies much above 1000 mc. Within a short time this upper frequency limit will extend to 2000 mc. However, with the development of heavier vehicles and solar-energy converters, this restriction will be removed, for it will then be possible to move into a new power class (10 to 100 watts) which is too far beyond the present horizons for solid-state devices. In this case microwave tubes of better than 10% efficiency will be utilized, and the useable space communications frequency range will again extend upward to 10,000 mc.

5. Practical Mechanics

Space vehicles at lunar distances and beyond will resemble fixed radio sources in the heavens—at least to the communicator. To an earth observer, the greatest components of apparent motion of the vehicle will be due to the rotation of the earth. In order to keep in continuous touch with the vehicle of the future, a network of listening posts must therefore be established around the earth, each post transferring its position data to the next. By all odds the simplest coordinate system to work in for such a problem is the astronomical or celestial system; the simplest, most reliable, and potentially the most accurate mounting system for the antenna to accept and generate celestial coordinates is believed to be the sidereal mount, almost universally used for optical astronomy. The drive system is also simple: a constant-speed motor. The other possibility, an azimuth-elevation mount, must be operated by conversion devices from a sidereal system. For the space communication problem, therefore, a sidereal mount is preferable if it can be built.

Because of a required set of counterweights in the sidereal mount, it is presently not feasible to build a sidereal mounting for an antenna which exceeds 140 ft. in diameter (NAS telescope planned). A very good sidereal mount has been designed and built, however, for an 85-ft diameter.

Mechanics (and cost) thus also tend to demand smaller earth antennas and consequently higher frequency. Using gain-limited design with the parabola diameter determined by a preference for sidereal mounting, a frequency above 1000 mc is preferred.

Mechanics also determine the maximum frequency which should be used. Vehicle antenna area has been shown to be an important parameter, at least until the vehicle antennas also become gain limited. It is important that the growth potential of vehicle antenna area not be jeopardized by selecting a frequency so high that the larger areas are of no value. For example, a 10,000-mc rigid vehicle antenna would be gain limited at a 12-ft diameter; however, reasonably accurate (1:2000) inflatable antennas to at least 20 ft in diameter appear achievable. To use the 20-ft-diameter efficiently, the frequency should not exceed 3000 mc. If still larger antennas of suitable accuracy can be developed, the upper frequency should be decreased.

6. Capabilities of the Indicated System to Meet Requirements Beyond the *Juno II* Program

A multiple station network consisting of 85-ft-diameter antennas has an extremely broad capability. It not only provides adequate performance early in the program when vehicle antennas are gain limited, but it also provides capabilities for the long-term space program which are very satisfactory. Table 8 shows predicted long-term capability. If it is desired to limit the range to only 400 million miles, this system is capable of providing a vehicle link operating with a 3-kc bandwidth in 1962.

Table 8. Long-term system capabilities

Characteristics	1958	1960	1962
Transmitter power, watts	0.1	10	100
Vehicle antenna gain, db	3	16	36
Receiver sensitivity:			
Noise temperature, °K	2000	400	40
Bandwidth, cps	30	30	30
Earth vehicle range for 10 db S/N ratio, miles	400,000	40 million	4 billion

A 20-ft-diameter reflector is necessary to provide the 36-db gain indicated for 1962 (operating frequency of 1500 mc). From the equations in Sec. IV-E-1, this same dish size is required regardless of the size of the ground antenna. It is obvious, therefore, that the communication system design and capability is directly dependent upon the vehicle and that this situation will remain so for many years. It is perhaps unfortunate that a larger ground antenna will not help to overcome this situation.

Conclusions:

1. A consistent space communications system can be built using frequencies between 1000 and 2000 mc. A gain-limited earth antenna, of about 85 ft in diameter and area-limited vehicle antennas should be used.
2. The penalties in using lower frequencies are increased Earth antenna size and increased galactic interference.
3. The penalty in using higher frequencies is the limitation on the useable vehicle antenna area.
4. The indicated system is sufficient for space communication from satellites of the Earth and lunar probes to deep interplanetary travel.

F. The Goldstone Tracking Station

A description of the Goldstone facility (Fig. 44) should provide an idea of the size and degree of complexity of a station in the *Pioneer III* and *IV* network. Except for the difference in antenna size and the relative permanency of the Goldstone Station, the Puerto Rico installation was very similar. In particular, identical electronic equipment was installed at the two stations whenever feasible. Elements of the station are shown in Fig. 45.

The antenna is 85 ft in diameter and is equatorially mounted. Significant parameters of the structure are:

1. Maximum tracking rate, 1 deg/sec in both axes.
2. Maximum acceleration, 5 deg/sec^2.
3. Reflecting surface accuracy, ¼ in.
4. Coverages, ±6 hr in hour angle from +90 to 50 deg declination.
5. Operation with good accuracy to 45 mph wind velocity, can survive 87 mph in any position and 120 mph in stowed position.
6. Accuracy of structure (constancy of axes alignment, etc.), an order of 1 min of arc.

The antenna uses a high-pressure hydraulic drive system. The reasons for the choice of a hydraulic system are that electrical interference problems with the sensitive receiving equipment are minimized and the rotating inertia of the drive is less than with electrical systems of comparable capacity. The system was made to have 2 speeds of operation, a high speed of 1 deg/sec for satellite tracking and a low speed capable of tracking the

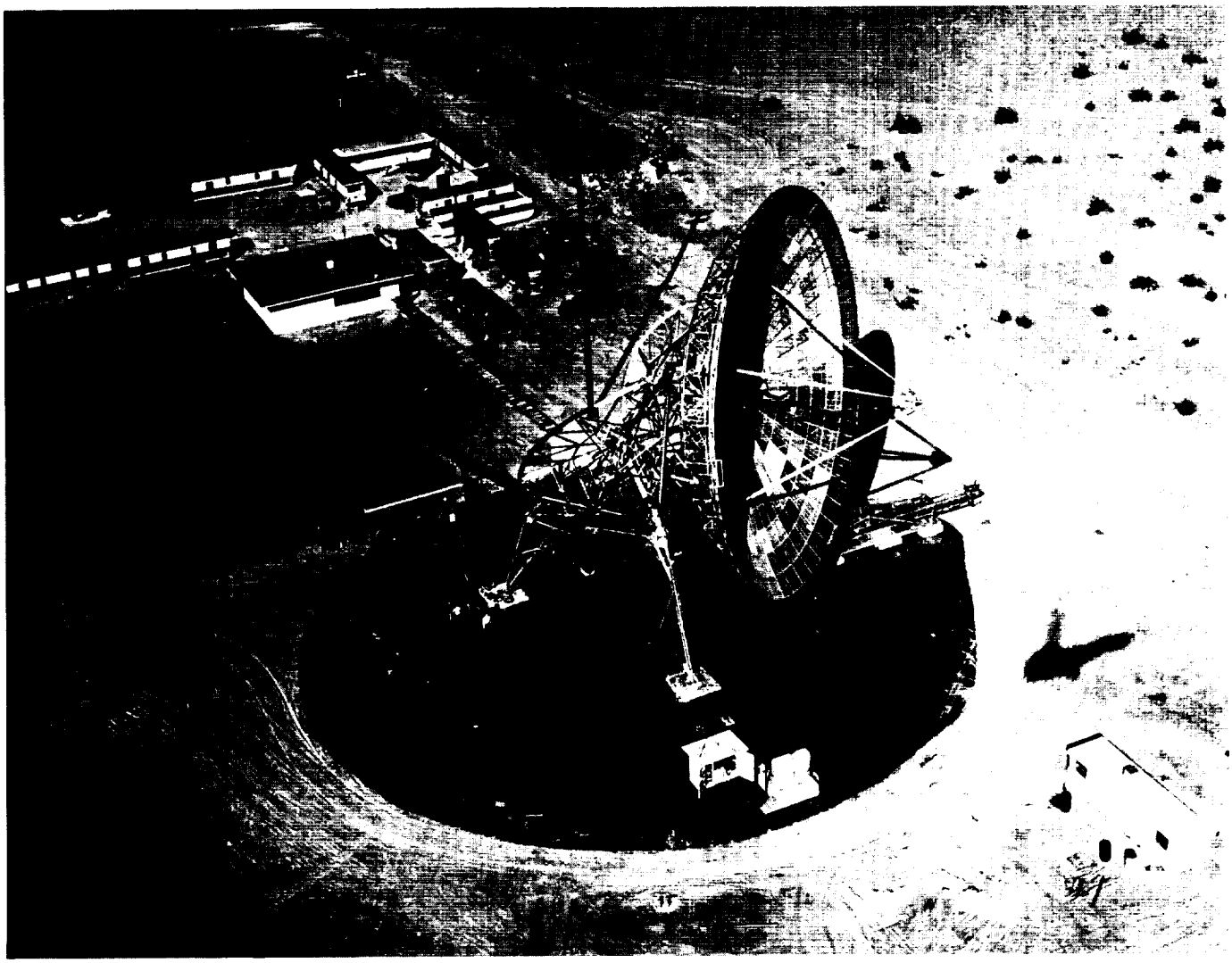

Figure 44. Goldstone tracking station

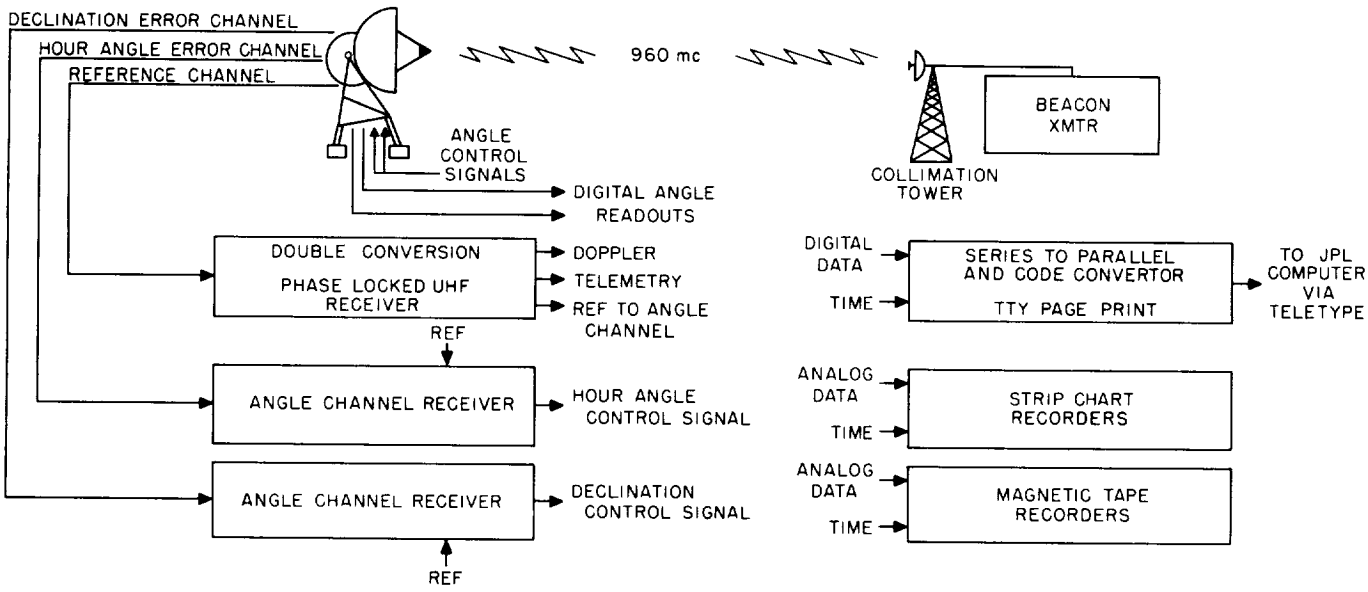

Figure 45. Elements of Goldstone tracking station

range of rates which might be encountered from a space target, 0.1 to 0.005 deg/sec.

The system was required to provide good tracking accuracy in a 45 mph wind. The wind load torques which amount to about 1.2 x 10^6 ft-lb and 0.6 x 10^6 ft-lb for the polar and declination axes respectively for a 45 mph wind dictate the power requirements for the drive which are 40 and 20 hp for hour angle and declination axes, respectively. The low-speed drives are less powerful by a factor of 10.

The control system for the antenna servo provided four modes of positioning the antenna.

1. Manual control at the hand-wheels which would insert a position error signal that the servo would null.
2. Manual insertion of a rate error signal at the hand-wheels. The antenna would move at the rate set in.
3. A saw tooth and a spiral scan with adjustable parameters could be inserted to control the antenna motion. This constituted the automatic search patterns available for angle acquisition.
4. Automatic track in which the amplified signals of the antennas' two axis simutaneous lobing error patterns were nulled by the servo positioning of the antenna.

The closed-loop bandwidth of the slow speed automatic track mode was adjustable from 0.025 to 0.1 cps. At low signal levels the narrow bandwidth was utilized to minimize noise jitter in the track.

The feed for the 85-ft-diameter antenna was a simultaneous lobing type, using four circular-polarized turnstile radiators located in front of a ground plane. The outputs of the individual radiators are combined in coaxial rat-race hybrids to derive the hour angle and declination error patterns and the reference channel pattern. Low loss rigid coaxial line is run down one of the feed support legs to connect the feed to the receiver mixers which are located in a small 6x8-ft mesh cage behind the reflector. The electrical performance of the antenna is as follows:

1. Gain, 41 db above linearly polarized isotropic.
2. HPBW of reference channel, 0.9 to 1.3 deg.
3. Separation of error channel peaks, 1.2 to 1.4 deg.
4. Reference channel on-axis ellipticity, 2.5 db.
5. Error channel cross coupling, 1 to 10.
6. Side lobe level, 15 to 20 db down for first side lobes depending on channel and polarization; wide side lobes, 45 to 50 db down on main channel.

The radio receiver utilized with the 960-mc tracking system is a narrow band phase coherent double conversion superheterodyne (Fig. 46). It has three separate channels, a reference channel for detection of the carrier and telemetry signals and derivation of the coherent AGC, and two similar error channels for the hour angle and declination error signals from the simultaneous lobing antenna. The high-frequency portion of the local oscillator frequency multiplier chain and the RF preselection, mixer and first preamp electronics are located

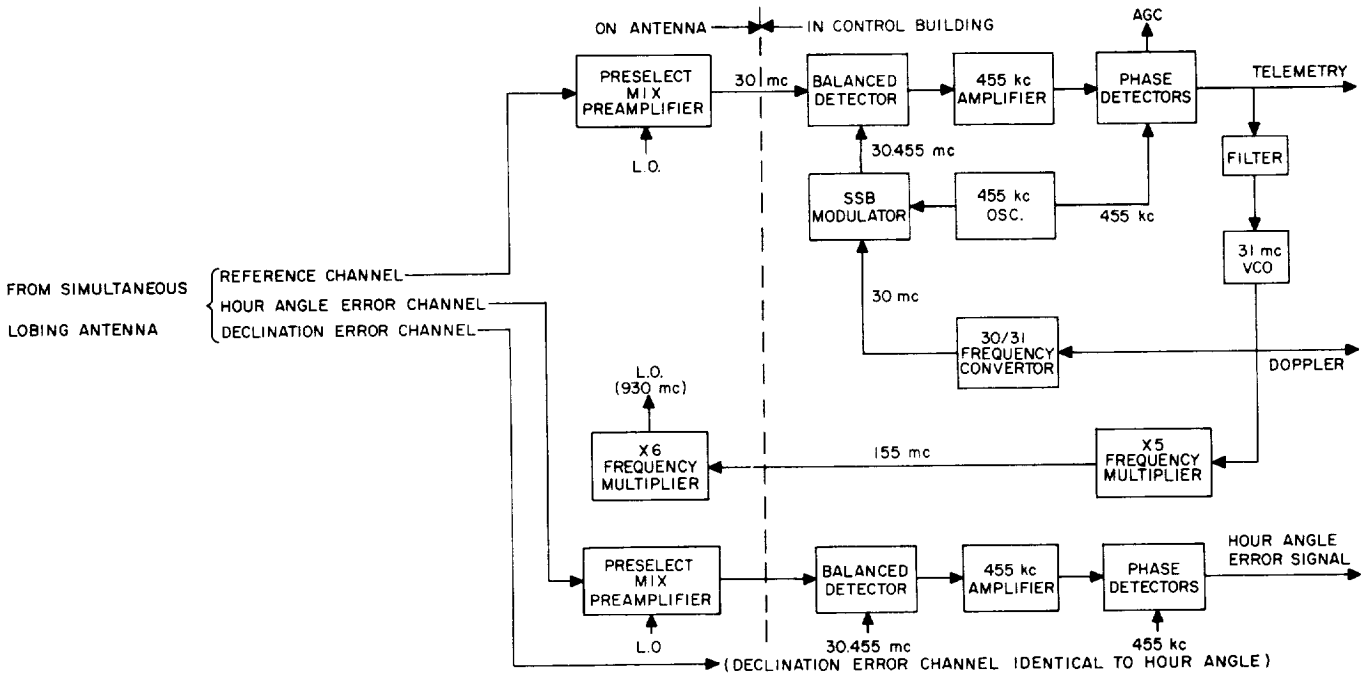

Figure 46. Basic Block Diagram of Goldstone TRAC(E) UHF Receiver

in the cage behind the dish surface. This cage also contains the test signal generator and noise-measurement equipment for maintenance testing and calibration of the radio frequency equipment. The remainder of the receiver equipment is located in the 30 x 40 ft control building approximately 100 yards north of the antenna. Parameters of the receiving system can be adjusted to provide best performance for a particular mission. For the *Pioneer IV* tracking mission the significant characteristics of the receiver were:

1. Noise bandwidth at UHF, 20 cps.
2. Noise temperature of receiver, 1330°K.
3. Approximate receiver threshold, −154 dbm = 4×10^{-19} watts.
4. AGC loop time constant, 11 and 300 sec.

For the above parameters, the maximum range for the *Pioneer IV* transmitter of 200 mw transmitted power was approximately 1 million miles for a unity *S/N* on the carrier signal and about 20-db *S/N* in the angle track and AGC loops. During the last phase of the *Pioneer IV* transmission, as the radiated power of the vehicle transmitter was falling off due to the batteries going dead, the bandwidth of the receiver was changed to a 10-cps value which increased the receiver sensitivity to about −157 dbm. This is equivalent to a range capability of 1.4×10^6 miles for a 200-mw transmitted power.

The functions of data handling and recording at the station may be divided into three areas: (1) measurement and handling of the signal source coordinates (limited to two earth-referenced angles and radial velocity from one-way doppler) utilized for determination of the vehicle trajectory; (2) recording and reduction of the information telemetered on measurements made in the vehicle; (3) recording of the receiver and tracking system performance and other information derived from the nature of the received carrier signal.

The first group of measurements is processed in real time and fed directly to the IBM 704 computer at the JPL control center. Hour angle and declination of the target are taken from digital encoders on the synchro follow-up system in the control room; there encoders follow the position of the drive pinion on the antenna bull gears. Also, the frequency of the oscillator, which is phase-locked to the received carrier signal, is digitally recorded to provide the velocity measurement. These three measurements together with a data condition indicator are sampled synchronously in time and time coded. They are then serialized, transformed to a teletype code, and transmitted as a teletype message to the computing center for insertion into the IBM 704 computer. This process is almost completely automatic; the punched cards from the incoming teletype message in the computing center do have to be manually placed in the 704 hopper. The purpose of the data condition indicator is to instruct the computer as to how to weigh the data

(good, bad, or in between). The resolution of the angle measurement is 0.004 deg and the resolution of the doppled measurement is one part in 3×10^7.

Recording of the telemetered information (the items of group 2) was done basically in two ways. First the composite signal with the three information carrying subcarriers was recorded on an Ampex magnetic tape recorder for permanent reproducible record and later reduction. The telemetry technique employed in the vehicle was FM of the conventional RDB subcarrier frequencies, and this composite signal was caused to phase modulate the transmitter signal to approximately 1.2 radians rms. In addition to the magnetic tape recording, narrow-band phase-lock discriminators provided signals to drive the pens of Sanborn strip chart recorders. This provides real-time reduction on the site of the three information carrying channels. The noise bandwidth of the audio discriminators was selectable in the range 1 to 8 cps, which provided a threshold of these channels within about 4 db of the receiver RF carrier threshold with the design values of payload modulation level. The functions which were recorded in this fashion for the *Pioneer* flights included:

1. Despin mechanism (memory).
2. Shutter trigger and memory.
3. High-intensity radiation (power level monitor).
4. Low-intensity radiation.
5. Internal temperature.

The third group of functions instrumented were also recorded on magnetic tape and strip chart, but in this case no discriminators were necessary. These functions included:

1. Received signal strength (also digitally recorded).
2. Spin modulation (from payload motion).
3. RF in-lock indicator.
4. Servo control mode switch.
5. RF static phase error in receiver phase-locked loop.
6. RF dynamic phase error in receiver phase-locked loop.
7. Hour-angle-error signal.
8. Declination-error signal.

The spin modulation recording was made to provide information on the motion of the payload. The essentially symmetrical dipole-like pattern of the vehicle was deliberately made slightly unsymmetrical to produce a modulation of the received signal as the payload rotated about its own axis. Some of the interesting motions of the payload were derived from that simple instrumentation.

To make the picture complete on the technical end of things, instrumentation utilized for preflight checkout and tracking evaluation should be included. The primary method of carrying out tracking evaluation tests was to use a helicopter which carried an optical target and a radio transmitter. The helicopter was programmed into a flight path resembling, as nearly as physically realizable, that of a space probe. The actual position versus time of the helicopter was derived by a high precision tracking phototheodolite, and those data were compared after a myriad of parallax and other corrections to the position data obtained from the tracking antenna. Also, a boresight camera was mounted in the antenna structure to directly determine tracking jitter and wander.

An interesting optical technique was used for checking the antenna and readout system. The basic reference for the antenna is an optical telescope which is very carefully aligned with the antenna axes and readouts. The radio axis of the antenna is in fact brought into parallelism with the optical system by sighting on a collimation pole which mounts suitable optical and radio targets. In order to calibrate systematic errors in the antenna structure and the readouts, the reference telescope was utilized to track optical stars and the positions indicated by the antenna axis readouts were then compared against the known star positions. For early preparations, stars nearby the expected path of the space probe were utilized. This technique, of course, does not account for any relative motion of the radio and optical lines of sight at various aspects of the antenna.

G. Trajectory Determination System

In order to handle the tracking and trajectory computations for the space probes, a data processing and computation center (Fig. 47) was established at the Jet Propulsion Laboratory in Pasadena. The center, built around an IBM 704 computer, had the following four main objectives:

1. To determine, in cooperation with ABMA, a series of standard trajectories that would make possible the achievement of the flight objectives.
2. To provide information to the primary tracking stations concerning look angle, doppler counts, expected time of probe acquisition and loss for each of the standard trajectories.
3. Computing the actual trajectory, utilizing information from the primary tracking stations.
4. Providing acquisition data to all stations in the net in the event that they lose contact with the probe.

The preflight trajectories provided for three or four firing times on each of seven days for *Pioneer III*. These

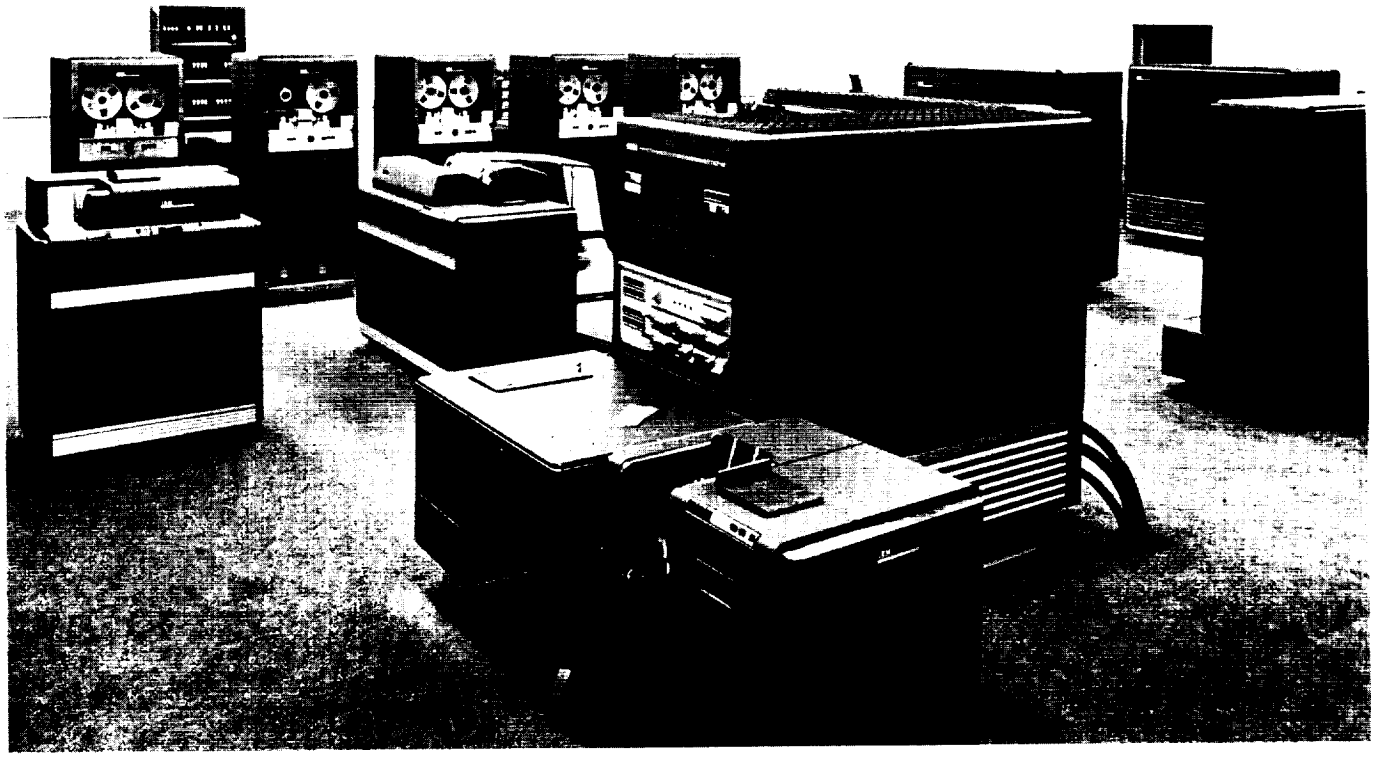

Figure 47. Pioneer III and IV computing center

firing times had tolerances of ± 5 minutes and were spaced approximately ½ hour apart. Preliminary information on each trajectory was then supplied to each tracking station in order that the stations would be able to shift their tracking programs according to which firing time was actually achieved.

The primary data-acquisition and tracking stations were connected to the computation center at JPL by teletype and voice communications. In addition, the center was in contact with a number of cooperating tracking stations and computing centers.

The doppler data from all stations and the angular information from the Puerto Rico and Goldstone stations, tagged with the exact Greenwich Mean Time, were automatically encoded into standard teletype format and transmitted to the computing center. Automatic teletype to IBM-card converters were used to put the received data into the proper machine input format.

The computing center in Pasadena utilized primarily an IBM 704 computer. The computer results were monitored with several independent procedures using smaller electronic computers, desk calculators, and precomputed charts. The IBM 704 computer at the RAND Corporation in Santa Monica served as backup. In the computing center the data were analyzed to provide rapid and precise acquisition pointing information for the tracking stations and accurate determination of the vehicle paths. The results of these computations were provided on IBM cards which were fed into a card-to-tape converter and transmitted to the appropriate tracking stations by teletype (Fig. 48).

The flow of data into and out of the computing center was regulated from a communications net control center located in the computer area which directed the switching of communications lines actually carried out by the two message centers located on the east and west coasts of the United States.

The primary tracking network was thus an almost completely automatic system which, when receiving a probe signal, would automatically count, encode, transmit, and convert tracking data, and then compute, convert, transmit, and display acquisition data. The only nonautomatic function in the system was the carrying of data cards the 25 ft between converters and machine input and output.

H. Data-Handling and Computation

The reduction of tracking data is essentially the problem of filtering, by statistical analysis, the random observational errors and the systematic bias errors.

Figure 48. Data handling facility

The basic procedure is as follows: A set of initial conditions is assumed or obtained from iterating within the program and is used to start the integration of the drag-free equations of motion, including the effects of the oblate Earth, the Moon, and the Sun. The computed trajectory variables are transformed into station-referenced coordinates and corrected for refraction and station anomalies. The differences between computed and observed values are used to determine those corrections in initial conditions which result in the minimum sum of squares of the differences between calculations and observations. The corrections in initial conditions are added to the previously employed initial conditions and this completes one iteration.

Figure 49 is a block diagram of the trajectory-computation program. The initial conditions at time of injection are assumed or specified from the tracking program. The input coordinates are distance from the Earth's center, geocentric latitude, longitude, and the magnitude, elevation, and azimuth of the velocity relative to the Earth. The integration of the trajectory is carried out in a right-handed, Earth-fixed, space-oriented Cartesian coordinate system where X is the direction of the vernal equinox and Z is the direction of the north polar axis.

For purposes of the tracking program, the trajectory computations are provided in terms of coordinates as

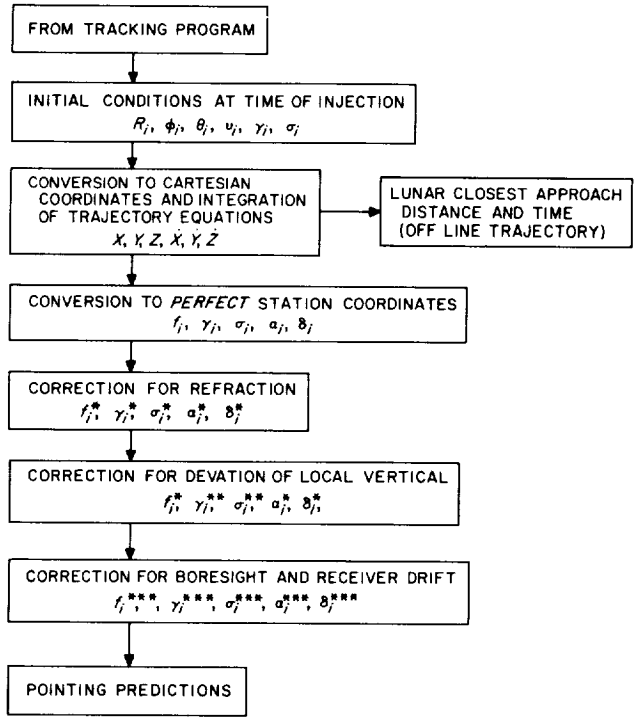

Figure 49. Block diagram of trajectory-computation program

similar as possible to those being observed at the tracking stations. The radial rate is converted to doppler frequency and then scaled and biased corresponding to the way in which the individual stations are mechanized. Angle data, corrected for refraction, are provided in elevation-azimuth and local-hour-angle local-declination coordinate systems.

The tracking program shown in Fig. 50 accepts as inputs the data obtained from the tracking stations and the computed values of the estimated trajectory in terms of the coordinates measured at the stations.

A sample of a data message received at the Computing Center from the Goldstone station is shown in Fig. 51. With machines adjusted for a transmission rate of 60 words/min, a single teletype line of data was transmitted in 7 sec. For use in the statistical evaluation of station performance after the completion of tracking, the comparatively high data-sampling rate of 6 samples/min was used throughout *Pioneer IV* operation.

Prior to full acceptance of a data point into the tracking program, the difference between the computed and observed values is compared with a standard deviation, which is either an externally specified number or one computed within the tracking program from earlier observation points. Measured values which differ from the computed values by more than three times the standard deviation are rejected.

Individual data points are weighted inversely as the variance of the deterioration in quality of the tracking data. The weighting used may depend on whether an automatic tracking mode is used, on the signal strength, and on the elevation angle.

The differences between computations and observations, properly weighted and the differential coefficients of the observations with respect to the initial conditions, are fed into a number of least-squares-fitting routines. In the primary method, each data type is weighted inversely as the previously computed variance from the mean for that type and then is combined. Changes in the six initial conditions and in constant biases in the five possible observation types can be solved for. Thus, the maximum matrix size provided for is 11x11. The new initial conditions and biases obtained by adding

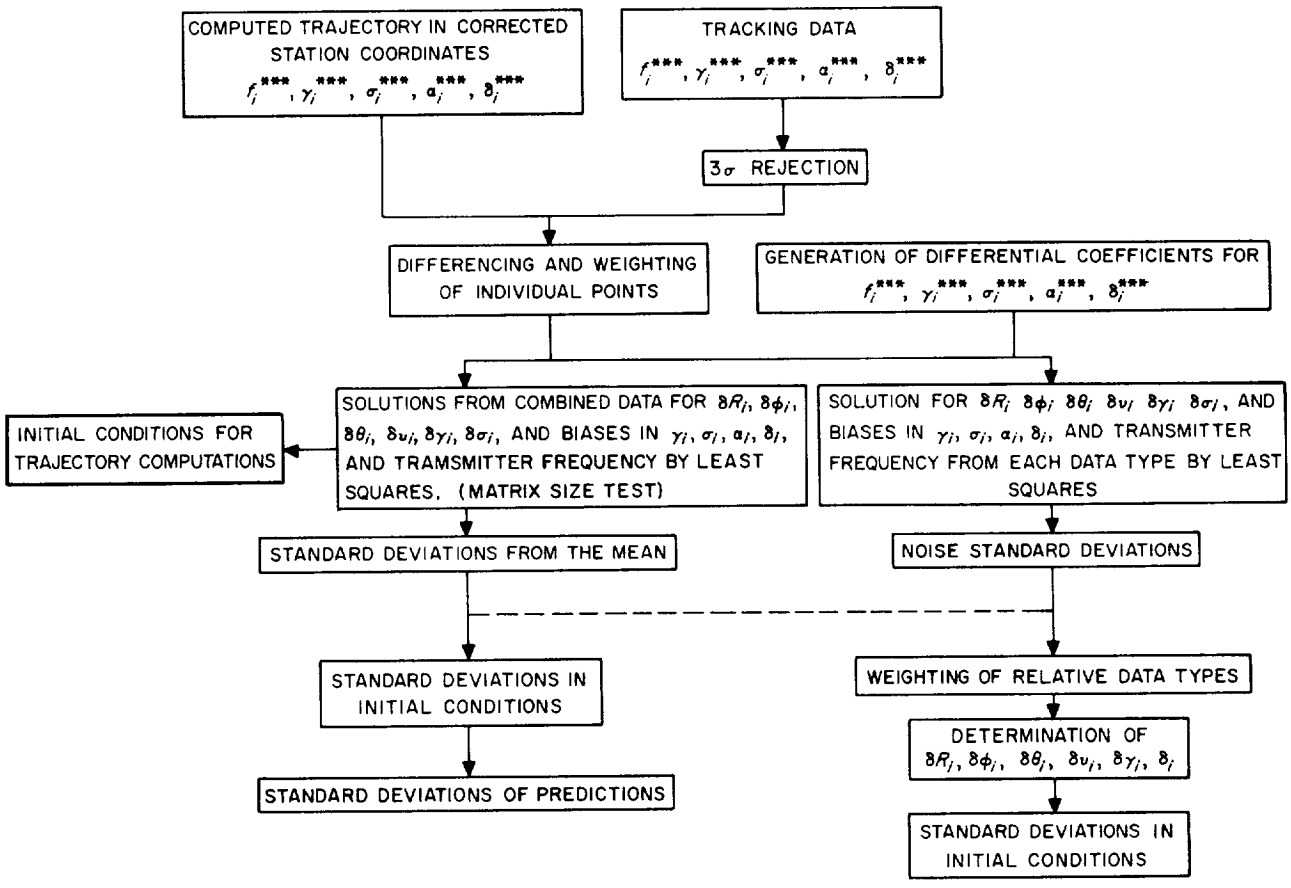

Figure 50. Tracking program

STATION IDENTIFICATION	DATA CONDITION	GMT hr, min sec	GOLDSTONE HOUR ANGLE deg $\times 10^3$	GOLDSTONE DECLINATION ANGLE deg $\times 10^3$	COUNTED DOPPLER FREQUENCY, cps
2	0	151401	335476	336524	11337
2	0	151411	335508	336524	11336
2	0	151421	335556	336524	11336
2	0	151431	335648	336524	11337
2	0	151441	335736	336524	11338
2	0	151451	335820	336524	11336
2	0	151501	335848	336524	11337

Figure 51. Sample of Goldstone Data Message

the changes solved for are used as input for subsequent trajectory computations. Standard deviations are always displayed. Standard deviations of predictions are computed on option.

For the tracking of the *Pioneer III* and *IV* probes, more reliance was placed upon the angular tracking measurements than upon the doppler measurements. The utility of the one-way doppler measurement rested on the assumption that the carrier frequency being transmitted by the payload did not change during the flight, and therefore the variations received by the stations represented actual variations in flight speed. Clearly, this assumption is open to question, and it would be much more desirable to have a doppler transponder carried on the probe which could be interrogated from the ground station giving an unambiguous measurement of range rate.

During the early portion of the flight, when the probe is still comparatively near to the Earth, measurements of angular position are sufficient to initiate the orbital computation. However, as the probe moves further and further from the Earth, its angular rate of motion across the celestial sphere becomes very small, and only extremely precise angular measurements could make any useful improvement on a computed trajectory. Thus, on future space probes the inclusion of a doppler transponder unit becomes of primary importance.

Acquisition predictions for transmission to the appropriate tracking station are generated on command and displayed on punched cards. The standard acquisition message provides data in 1-min intervals. For long-range predictions less frequent intervals were used. Figure 52 shows a sample of a standard message sent from the computing center to the Goldstone tracking station. The

GMT hr, min sec	GOLDSTONE HOUR ANGLE deg $\times 10^3$	GOLDSTONE DECLINATION ANGLE deg $\times 10^3$	COUNTED DOPPLER FREQUENCY, cps	GOLDSTONE HOUR ANGLE RATE $\times 10^3$, deg/hr	GOLDSTONE DECLINATION ANGLE RATE $\times 10^3$, deg/hr	RANGE, km
131201	304776	336507	11329	015102	-00048	492858
131301	305027	336506	11329	015102	-00048	492954
131401	305277	336504	11329	015103	-00048	493050
131601	305779	336501	11329	015104	-00048	493242
131701	306029	336500	11329	015105	-00048	493338
131801	306280	336498	11329	015105	-00047	493435
131901	306531	336497	11329	015106	-00047	493531

Figure 52. Sample of Goldstone Acquisition Message

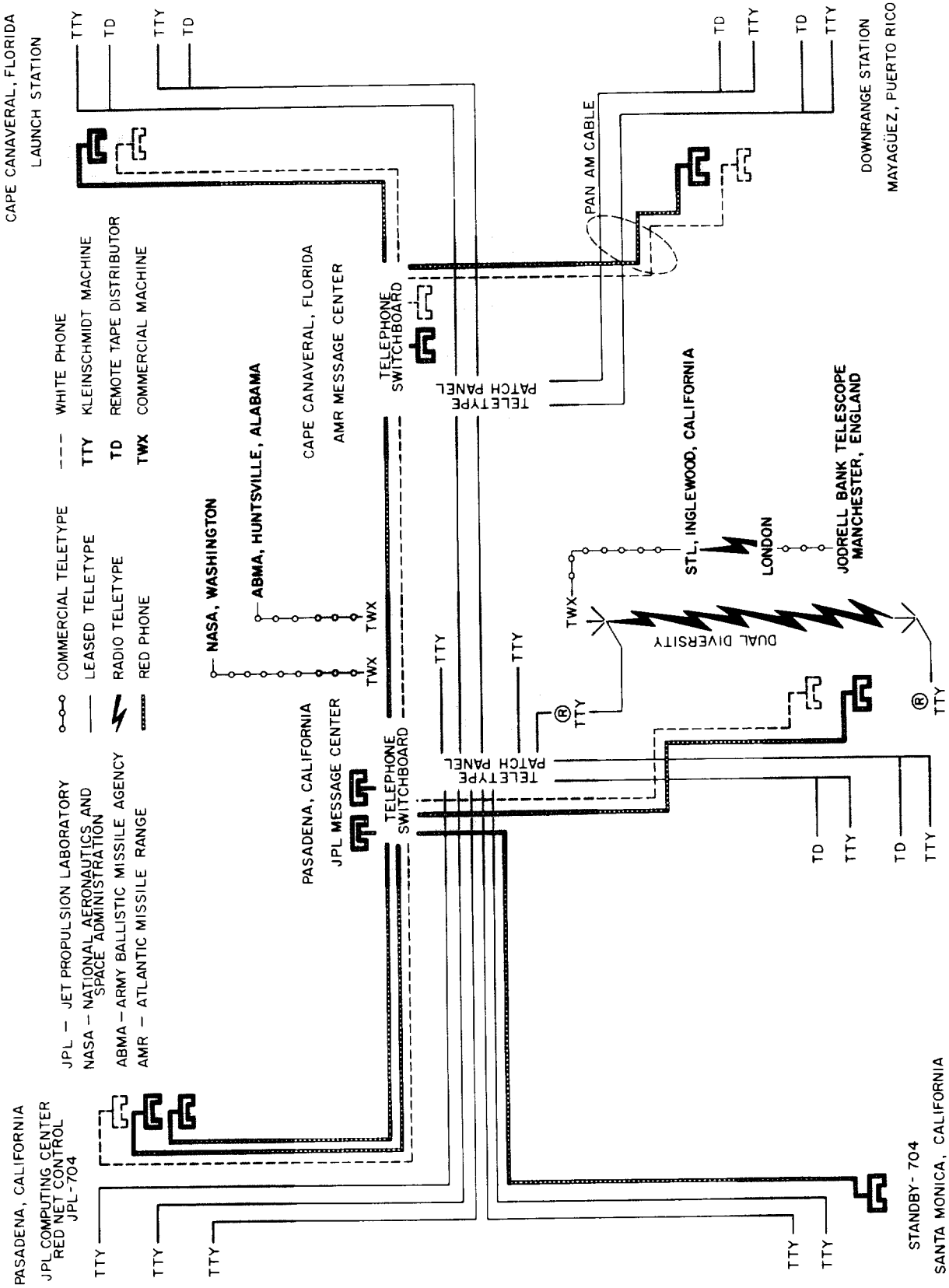

Figure 53. Pioneer III and IV communications network

first four columns represent time, local hour angle, local declination angle, and counted doppler frequency in the same format and in the same coordinate system (including refraction corrections, etc) as the expected data message. The remaining three columns represent local hour angle and local declination angle rates in thousandths of degrees per hour, and range in kilometers.

I. Data Transmission Network

A communications system made up of voice and teletype facilities was established early in November 1958 to provide a reliable, rapid, and flexible means of transmission of digital data, technical information, and administrative messages between the various tracking stations, computing centers, and communications centers. This network provided full-time voice and 60 word/min teletype communication between stations at the Jet Propulsion Laboratory, the Goldstone tracking station, and the Atlantic Missile Range by means of trunk tie-lines with existing administrative exchanges at these areas. The Mayaguez tracking station was linked to the net through the submarine cable which extends from Cape Canaveral to the southeastern range stations.

The over-all network, as illustrated in Fig. 53, provided for at least two half-duplex teletype circuits and two voice circuits between all points, with switching capabilities at the two message centers to provide for any makeup from a single point-to-point connection to a full party line.

The data transmission equipment is described more fully in the tracking station descriptions in this Section.

V. SYSTEM TESTS AND PERFORMANCE EVALUATION

A. Introduction

The launch phase of the *Juno IIA* operation at Cape Canaveral followed in most respects the pattern set for the *Explorer* or *Jupiter C* firings, namely: cluster assembly and checkout, payload or probe checkout, integration of probe and cluster, installation of cluster on booster, RF interference test, and finally the launch countdown. Although this operation represented the first time that a cluster had been used on a Jupiter (Fig. 54) and under a shroud (Fig. 55), none of the complications that were encountered was attributable to these conditions. The firing was complicated, however, by the need for close tolerance firing times and for alternate firing periods, and these items are discussed briefly prior to describing the actual operation.

The firing period was influenced by the following:

1. The objective of a close approach to the Moon.
2. Goldstone to be in contact with the probe at the time of closest approach.
3. Continuous radiation information from launch until the probe passed out of the field of view of Goldstone.
4. Vehicle performance.
5. Payload weight.

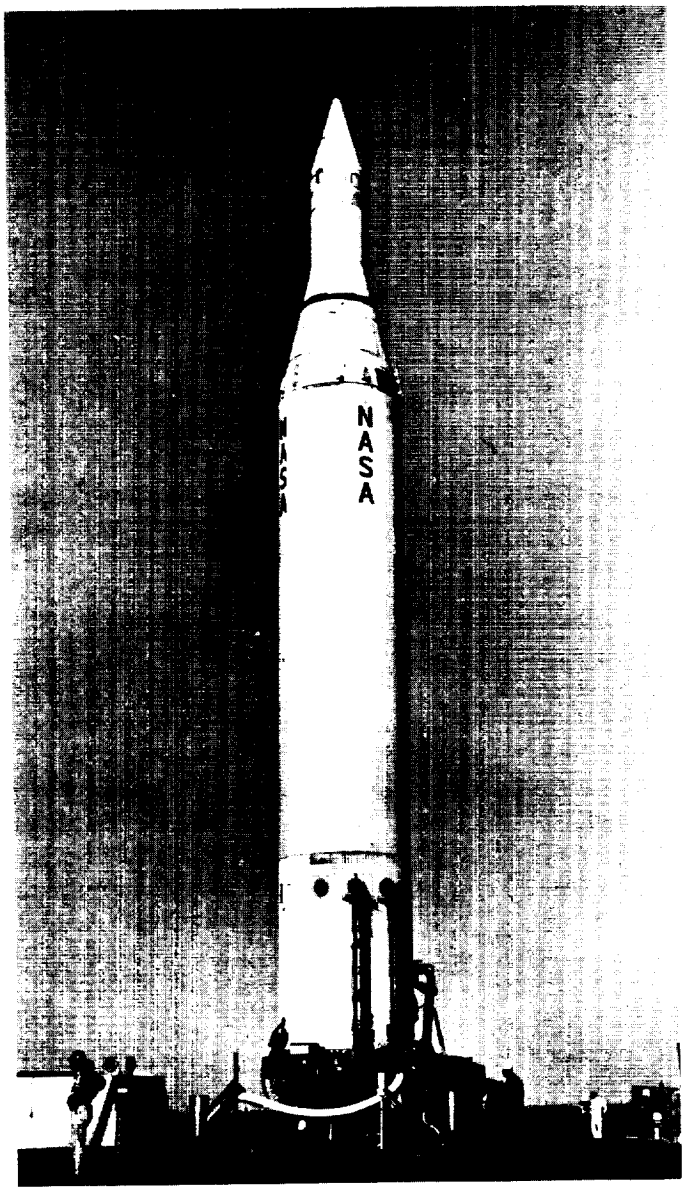

Figure 54. Jupiter

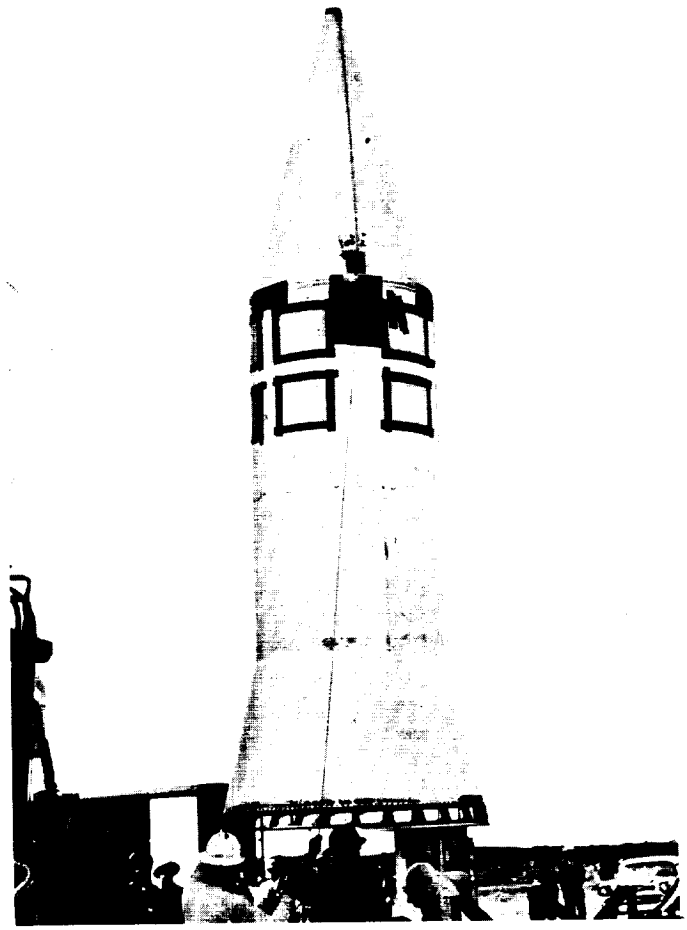

Figure 55. Shrouded Jupiter cluster

A consideration of these items resulted in an available firing period of approximately 50 min on December 6 and approximately 80 min on December 7 through 12. A particular firing time had associated with it an azimuth setting, a booster cutoff velocity, and a tilt program. In order to change these settings, a period of 30 min would be required. Therefore, possible firing times with a tolerance of plus or minus 5 min were spaced approximately 30 min apart for each day in the firing period. Fortunately, the range of firing azimuth from 79 to 95 deg would result in booster impact in a safe area, thus avoiding a range safety problem. In order to assure that a particular firing time be met, 185 min of hold time was allowed for in the countdown.

B. Operations

The cluster was moved to the pad and mated with the booster at 0800 hr, December 1. Countdown procedures were checked in preparing the cluster for the interference test. With all RF equipment operating, the cluster was brought up to a rotational speed of 250 rpm, held for a few minutes, then accelerated to 400 rpm momentarily. Observation of the probe motion during spin was obtained by leaving a pair of shroud RF windows off and focusing a closed circuit TV camera on the probe. No lateral motion was observed during spin up. The launcher base accelerometers also indicated no significant vibration during cluster spin.

No RF interference was encountered during the test.

The final countdown was begun at 1240 hr EST, 5 December, at X-540 min plus 185 min of builtin hold time.

Probe preparation was completed satisfactorily at X-360 but transportation to the pad was delayed 55 min to complete preflight radiation experiment calibration checks.

Measurements of the assembly 3 timer-battery voltages indicated an apparent excessive drop with a dummy load. Use of the satisfactory backup battery required rerunning the timer to record event times which required returning the shop trailer to the pad. However, the excessive time consumption of using the trailer recorder was avoided by measuring the event times with a stop watch.

Cluster work was delayed somewhat by the battery problem, but the probe delay was moderated by pad time in the probe schedule so that by X-290 min, JPL work was about 20 min behind.

The RF power measurement meter plugged into the assembly 2 ignition harness was watched closely during the operation of the *Thor* ground guidance transmitter up to X-320 min, but no indication was observed.

At X-275 the range requested permission to break RF silence to tune up the command transmitter. Igniter insertion was delayed until X-265 for this reason, placing cluster work 25 min behind at X-255.

The first scheduled hold was called at X-220 and lasted from 1800 to 2000 hr EST. Work on the cluster was completed and shroud installation done during this period.

The payload timer was started at X-139, 2120 hr EST.

A 1-hr hold occurred at X-60, 2249 hr EST, during which time difficulties with the LOX topping system for the booster were ironed out.

Failure of a receiver component at the launch station at about X-20 min required replacement of a subassembly and a readjustment of the receiver. After the readjustment, the channel showing the signal-strength modulation due to the unsymmetrical antenna on the rotating payload did not look the same as that seen during the RF interference check on December 1. This difference was finally attributed to the fact that the service structure was surrounding the vehicle for the interference test and now it was not. The ABMA Gold Microlock Station indicated that the payload beacon was functioning properly insofar as they could tell and thus increased the confidence that the system was functioning properly.

The last 5-min hold was called at X-2 in order to adjust the firing time to coincide with the optimum. Launch occurred at 5:44:52.3 hr on GMT December 6.

C. Vehicle Performance

Jupiter Round AM-11 which was to place *Pioneer III* into the vicinity of the Moon was fired 6 December 1958 at 05:44:52.3 GMT, 4 sec later than the optimum launch time. In order to minimize the danger of explosion from premature depletion, the depletion cutoff circuit was to be armed prior to earliest possible depletion time. Arming of that circuit occurred 176.1 sec after liftoff (05:47:48.4 GMT) corresponding to the approximate 2-σ value of the earliest possible depletion time.

Due to a failure in the depletion circuit, cutoff occurred at X + 176.2 sec, 3.6 sec earlier than expected. The failure is believed to have been caused by an electrical or mechanical failure in the depletion switch or by a mechanical failure in the shuttle valve.

At the time of early cutoff, the velocity was approximately 364 meters/sec below the value expected normally and resulted in a decrement of 382 meters/sec at cluster ignition. At cluster ignition, the standard

trajectory was to have a velocity 215 meters/sec in excess of escape velocity and 350 meters/sec in excess of that required to reach the Moon's altitude.

The circuit which was to provide cutoff was armed at X + 178.2 sec approximately 2 sec prior to the standard cutoff time. The cutoff time was selected to provide 2-σ assurance that the Moon's altitude would be reached even if failure of the guidance system resulted in cutoff when the system was armed.

At the end of the lamp spinup period and prior to *Jupiter* cutoff, telemetering data indicated that spin motor currents and voltage fluctuated over a fraction of their full-load values. The frequency of the oscillation appeared to be of the order of 2½ cps. Although no definitive explanation of the action of the drive motors is available to date, it is believed that no detrimental effects were caused by this behavior.

The instrument compartment separation signal was given X + 184.2 sec from liftoff and the shroud separation signal was given at X + 196.95 sec. Both separations appeared to be normal.

During and after tilting of the cluster, the control-jet needle valve positions showed small oscillatory motions with a frequency of approximately 5 cps. The oscillations appear to be a result of instability within the control loop. Analysis of the motion indicated by the guidance platform and the rate gyros and of the forces produced by the control jets shows the possible angular rates and positions to have been too small to significantly affect the subsequent dispersion of the cluster.

The coast period was 2.2 sec longer than nominal. Stage 2 ignition signal was given at X + 235.6 sec, and burnout occurred approximately 5.7 sec later. Stage 3 ignited at X + 244.3 sec and burned out approximately 5.8 sec later. Stage 4 ignited at X + 253.1 sec and burned out approximately 6.5 sec later.

Reduction of the Doppler data from three stations located in Miami, Florida; Fort Stewart, Georgia; and on Cape Canaveral, shows the following deviations in the mean direction of the velocity vector, with respect to the performance of a nominal cluster.

Stage	*Pitch*	*Yaw*
2	1-deg pitchup	2-deg yaw north
3	4.5-deg pitchup	5.9-deg yaw south
4	7.7-deg pitchdown	14.8-deg yaw south

The total angular deviation of the velocity vector at injection was 1.1 deg down and 4.6 deg south with respect to a nominal cluster. This deviation, in conjunction with the lower booster velocity prevented the probe from reaching escape velocity. Maximum altitude actually reached by the probe was 63,500 miles. Results of the stage-by-stage integration of the equations of motion using the mean directions of the velocity vector are in good agreement with the cluster burnout conditions determined from the subsequent tracking of the payload. Photography from ballistic cameras also shows the substantial deviation in the exhaust flame trace expected from the dispersion of the velocity increment vector. Signal strength records from the Cape station as presently interpreted indicate the existence of precessional motion at burnout of stage 2, but not at burnout of stage 4.

The spin rate prior to stage 2 ignition was within less than 1% of the expected value of 400 rpm. During cluster burning, the over-all change in spin rate was approximately 100 rpm. The over-all change in spin rate can be explained by examining the statistically distributed effects of cluster motors with reasonable jet misalinements. However, signal strength records suggest abrupt changes during ignition of the three high-speed stages. If these abrupt changes in the frequency with which the signal strength records are modulated represent equally abrupt changes in the spin rates, then there is, at present, no acceptable explanation.

The dispersion of the cluster could, of course, have been caused by a number of things. It is at present believed that the most likely cause is that it was due to slight differences in burning time between motors within a stage.

At least two pieces of data are in apparent contradiction of this conclusion. The mean velocity vector during second-stage burning suggests the existence of a disturbance prior to burnout of that stage. Although the numerical values of the angular deviation during second-stage burning cannot be considered to be known to high precision, it is estimated that an angular deviation of at least 1 deg existed.

If it is assumed that slight differences in motor burnout times were the principal cause of the deviation of the velocity vector during cluster burning, the motion of the cluster can be reconstructed analytically. These calculations give the correct velocity increment stage by stage and the correct direction of the mean velocity vector for each stage. However, all such calculations result in significant precession angles at burnout of the last stage, in apparent contradiction to the result of the analysis of signal strength data. Since cancelling of the precessional motions could, at present, only be explained by a highly fortuitous and, therefore, unlikely circumstance, the signal strength data is in apparent contradiction to the cluster motion postulated.

D. Probe

The payload separated from the empty stage 4 at X + 268 sec. Signal strength records suggest that the payload after separation precessed with a half-cone angle of about one with an uncertainty of a factor of two.

At 06:00:30 GMT telemetering channel 1, which was to show triggering of the optical sensors whenever an illuminated body was in view, indicated passage of the crescent of the Earth in front of the optical axis. The Earth was in view for less than 10 min.

Based on the present best estimate of timer performance, corrected for the measured inflight payload temperature, despin of the payload should have occurred at 15:30:00 GMT (9¾ hours after liftoff). Signal strength records from Goldstone, which had the probe under surveillance at that time, and records from Puerto Rico for a later time show conclusively that no changes in spin rate occurred at any time between payload separation and re-entry. The reason for the failure of the despin device to function is not known.

The shutter-trigger memory circuit was to arm between 21:30:00 GMT on 6 December and 01:30:00 GMT on 7 December. At 22:10:00 GMT (16 hr and 25 min after liftoff) the channel 1 oscillator changed frequency, indicating a change of state of the memory circuit. No subsequent changes were observed. Although the Earth could have been in view at approximately the time the memory circuit changed state, the fact that the angle to the Earth changes very slowly at that time makes it very unlikely that only a single sighting could occur. Final conclusions were that the memory circuit triggered shortly after arriving and that the scalers were damaged before the memory circuit triggered.

Estimates of payload temperature were made from the subcarrier oscillator frequency of channel 1 which responded to the temperature of a thermistor in the circuit and from the transmitter frequency which had been calibrated against temperature. Both estimates gave temperatures of approximately 38°C and were in agreement within 2°C. An analysis using the best available estimate of payload altitude with respect to the sun and neglecting the heat transfer into the nose cone results in an equilibrium payload temperature of 40°C. The difference between the observed and computer equilibrium temperatures is of the correct order of magnitude to be accounted for by the neglected heat transfer to the nose cone.

The performance of the scaler in channel 3 was normal. Nonstandard performance, however, did occur in two noncritical instances. When the payload was turned on, the subcarrier frequency in channel 3, the scaler channel, was not one of the eight calibrated stable states. The auxiliary flip-flop, stage 18, assumed a nonstandard state thus cutting off the buffer amplifier driving the VCO. Ordinarily, the digital output from the 9th stage would be obscured by the cutoff buffer until stage 18 had received its reset pulse from the 13th stage. This would normally occur after about 3000 counts. Strangely, the reset of stage 18 occurred precisely at second stage ignition, indicating that spurious triggers were generated somehow at that time. As indicated before, normal performance ensued.

Both counters in *Pioneer III* operated in the Geiger region, so that they measure only the number of particles entering their sensitive volumes.

The peak counting rate, encountered at about 16,000-km altitude, was 10.5K counts/sec on the channel 3 digital counter during ascent and 11.3K counts/sec during descent. Both peaks were flat-topped, indicating saturation, and the maximum counting rate observed during calibration was 11.5K counts/sec.

The channel 2 analog did not reach its saturation level at the peak counting rate. Figure 56 is a plot of the *Pioneer III* trajectory on the probable shape of the Van Allen radiation belt. Counting rates at distinct points along the trajection are indicated by the contour lines drawn through those points. At low altitudes, these contour lines coincide with those discovered by the *Explorer* satellites. At high altitudes the contour lines are drawn to reasonably fit the data obtained by *Pioneer III*. The contour lines in regions not actually traversed by the probe are speculative but are drawn consistent with both *Explorer* and *Pioneer III* data.

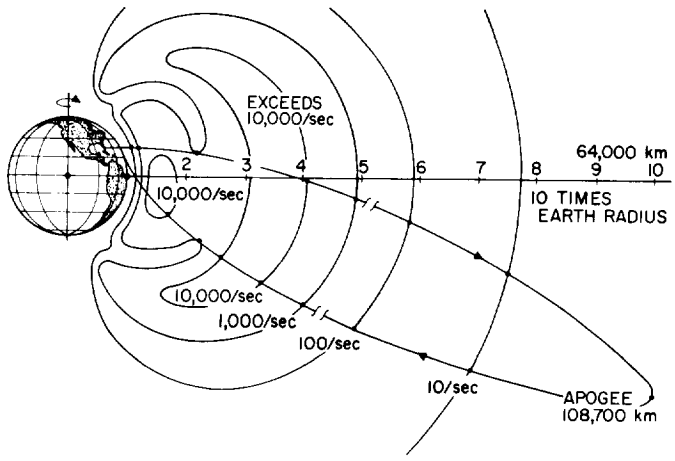

Figure 56. Van Allen Radiation belts

E. Tracking Network

1. Transmitter

Measurements of the transmitter power output and the effective radiated power of the payload at JPL and a comparative radiated power measurement at Cape Canaveral prior to launch indicated normal transmitter power output. An analysis of the received signal level during the first *Juno IIA* experiment has revealed the following. Comparison of measured signal level with the expected level is shown in Fig. 57 for the Goldstone Station. Within the uncertainties of measurement and calculation there was moderate agreement between the expected values and actual received signal levels. If the lock angle were increased by 20 deg for Goldstone, the agreement would be improved (see Fig. 58), or if the transmitter carrier power were low 1-3 db, better agreement would result. While it is possible that the received signal level was less than expected, it is not possible to establish this accurately on the basis of the available data. The results are generally in agreement with those obtained from the analysis of signal level at Puerto Rico.

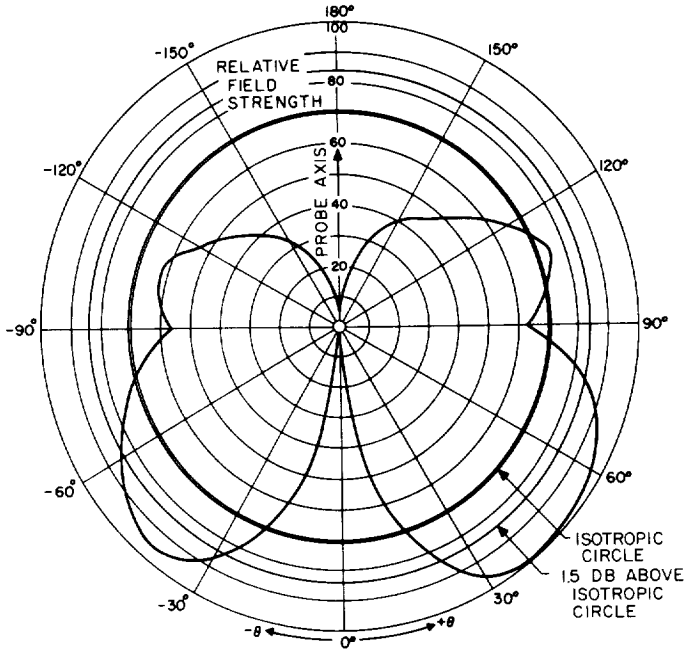

Figure 57. Pioneer IV antenna pattern

Due to the large number of factors involved in the analysis of in-flight signal strength data, it is not possible to meaningfully correlate predicted and observed antenna gain. The in-flight observed spin modulation is in the range of 1.5 - 3.0 db. Predicted modulation, based on calculated look angles and Fig. 59, is in the range of 1.0 - 1.5 db. Receiving instrumentation uncertainties and

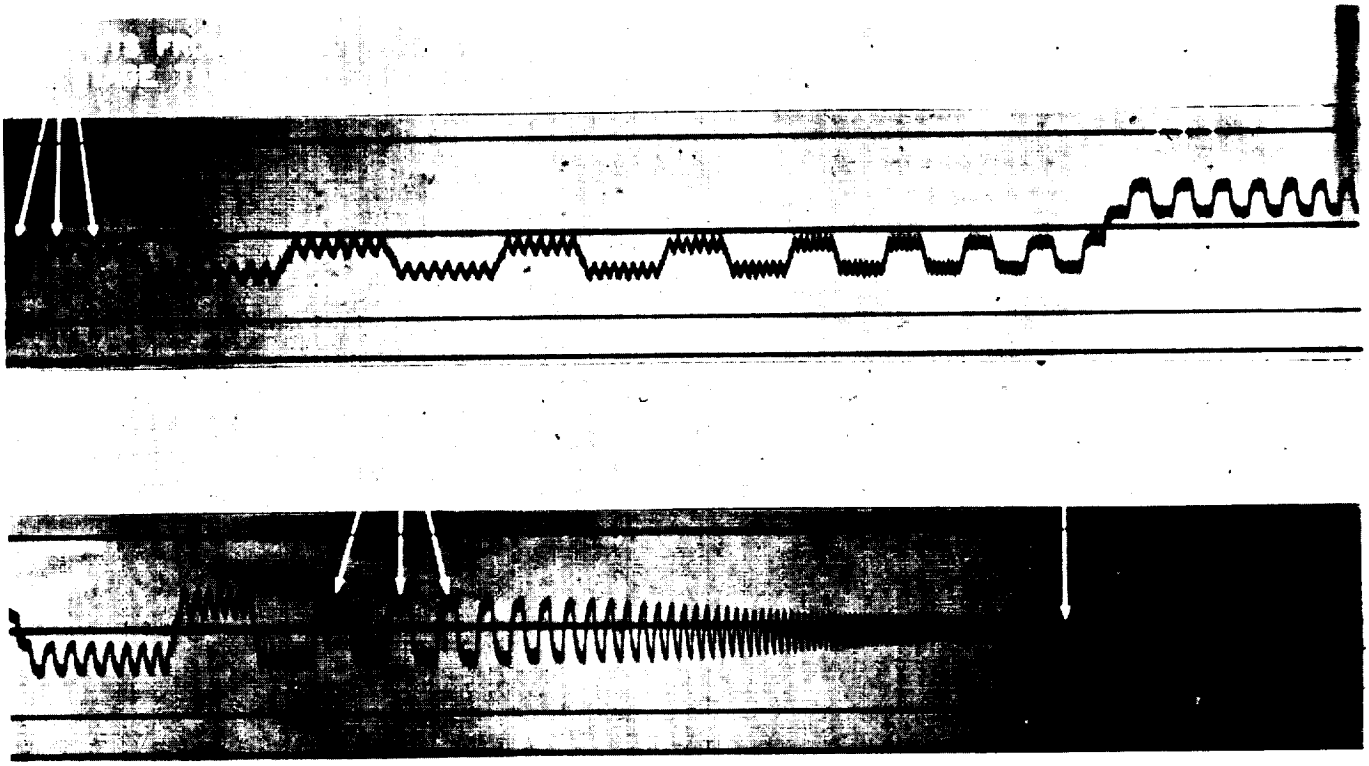

Figure 58. Pioneer III radiation data as monitored at Puerto Rico

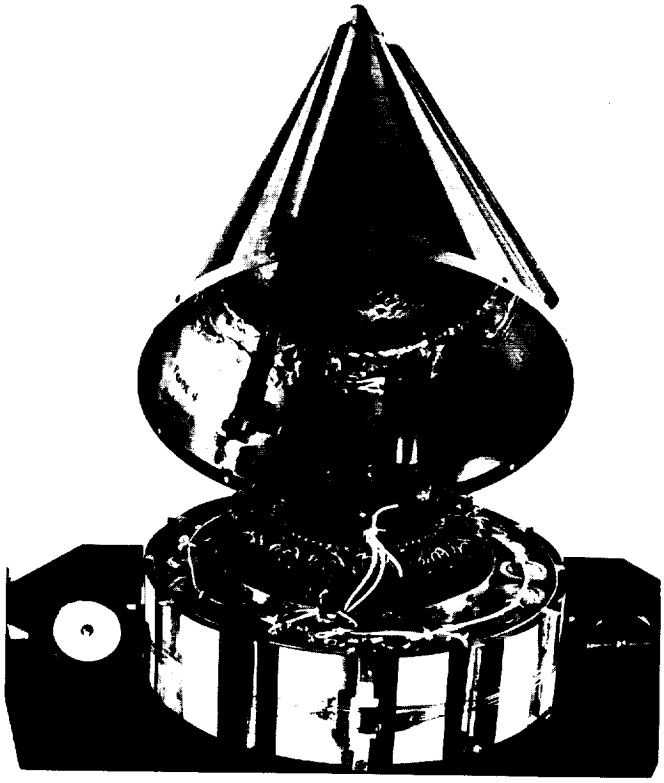

Figure 59. Pioneer IV: crosssection of nose cone

in-flight look angle uncertainties are sufficient to account for the discrepancy between predicted and observed spin modulation.

Analysis of carrier frequency for the *Pioneer III* probe transmitter reveals that agreement between measured frequency vs temperature (during flight) and laboratory temperature calibration is excellent. It is concluded that the transmitter has met the design frequency stability requirements of 1 part in 10^6 long term and 1 part in 10^7 short term. The analysis also demonstrates that the digital frequency readout equipment used with the TRAC(E) receiver is accurate to 1-3 parts in 10^8 and is not only useful in providing one-way Doppler measurements of radial range and velocity but is also useful in evaluating the performance of the vehicle transmitter itself.

2. Radio Receiver

The receiver checkout and calibration proceeded satisfactorily during the final countdown until a malfunction occurred at X-30 minutes. The difficulty was traced to the voltage controlled oscillator and the spare unit was installed immediately. The receiver was then recalibrated and found to be operating satisfactorily. At X-13 the receiver was again locked to the probe signal and operated satisfactorily during takeoff and up until four seconds after second stage ignition at which time loss of lock occurred. Experimentation at JPL indicates that this was primarily due to excessive static phase error due to the low leakage resistance of the nonpolarized tantalum capacitors used in the loop filter. At present, a study is being made to determine quantitatively the effect of these capacitors upon the RF loop characteristics. It might also be mentioned that there was a possibility of a transient phase instability occurring at the start of second-stage ignition. This was evidenced by an apparent change of state of the cosmic-ray channel at this time.

The probe signal was reacquired after injection and lock was maintained until the probe disappeared over the horizon 17 min after launch. Figure 60 shows the measured and calculated signal values during this period along with a list and the range of the uncertainties present. The calculated curve is not presented during the initial period prior to loss of lock because of insufficient and inaccurate lock-angle data.

The probe reappeared over the horizon and lock was again attained 3½ hours after launch. The launch station receiver maintained lock for an additional period of 2½ hours, the probe slant range being 69,147 km at the end of this tracking period. During this period the measured signal level was below −150 dbm at the receiver input. The greater discrepancies between measured and calculated signal levels occur in the first hour of this tracking period, during which time the probe was rising above the horizon to an elevation of 10 deg. Signal level values at these low elevations angles become inaccurate due to ground reflections. After the probe rises above an elevation of 10 deg correlation is better, the differences between measured and calculated values of signal level being in the order of 2 db (Fig. 61).

The re-entry of the probe was monitored on the following day for a period of about 1 hr. When acquisition was attained the slant range was slightly over 30,000 km and when the probe disappeared over the horizon the slant range was slightly less than 17,000 km. Measured and calculated signal levels for this tracking period are also shown in Fig. 61. These measured signal level plots are not the actual measurements made at the receiver input but are the corrected values taking into account the position error of the antenna.

3. Telemetering and Recording System

The main function of the telemetering system at the launch site was to check out the payload telemetering

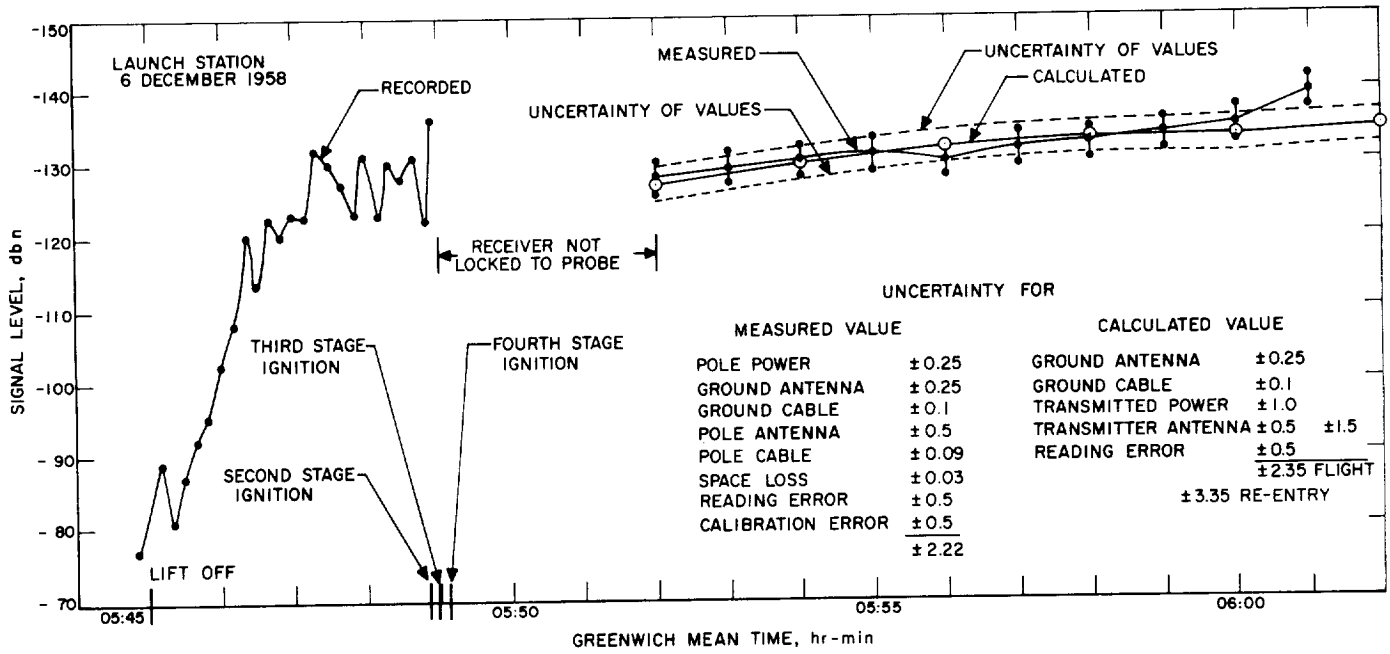

Figure 60. Signal valued

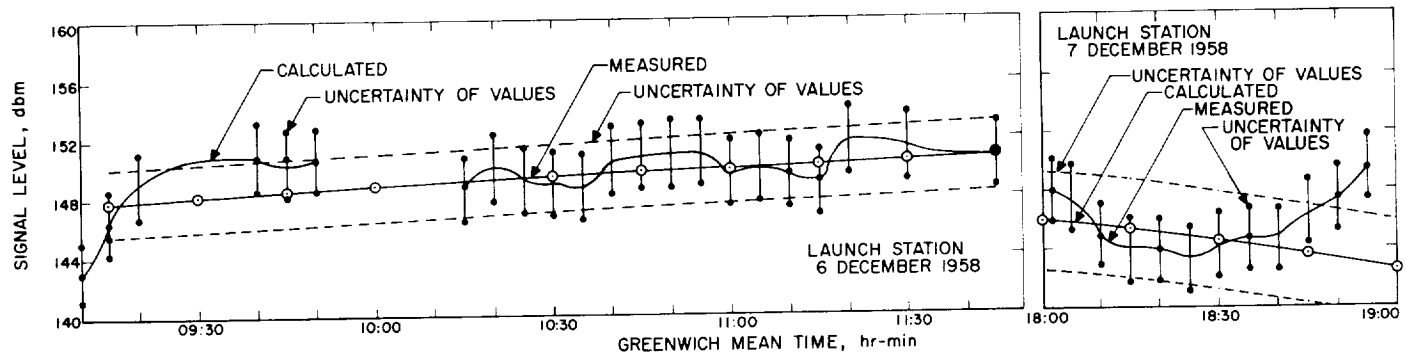

Figure 61. Signal levels for tracking period

during countdown and to make a magnetic recording of payload telemetering prior to acquisition of the Puerto Rico Station.

The telemetering system as delivered to the launch site performed very well throughout the checkout and flight operations. Several minor changes and additions were made which are listed below.

1. The discriminator tracking VCO output was fed to the mixer and recorded on track two of the magnetic tape recorder.
2. The discriminator was modified to bring the output of band-pass filter channels one and two out to test points. This permitted the operator to measure the frequency of either channels one and two while making a continuous recording of channel three.
3. The magnetic tape recorder was reworked to reduce the amount of wow and flutter. This rework consisted mainly of replacing the capstan fly wheel and aligning the drive mechanism.
4. A backup timing system was wired into the station by using the one pulse per second from the HP counter as a timing signal source. This 1 pulse/sec signal was used to drive an amplifier relay circuit which gave a contact closer for the oscillograph timing circuit. This 1 pulse/sec voltage was also used to modulate a voltage controlled oscillator which was recorded on the magnetic tape. This backup timing signal was not a coded signal, therefore WWV time must be marked on the oscillograph and voice labeled on the tape recorder.

A switch was mounted on the control panel to select either range time, or the backup timing signal. During the flight the range timing performed very well, and it was not necessary to use the backup timing signal.

The launch station countdown started at X-435 minutes. At X-405 the payload signal was received and recorded from the spin building. Between X-405 and X-280 the telemetering system was checked out and calibrated. At X-280 the payload signal was recorded from the missile. Between X-280 and X-47 the telemetering system calibrations were completed and the receiver functions were calibrated. At X-47 the payload signal was again checked and recorded. At X-25 the Launch Station reported status of the payload. At X-15 the direct writing oscillograph was turned on to record spin of the payload and at X-2 minutes the magnetic tape recorder was turned on. During the flight, telemetering channel 3 was recorded on the oscillograph and the frequencys of channels 1 and 2 were counted and written down on a log sheet. The launch station recorded good telemetering data from launch to horizon (X-17 minutes) and from horizon to 69,147 km distance on December 6 and for about 1 hr on re-entry.

4. Data Processing

The data-handling equipment for the Launch Doppler Station was constructed by Collins Radio Company, Burbank, and was delivered to the Laboratory on approximately 13 October 1958. The equipment was installed in the launch Doppler van and checked out. Unfortunately, the data-handling system did not work. The main problem areas were in the 100-kc Doppler count board, the sample and Doppler control circuits, and the tail break or lift off signal circuits. Considerable effort was expended rectifying the existing problems; in fact, no qualitative tests or reliability runs were made because all available time was spent in troubleshooting, modifying, and repairing the equipment.

The data-handling equipment was shipped with the launch Doppler van to Cape Canaveral on 31 October 1958. Further problems were encountered in the 100-kc counter, sample, and doppler control circuits. These problems were resolved by 1 December 1958. The Gertsch FM 6 frequency multiplier was checked and was functioning properly; there was a loading problem associated with measuring the frequency on the HP counter, but this had no effect on the normal operation of the system.

The clock and the frequency standard worked properly, however a complete check on the frequency stability and on the actual frequency of the frequency standard was not possible. Primary power failures would not allow test runs of sufficient length to obtain the accuracy required. During the last week before the flight operation, the rough measurements taken indicated a frequency error in the vicinity of 3 to 6 parts in 10^8; in any case, the frequency error was well below 1 part in 10^7.

In general, the sample rate controller and the parallel-to-serial converter worked well. There were a few circuit problems, but they were overcome without major equipment modification. There were 42 errors in the punched paper tape of which 35 were associated with one combination of Doppler digits (i.e., 11,400 became 11,480). There were two errors due to sample rate switches; this is a design problem. There were five errors due, apparently, to random missing pulses.

The teletype equipment worked reasonably well but did show signs of mechanical wear. Preventive maintenance was performed on this equipment, but the experience of this operation indicates that it should be more frequent.

There were three errors which can be attributed to the TD bit error. The TD missed reading one hole in the tape in each case. There is one sample which was scrambled and was probably due to teletype line trouble.

5. Puerto Rico Downrange Station

The acquisition of the space probe at Puerto Rico required coordination between the pointing of the antenna in azimuth and elevation and in the tuning of the receiver in frequency in accordance with the expected motion of the probe. Since the subsequent acquisition by the Goldstone tracking station was dependent on tracking data from the downrange tracking station, this acquisition was vital to the success of the tracking network. The receiver tuning was the most critical part of the operation, for without RF lock, angular acquisition and telemetering reception were impossible. The acquisition problem was complicated because the pointing and tuning are manually controlled by three human operators.

A study of the available nominal trajectories indicated that the spread in azimuth and elevation angles would not exceed 1.3 antenna beamwidths for any given time from launch and that the maximum angular rate would not exceed one antenna beamwidth in 15 sec. Thus, if the operators were trained to smoothly position the antenna in accordance with a precomputed nominal trajectory, the antenna would be pointed at the probe to within 1 beamwidth during the acquisition phase.

The nominal trajectory data indicated that the signal frequency would vary over a 47.4-kc range during the first 6.5 min of the flight with a maximum rate of 0.475 IF bandwidths per sec. In addition, the spread about the nominal frequency could be as large as 1.9 IF bandwidths due to trajectory variations, and 5 bandwidths due to the static transmitter frequency error. In order for the receiver operator to intercept the signal, it is necessary to sweep the receiver tuning about the frequency obtained from a precomputed nominal trajectory. Since the error in the static transmitter frequency could be measured at the launch station, the necessary sweep width could be reduced by biasing the receiver tuning calibration accordingly. At the large signal level expected during the early portion of the trajectory, experience has shown that a receiver operator requires only 1 or 2 sec to accomplish RF lock when the signal is within the 2-kc IF pass band of the receiver.

In view of the above situation, the acquisition operation was conducted as follows:

1. During the countdown the static transmitter frequency was obtained from the launch station, and the receiver tuning indicator was adjusted to compensate for the difference from the nominal value.
2. Just prior to the time that the space probe was to rise above the horizon, a person read the azimuth, elevation, and frequency to the console operators from a precomputed nominal trajectory at 15-sec intervals.
3. The trajectory reader gave a "mark" at the time corresponding to each trajectory point.
4. The azimuth and elevation operators moved the antenna position controls such that the antenna was pointing in the direction read from the trajectory when the "mark" is given.
5. The receiver operator tuned the receiver about the frequency given by the trajectory reader.

This procedure was to be followed until acquisition or a similar "failure" search mode was to be followed.

Acquisition tests, using the helicopter simulating the space-probe trajectory were conducted at both Dallas and Puerto Rico. A flight trajectory was established after several runs. After several practice runs, acquisition time for the radio signal and servo system was approximately 5 to 8 sec for a strong signal and a wide bandwidth. Acquisition time with weak signals and narrow bandwidths was 15 to 30 sec.

On the night of the experiment, the acquisition was not as difficult as anticipated. Solid RF lock was obtained (05:49:11.5 GMT) within 12.8 sec after the space probe came above the horizon; complete angle track was obtained 14 sec later (05:49:25). Radio acquisition did occur at 05:49:03 and was maintained for 3.5 sec but was then lost. Radio and angle tracking of the space probe continued until acquisition by the Goldstone tracking station. The signal strength at this time was −151 dbm. The receiver and servo systems were operated in their wide bandwidths during acquisition and the period following due to high doppler and angle tracking rates. The bandwidths were switched to the narrow position when the signal strength was −139 dbm and the doppler and angle tracking rates had decreased considerably. It was then possible to take advantage of the greater sensitivity and to obtain smoother tracking.

Search for the space probe on re-entry was started at 11:00 GMT with the radio lock and angle track being accomplished at 11:51:21 GMT. The signal strength at acquisition was −152 dbm. The acquisition was greatly aided by predictions from the computer. Angle tracking was maintained until the space probe disappeared over the horizon at 19:28:00 GMT. The signal strength at this time was −135 dbm.

6. Goldstone

Goldstone acquired the probe signal at 13:15 GMT, 6 December 1958 and lost it at 22:10 GMT. During this period the range to the probe varied from about 80,000 to 107,000 kilometer. The operation of the tracking station was very satisfactory.

The expected received signal level for the Goldstone station was calculated (Fig. 62) on the basis of the

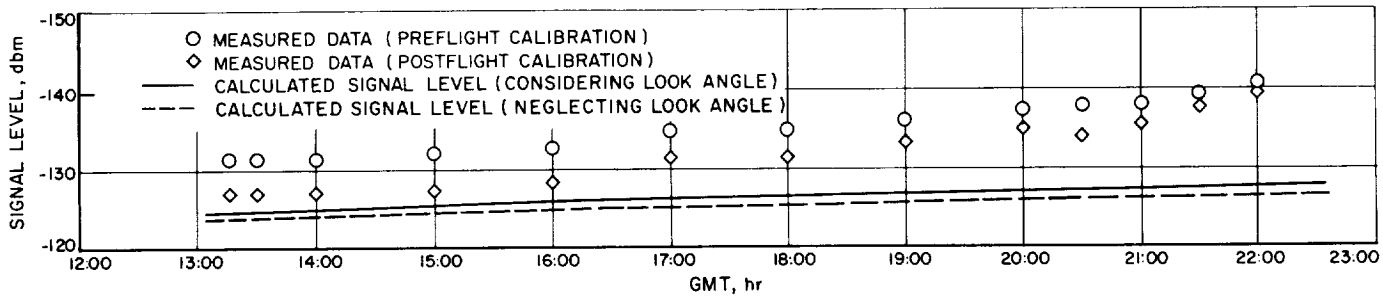

Figure 62. Comparison of calculated and measured signal levels

following values: transmitted carrier power, 20.5 dbm; vehicle antenna gain, 3 db; ground antenna gain (net), 42.7 db; and space loss (db), 92.1 + 20 log R, where R is the radial range in kilometers. One calculated curve (dashed line) is based on the maximum vehicle antenna gain and the other (solid line) considers the effect of the calculated look angle on the vehicle antenna gain. The look angle is calculated on the assumption that the spin axis of the probe is essentially colinear with the velocity vector at injection. The transmitted carrier power and vehicle antenna gain agree with measurements of effective radiated power performed at JPL and Cape Canaveral. The net ground antenna gain as obtained by direct measurement (Section V-D-3 of this report) is 42.7 db with the polarization of the signal at its expected value for the flight, neglecting Faraday rotation due to the ionosphere.

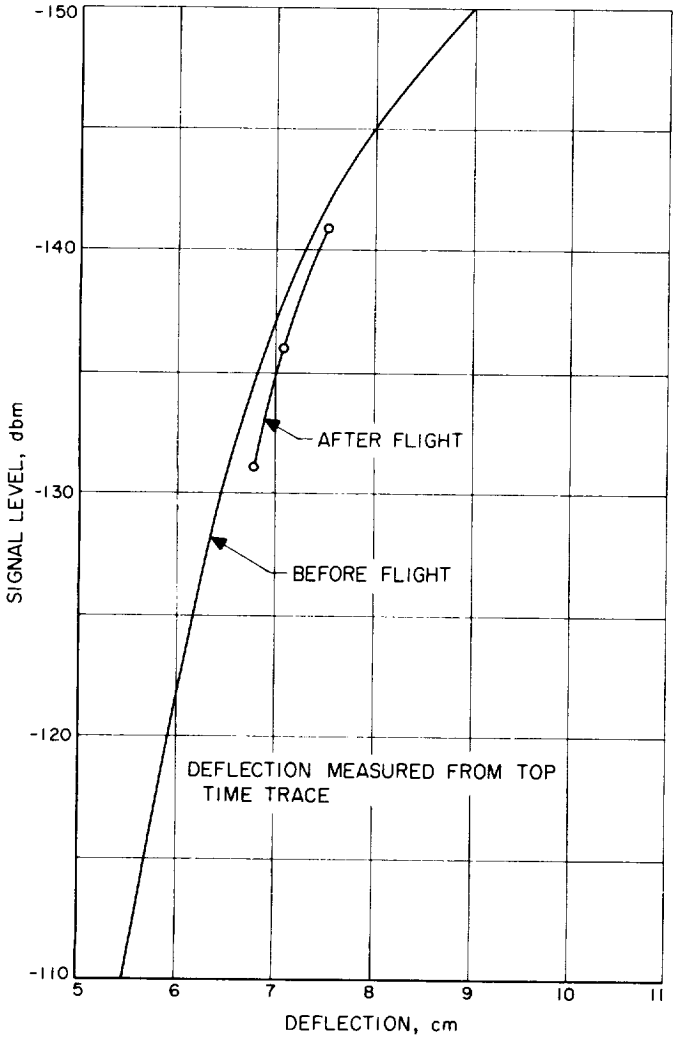

Figure 63. Signal level calibration

The signal levels as reduced from the Sanborn recordings are shown in Fig. 62 for comparison with the expected signal levels. A discrepancy was observed in the calibrations which were performed prior to liftoff and those which were made immediately following the end of the tracking period. The difference between the calibrations appears to vary from 1 to 4.5 db for the region of interest (Fig. 63). Therefore, the measured values for both calibrations are shown in Fig. 62 for comparison. On the basis of time, the postflight calibrations should be the more accurate.

The hour angle and declination of the probe during the Goldstone tracking period are plotted vs time in Fig. 64 and 65. An indication of the tracking accuracy is provided by comparing the hour angle and declination data from Goldstone with the best calculated trajectory data available at the present time. The comparison of the Goldstone angle tracking data with the calculated trajectory is shown in Fig. 64 and 65. The error curves represent the total error of the system due to refraction, boresight shift, mechanical collimation and alinement, mechanical deflection errors, and shaft-to-digital pickoff errors. The error curves were obtained by subtracting the measured angles from the calculated trajectory. The positive errors indicate that the antenna points east and south of the vehicle position indicated by the trajectory. Initially, the hour angle error is 0.17 deg; at this time the hour angle is approximately 300 deg; the vehicle is low in the east; and the antenna points below the vehicle. When the vehicle is low in the west, the antenna points below the vehicle again as indicated by the error −0.05 deg. The hour-angle error is zero when the position of the probe is near the meridian. The hour-angle error is almost linear in time and is less than 0.2 deg over the entire tracking period. The declination error is zero initially and increases linearly with time to a value of 0.1 deg at the end of the tracking period. The antenna points below the probe over the latter portion of the period.

The error curves generally show good agreement with the calculated trajectory. It is assumed that these errors are due to all or a portion of the following:

1. Boresight misalinement or boresight shift with antenna angle.
2. Mechanical collimation and alinement.
3. Mechanical deflection errors.
4. Shaft-to-digital pickoff errors.
5. Refraction.

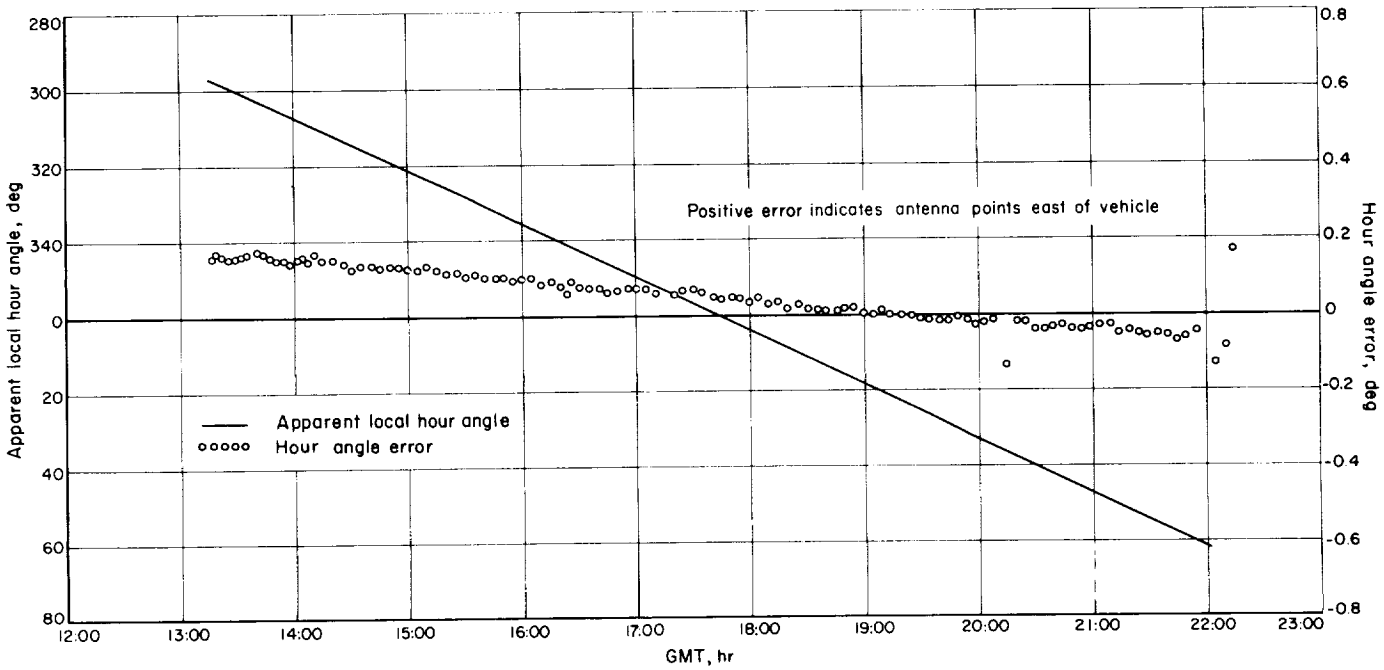

Figure 64. Comparison of hour angle with calculated trajectory

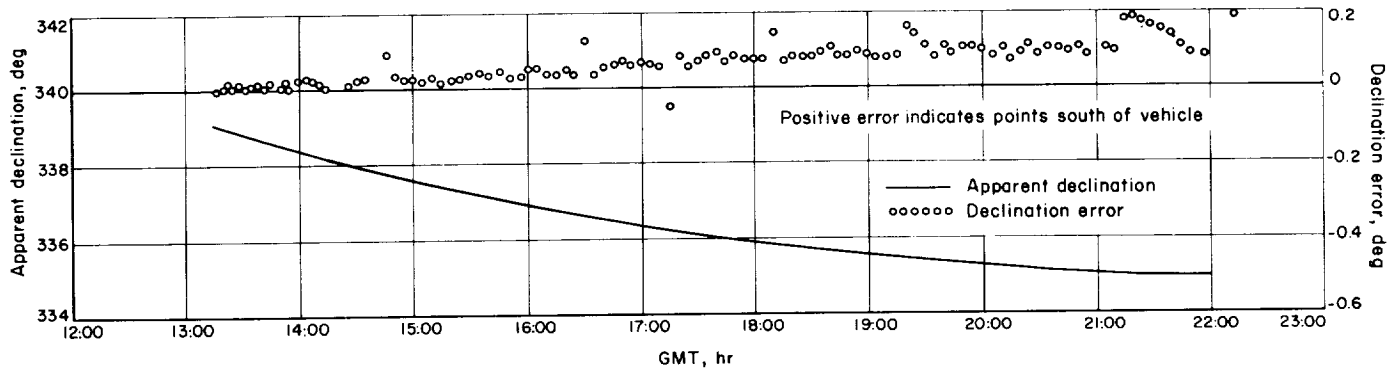

Figure 65. Comparison of declination with calculated trajectory

The investigation of the angle-tracking accuracy will be continued in order to determine the sources of error. New trajectories will be calculated with boresight shift and mechanical errors being considered.

All telemetry equipment functioned satisfactorily during the mission with one exception: an amplifier used to boost the signal strength data to obtain adequate VCO deviation failed. As a result, this information was not recorded on magnetic tape; however, the real-time analog recordings of this function were normal. Good data was obtained throughout the entire tracking period for all payload channels and receiver-servo functions. After approximately 9 hr of tracking, the probe was lost below the horizon and at that time the discriminators exhibited the thresholds as shown in Table 9.

Since these results are referenced to the equivalent received RF signal strength, they are subject to errors or uncertainties in this measurement, as well as the uncertainty in the actual carrier-to-side-band power as received during the mission.

Table 9. Tracking thresholds

RDB channel	In-lock	
	100%	50%
1	−147 dbm	−149 dbm
2	−148 dbm	−150 dbm
3	−147 dbm	−149 dbm

PART 2. JUNO IIA' (PIONEER IV)

Pioneer IV was the second experiment in the *Juno II* series, for which the vehicle is a modified *Jupiter* booster and a modified JPL cluster of three high-speed upper stages. Since the objectives assigned to *Pioneer III* were not fully accomplished, the same objectives were assigned to the *Pioneer IV* mission. The payload or probe was a spare from the *Pioneer III* operation; it had been modified to improve over-all reliability and to increase the scientific-data-gathering capability. Because of the close similarity between this system and the *Pioneer III* system, only the system modifications are described, as well as the results of the launching.

VI. SYSTEM MODIFICATIONS

A. Vehicle

1. Booster

The modified *Jupiter* booster, No. AM-14, used in this experiment consisted of the main body section with its propulsion system, and the instrument compartment which housed the guidance spatial-attitude control, events programmer, and cluster-drive motors, substantially the same as missile 11, the first stage for *Juno IIA*.

Since the failure of the *Juno IIA* booster to reach a proper booster-cutoff velocity was due to a malfunction in the depletion-switch circuitry (corrosion), new components were installed during testing in Florida. In addition, the arming of the cutoff devices (guidance cutoff and depletion cutoff) was rearranged.

The cutoff devices (guidance computer and depletion switch) were armed at such a time in the flight that even in the event of an early cutoff sufficient booster velocity would have been attained to insure reaching Moon velocity. Arming of guidance cutoff was set for 176.1 sec. This was the earliest feasible time for reaching proper booster velocity due to high engine performance.

The timing was selected as a 2-σ dispersion, mainly due to high flow rates. Arming of the depletion switch was to occur at 177.6 sec. This time represents the burning time required to reach a booster velocity increment, for standard engine performance, sufficient to reach the Moon. The chosen time sequence was considered an optimum solution with respect to failure possibilities.

2. Rotational Launcher

The rotational launcher was permanently attached to the forward end of the booster's guidance compartment. The launcher drive motors and their power supply are located in the instrument compartment along with the launcher-rpm control equipment. For this round this control equipment was set to maintain a constant rotational speed of 420 rpm during the first 133 sec of flight; it is then increased to 600 rpm and remains constant until Stage 2 ignition.

Six 4-in. nylon rollers were installed on the inner side of the shroud support at the level of the top of the rotational launcher. These rollers, preloaded to 100 lb each, provided lateral stability for the launcher and cluster, thereby raising the first cantilever mode frequency sufficiently above the spin rate of 600 rpm. This modification was primarily a test of a system that would be required on the future *Juno II* Earth satellites, and as such was not actually required at this time.

3. Cluster

The fairly large angular dispersion encountered with the *Juno IIA* high-speed stages suggested the addition to the *Juno IIA'* cluster of instrumentation to aid future dispersion analysis. Considering the limitations in time, weight, and telemetry, it was decided that only the determination of whether the second stage bumped the side of the launcher during firing would be attempted. The necessity of using the booster telemetry link made even this measurement difficult, since it meant maintaining electrical contact between the second-stage transducers and the launcher as the stage moved out of the launcher.

Two crystal accelerometers, Gulton Model A320, were installed on the outer rim of the aft bulkhead of Stage 2. These were connected to a dual-channel transistorized amplifier also on Stage 2. The two outputs were then carried to four wire-capsule devices mounted on the upper rim of the launching tub which allowed small wires (0.003-in. diam.) to pull out under tension, keeping the amplifier in electrical contact through slip rings with the booster telemetering system for the 42-in. length of the wires. Two channels, 9 and 13, were made available by ABMA in the booster telemetering system for these two measurements.

The wire capsules were designed to keep the small wire under tension while the second stage was leaving the launching tub and to break after 42 in. of travel with a maximum tension of 3.8 lb. A cutaway drawing showing the small wire peeling off the conical interior of the capsule is shown in Fig. 66. Since the cluster was

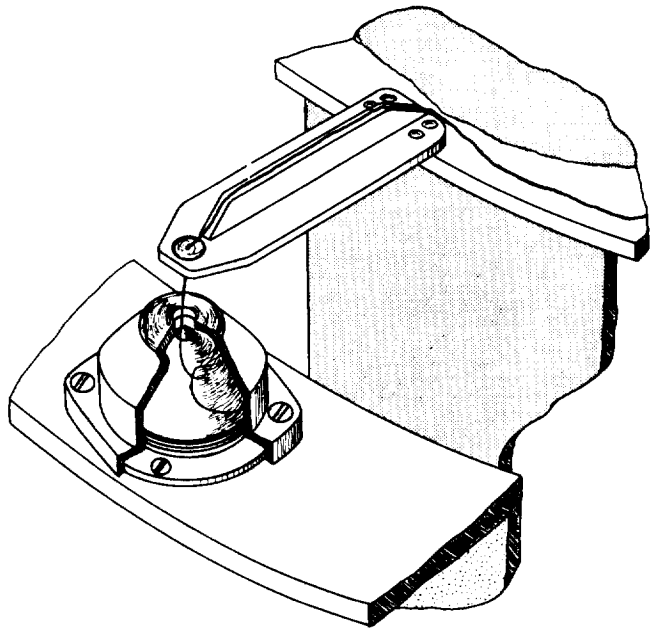

Figure 66. Wire reel

rotating, it was necessary to keep the wires under tension to prevent their contacting the shroud, only about 3.5 in. away.

The dual-channel transistorized amplifier was powered by self-contained rechargeable nickel-cadmium batteries sealed into a Micarta block. Figure 67 shows the amplifier with the two accelerometers and interconnecting cables; Fig. 68 shows a system block diagram. The amplifiers were calibrated to a full-scale range of ±100

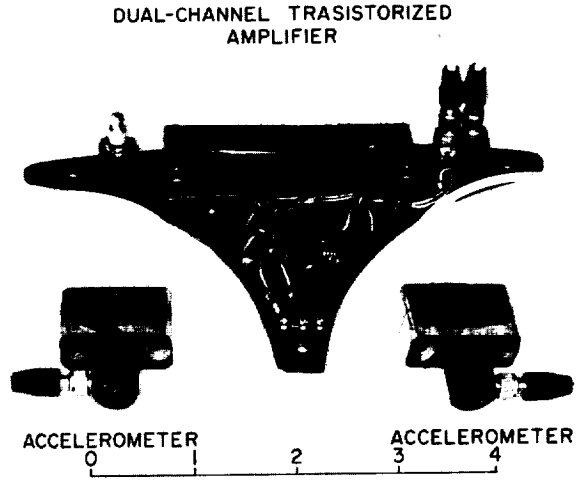

Figure 67. Dual-channel transistorized amplifier and accelerometers

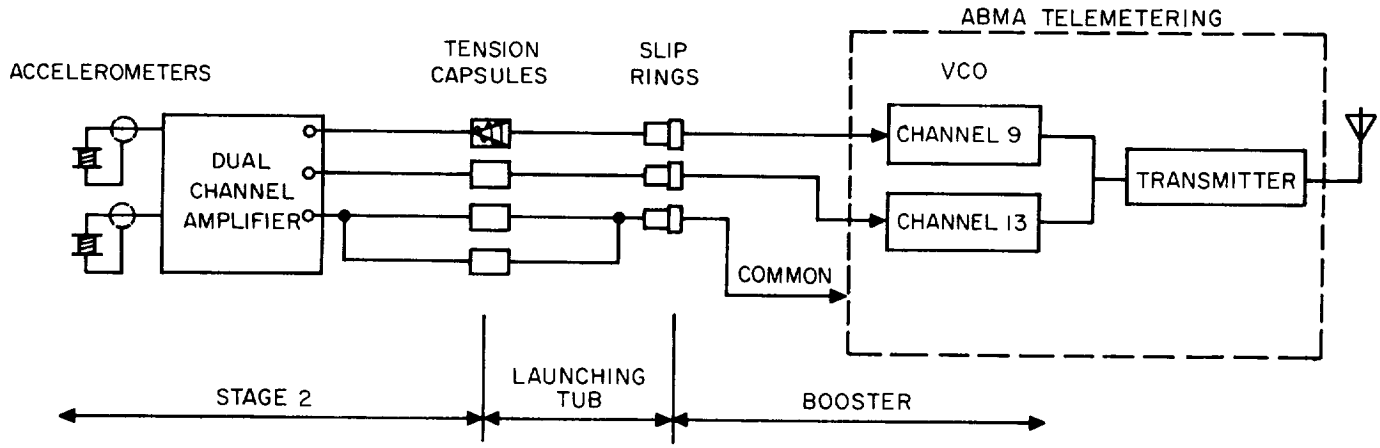

Figure 68. Vibration measurement system

g peak, based on a ±10 g-peak shake-table calibration of the accelerometers.

B. Moon Probe

Two payloads were prepared for *Pioneer IV*. These were the spare flight units, Serials No. 3 and 4, of the *Juno IIA* firing in December. In order to meet the slightly different requirements of the *IIA'* mission, the payloads were modified.

1. Scientific Experiments

The cosmic-ray experiment, consisting of an Anton 213 and an Anton 302 GM tube with their associated circuitry, was modified to the extent of shielding the 213 tube with 4 gm/cm² of lead. The shielding covered the forward end of the tube, subtending a solid angle which overlapped the angle subtended by the battery pack and the rest of the instrument package. Figure 69 shows the radiation deck and the shielded GM tube. These modifications were intended to provide additional information concerning the nature of the particles encountered in the radiation bands.

There were no modifications to the optical-trigger experiment of the *Pioneer III* probe. As mechanized previously, it shared channel 1 with the internal-temperature measurement. The design figure for the threshold distance of the optical trigger was 20,000 mi, based on a lunar-surface brightness of 1,000 ft-lamberts. The measured values for this distance made during preflight calibrations agreed closely with this design figure.

2. Engineering

Owing to an apparent 4-db discrepancy of received signal strength in the *Juno IIA* experiment, a modification was made to permit inflight monitoring of the RF power delivered to the antenna. The measurement was made at the antenna-feed connector by tapping a small percentage of the available radiofrequency power, detecting with a crystal diode, and telemetering the rectified dc current. Time sharing of channel 2 with the high-level radiation experiment was used for this measurement, with switch-over at X+5 hr.

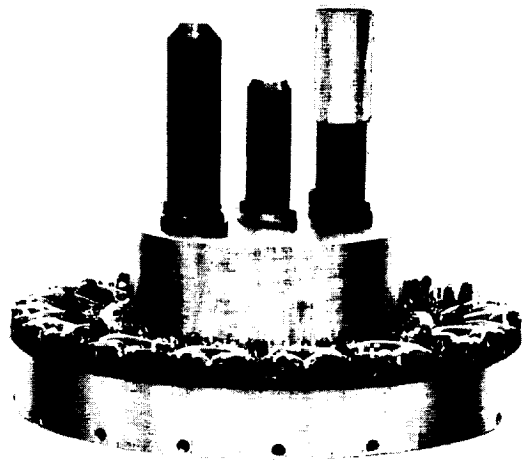

Figure 69. Radiation deck

Two minor changes were made in the telemetering system. The first provided for the power-monitor measurement of the transmitter. The second change permitted telemetering of the despin functions. Proper functioning of the despin mechanism was designed to cause a step change in the channel 1 frequency. The ultimate telemetering-channel assignments are listed in Table 10.

Table 10. Telemetering Channels

Channel	Center frequency cps	Measurements
1	400	Shutter-trigger operation Internal temperature Despin
2	560	Radiation, analog (shielded GM tube) Transmitter RF power
3	730	Radiation, scaler

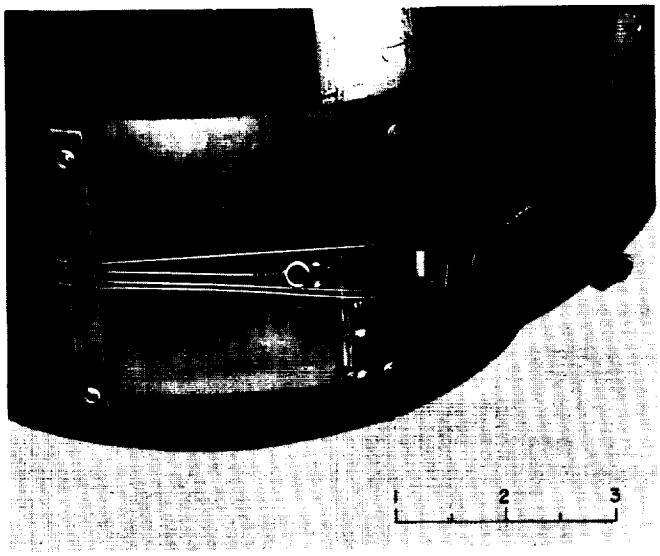

Figure 70. Despin mechanism

The despin mechanism (Fig. 70) was modified from the all-mechanical mechanism to an electromechanical system. An electrical signal from a timed switch closure actuated a pair of dimple motors associated with each despin weight. Extension of the dimple-motor bellows was arranged to withdraw the retaining pin, thereby releasing the weights. Power for the dimple motor was supplied by four nickel-cadmium cells arranged in series and located in the center of the payload on top of the transmitter desk. Two motors were used for each weight as a redundant feature to enhance the reliability of the system.

The hydraulic timer was modified to the extent of replacing the mechanical despin-release mechanism and trigger-arming switch with an arrangement of three improved switches. These single-poles switches were designed to close when the shaft of the timer had moved a preselected distance. The relative timing of the switch closures was fixed by their relative physical spacing. The functions of the switches in their order of occurrence was as follows:

1. RF monitor transfer (X+5 hr).
2. Despin (X+9 hr).
3. Trigger arming (X+12 hr).

C. *Tracking and Communications*

1. Launch Station

Located near the launching pad, the launch doppler station is mechanized with a 6-ft parabolic-reflector antenna.

The four-turn helical feed which illuminated the 6-ft reflector during the *Juno IIA* launching was replaced, for *Juno IIA'*, with a turnstile feed. Consisting of a turnstile mounted 2.9 in. forward of a 12-in. ground plate (both silver-plated for weather protection), the new feed afforded antenna gain of 21.6 db to a vertically polarized wave and 19.5 db to a horizontally polarized wave, compared to 16.4 db and 17.5 db, respectively, for the helical feed.

Alterations to the receiving system included installation of the test beacon on a 65-ft tower 275 ft from the receiving antenna. In the receiver proper, an additional 240-cps RF-loop noise-bandwidth position was added to the loop filter, and the foil-type tantalum capacitors used in the loop filter for *Juno IIA* were replaced with Mylar capacitors.

The following items were added to the telemetering system: three modified Hallamore phase-lock-loop discriminators, and a Midwestern 36-channel direct-writing oscillograph.

Only minor changes were made in the data-handling system; it operated without malfunction for *Juno IIA*.

2. Downrange Station

The downrange tracking and telemetry-receiving station again had the same mission of bridging the gap between the launch station and Goldstone station in point of time and, in fact, of providing Goldstone with necessary information for its acquisition of the probe. The station location near Mayaguez, Puerto Rico, was still considered satisfactory. This station had been deactivated following the *Pioneer III* operation, and was reactivated on 16 Feb 1959.

Although the station was in good repair when reopened, certain modifications were accomplished. In the receiving and antenna system, the loop filter was replaced with a unit using Mylar-dielectric capacitors

instead of liquid tantalum capacitors, to prevent leakage. The pole beacon antenna was provided with an antenna feed rotor, to permit ground control of antenna polarization angle, in 10-deg increments, affording more complete antenna calibration in less time; in addition, the pole-beacon attenuator system was revised. A variable attenuator was placed at the output of the beacon. Substituting fixed pads as standards and utilizing the receiver as a monitor, the variable attenuator was accurately calibrated from 20 to 90 db. Control of signal level was then smoothly controlled to the threshold of the receiver. Some leakage was detected at the output connector of the beacon when operating at low signal levels however. Substituting fixed pads, the first two steps of the beacon attenuator were calibrated. The resultant method of operation utilized the variable attenuator exclusively for signal levels greater than −110 dbm. For signal levels lower than −110 dbm, 20 db of the pole beacon attenuator was used additionally.

The data-handling system was modified to improve circuit operation of the signal gate in the doppler counter by replacing a diode gate with an RC network; the digital visual-display units were redesigned and modified by Collins Radio Co.; and frequency dividers in the clock and the doppler counter were made more reliable by the substitution of 2N460 transistors for 2N44's.

In the telemetering system, the phase-coherent discriminator loop bandwidth mechanization was altered to provide constant loop gain in all bandwidth positions, thereby improving threshold performance. Loop bandwidths were as indicated in Table 11.

The time encoder was modified at Goldstone.

A Hallamore dc amplifier was added following the data-conditioning chassis in the receiver signal-strength line to compensate for attenuation in the data chassis, giving greater deviation in RDB channel 5. The discriminator manual search potentiometers. The Ampex tape transport hubs were adjusted to accommodate the precision reels used with Mylar backed tape.

A Krohn-Hite adjustable bandpass filter was inserted into the spin-modulation line ahead of the Sanborn A input. This narrowed the passband so spin rate could be read more accurately. Tests using the spin-modulated (10 cps) pole beacon showed improved readability using a 9-11 cycle passband at receiver signal strengths greater than −130 dbm.

Table 11. Loop Bandwidths

Channel	BW, nominal	BW, measured
1	2	1.93 (3.5% narrow)
2	2	1.91 (4.5% narrow)
3	4	3.94 (1.5% narrow)

D. Goldstone Deep Space Tracking Station

Modifications in the Goldstone station for the *Pioneer IV* flight were generally on a design-detail level, and were more in the nature of one phase of a continuing program of improvement than of a single series of changes for a specific mission. For example, in the receiving system, filament wiring was altered by using shorter runs of heavier wire, to provide higher and more uniform filament voltages throughout the receiver; manual switches were wired across the power-distribution relay contacts, to avoid transients due to relay-contact failure; and a digital voltmeter and printout unit were connected to the AGC bus. In the antenna servo system, a battery box with a 10K 10-turn helipot was installed in the optical cage, to give the observer direct adjustment of the hour-angle rate; variable bandwidth networks for the servo networks in both the declination and the hour-angle axes were installed; and a pressure interlock was added to the hydraulic system. The data-handling system was modified in that the toggle and clock boards were improved (the same replacement of 2N44 with 2N460 transistors later accomplished but already described for the downrange station) and blowers were provided to lower transistor-board operating temperature. In telemetering, the mechanization of spin-modulation recording and of loop bandwidth in the phase-coherent subcarrier discriminators was improved, the first to provide greater bandwidth versatility and the second to improve over-all threshold performance.

VII. PREFLIGHT PREPARATION

Preparation for the *Juno IIA'* mission was essentially identical to that for *Juno IIA*, with the exception of certain matters related to system modifications. Particularly these differences had to do with the installation of a cluster telemetering package and an additional cluster support system; other modifications had less obvious effects on preparation and checkout operations.

A. Cluster

Cluster No. 12 was received at Cape Canaveral on 21 January, and was unpacked and readied for inspection. Inspection showed that one set of wires on the stage 4 motor case was not properly bonded to the case. No other damage was observed. The motor pressure checks were satisfactory, and the igniter birdcages were all in their proper positions.

1. Launcher

After inspection, work began on the installation of the wiring modification for the stage 2 accelerometers. Since the booster telemetry system was to be used for the data link, a system was devised for the proper routing of the accelerometer amplifier signals. These signals were fed through four 0.003-in. steel wires, two for return leads, and one for each amplifier output. They originated in the amplifiers on the top bulkhead of stage 2, and were then fed to the top rim of the tub, down the outside of the tub through an exhaust port in the tub base, into the tub wiring, and finally through the slip rings into the instrument compartment of the booster. The leads through the exhaust port were protected from the motor flame by running them through an asbestos-covered metal tube.

On 4 February, the first cluster electrical checkout was made. On 18 February, the final electrical checkout was made. There were no troubles encountered in either check.

After moving the cluster to the gantry, the telemetry was checked by placing standard calibrating voltages in series with the accelerometers, and reading the output of the accelerometer amplifier in the ABMA telemetry trailer at the pad.

Ten lines were provided from the launcher distributor terminal strip E-420 into the blockhouse. Slip-rings 6, 7, 8, 9, and 10 were connected to the payload control panel in the blockhouse, from which payload checkout functions could be switched. These functions were 1) commit payload transmitter; 2) turn on and off payload transmitter; 3) transmitter filament preheat. A block with a meter and resistors was made to engage the finger contacts in order to simulate the payload to the control panel, and to check the control wiring during flight countdown.

The first opportunity to observe the effect of the nylon rollers on the cluster occurred on 24 February after the cluster was mated with the booster. A dial indicator was set up using the shroud as a base, and readings were taken on the ring at the top of the stage 3 cone. With no preload on the rollers, the TIR was 0.002 in.; with a maximum preload of 100 lb on each roller, the TIR increased to 0.012 in. This increase was primarily due to the fact that the contact surface between the tub and rollers had a runout over 0.020 in., and the preload spring constant was in the neighborhood of 10 lb/0.001 in.

At the scheduled time for checking out the ABMA speed-control box with the cluster, the speed-control program was still being discussed. Therefore a guess was made, and the control box was checked out under these conditions. Essentially it was assumed that the initial speed would be 420 rpm, and the terminal speed would be 600 rpm. The battery step occurred at 133 sec, and the pulse change at 135 sec. It took 32 sec to make the step from 420 rpm to 600 rpm, with an approximate 10-rpm spin overshoot.

A spare box was checked out under the same assumptions just before the cluster was removed from the spin building.

2. Stages 2 and 3

All the motors in Stages 2 and 3 were pressure-tested five times. They were checked at JPL after they were cast, at the vendor assembly area before they were shipped to Florida, in Florida immediately after receipt, in the spin facility after all assembling, balancing, and aligning operations had been performed on the cluster, and just prior to removal of the cluster to the pad for assembly on the booster. During the pressure test at the vendor assembly facility, it was noted that two motors in Assembly 2 did not hold pressure. Examination revealed that this was due to faulty soldering where the diaphragm is sealed to the convergent section of the nozzle. Consequently, both nozzles were replaced. These motors were again pressure-tested with satisfactory results.

At each of these pressure-check intervals, the alignment of the grommets in the igniter support assembly was checked. No irregularities were uncovered in any of these tests.

The standard RD-7 igniters, which had been used in the motors of Assemblies 2 and 3 on all previous flight rounds, were used on this vehicle. They were checked for continuity three times. These checks were conducted at the point of manufacture, at JPL before shipment to Florida, and finally, in Florida several days prior to flight.

3. Stage 4

The last-stage motor was first pressure-checked at JPL before shipment to Florida. The result of this test was satisfactory.

The motor, TC-25, was prepared for arming by removing the paint from the area adjacent to the nozzle-case mating surfaces with acetone and MEK. The threads were also cleaned with these solvents to remove Celvacene which had been placed there before the motors were shipped. The igniter was inserted into the motor, Celvacene was placed on the nozzle thread relief, and the nozzle was bottomed into place. The pressure check was started. It was observed immediately that the motor would not hold pressure, and leakage at the nozzle was considerable. The nozzle was removed, and the igniter was taken out. Inspection of the diaphragm revealed that a piece of the nickel plating, about $\frac{1}{8}$ x $\frac{1}{16}$ in. had broken off from the copper near the seat. Another igniter was substituted and inserted in the motor. Again Celvacene was applied to the nozzle thread relief, the nozzle was bottomed in place, and the motor was pressure-tested. After 19 min, the pressure remained constant at 15.0 psig Armstrong cement was applied to the nozzle-case mating surface.

The motor was again pressure-tested after the Armstrong cement had cured. Pressure remained constant at 15.0 psig for 19 min. The pressure test plug was removed, and the flight head-end plug with stud, spring, and pedestal attached, was inserted in place. The igniter was then checked for continuity with the following results:

Resistance across igniter ..... 0.29 ohms
Leakage resistance igniter-to-ground ..... ∞

Several minor difficulties were encountered during operations on the assembly 4 motor. Upon receipt of this motor in Florida, it was noted that the potting on one side, where the wires had been laid up, had come loose from the case. This was attributed to the use of potting compound beyond its pot life. The old potting was removed, and the wires were repotted in place. It was estimated that there was no weight change as a result of this operation.

Just prior to flight, as the payload adapter was being mated to the motor, one of the nut blanks, which had been potted to the forward support sleeve, fell off. It was removed and the screw was held in place on the fractional threads in the support sleeve.

B. Payload

The preflight preparation for *Pioneer IV* commenced with the shipment of the payloads to SUI for radiation calibration by Dr. Van Allen. The first package (serial 3) arrived at SUI on 9 February, and was calibrated and then sent directly to CCMTA, arriving there 11 February. The second assembly (serial 4) followed three days later.

The first few days at the Cape were almost completely devoted to setting up the checkout area, and to repairing the test gear which had suffered some deterioration since the December firing. In the meantime, the payloads were mechanically mated to the cluster, and preparations were made for spin-up.

Following the payload cluster checks, performance tests were begun on both units prior to final assembly. In general, the performance tests were a review of the temperature – supply-voltage calibrations made at JPL, performed at the ambient temperature. Evaluation of the payload performance was based on how well the data recorded in the field fitted the calibration data taken at the Laboratory.

In the afternoon of 23 February 1959, measurements were begun on side-band power level of serial 4, using the SB 12A spectrum analyzer. It appeared that the modulation level was considerably less than it had been a few days earlier. The carrier shrinkage was reduced from 3 db to 1 db. Some question was immediately raised over the fidelity of the test equipment. A measurement was therefore made on the other payload; the results were the same. At this point operations were suspended for dinner, and when they were resumed after about an hour, measurements on both payloads were normal again. It was then concluded that something was wrong with the test equipment. Although nothing definite was established, it was resolved to check the side-band level measurement frequently for recurrence.

On 26 February 1959, the RF monitor measurement on serial 3 evidenced a large, unexplainable level shift resulting in the nominal full power rest frequency changing from 525 cps to 565 cps. This had no effect on the radiation measurement which time-shared the same channel. After several hours of investigation, no cause for the change could be found.

The same day, the sideband anomaly reappeared on serial 4 but not on serial 3. On the following day, serial

4 sideband levels were normal again, and the payloads were again open to suspicion. A calculation of the total power in the sidebands for the low modulation case showed that the levels fell short of the system specification by only 1 db, owing to the margin of total power delivered by the transmitters. With less than two days remaining before firing, any major tear down or trouble shooting would certainly have resulted in a hold, and possibly a complete cancellation. The decision was therefore made to proceed regardless of the sideband levels.

Serial 4 was selected for the flight unit, first because of the RF monitor change in serial 3, and second because it was judged to have more desirable characteristics on the basis of the performance tests. Subsequent events were to dictate, however, that serial 3 must carry out the flight. These events are covered in Sec. VIII.

Final preparation included surface sterilization of the lunar probe, to preclude the possibility of biological contamination of the Moon in the event of impact.

C. Tracking System

Preflight operations consisted of a number of equipment modifications and additions to correct deficiencies noted in the *Juno IIA* operation. Systems tests were then conducted at all stations to check over-all station operation. Helicopter tests were performed at the down range and Goldstone stations. These tests served a dual purpose: (1) to increase operator familiarization and (2) to evaluate over-all system operation. Additionally, the Goldstone station conducted several star tracking tests to evaluate further the antenna positioning and accuracy. Two dummy runs were successfully conducted.

Countdown for the operation was first begun on 1 March, and satisfactory status reports were given for all tracking stations. However, payload trouble at approximately X−10 min caused a reschedule. The second and final countdown started 2 March. This countdown continued successfully with lift-off occurring at 05:10:56 GMT, 3 March 1959.

1. Launch Station

The alterations and additions to the receiving and telemetering systems described in Sec. VI-C were accomplished; the data equipment was turned on and checked, and was modified to include the data-condition word. During the preflight checkouts, several problems, the results of inadequate design or poor construction practice, were discovered. The automatic sample-rate selector circuit was damaged during checkouts, and all sample-rate changes had to be accomplished manually during the flight. The standard-frequency-oscillator accuracy evaluation was complicated by equipment problems, but sufficient measurement time was available to determine that the frequency was approximately 7 parts in 10^9 of WWV (transmitted).

System tests consisted of receiver sensitivity measurements, data handling tests, telemetering and recording tests and calibrations. All equipment operated normally.

D. Communications Net

Modifications and additions to the communications and data net, which experience gained during the *Pioneer III* activities indicated were necessary, were installed and checked out by 1 February. Teletype maintenance and operator support were again provided by Signal Corps and RCA personnel, augmenting Laboratory personnel, particularly at the off-Laboratory tracking stations.

A more extensive program of pre-operation practice runs and circuit tests was conducted during the six weeks prior to the launching in order to test the modifications made, to gain a better statistical record of equipment and circuit reliability, and to provide further training of communications personnel. Seventeen such tests were performed, including two over-all systems tests prior to launching.

1. Equipment

Equipment reliability was quite satisfactory in that very few malfunctions were encountered. Although some malfunctions are considered unavoidable, the reliability of equipment will be further improved by the introduction of a preventive maintenance program, now being formulated, to cover the between-operations periods.

2. Leased Circuits

A marked improvement was noted in the reliability of leased teletype circuits between Pasadena and Florida. This resulted in part from improvement of Telco equipment in the Jacksonville and Atlanta stations, and from diverting one of the circuits through Washington, D.C. Other than the increased gain on the White voice net as a result of the system modification, the over-all voice nets were acceptable, as was the case in the December operation.

3. Personnel Training

The series of tests and checks served as a refresher for the personnel previously involved in this system, and as training for new JPL and Signal Corps operators recently assigned on a temporary basis. Proper message center procedures and net discipline were fully documented and stressed; this resulted in improved message handling and interstation contacts.

VIII. PAD OPERATIONS

The possible launching period for *Juno IIA'* was a five-day period from 28 February to 4 March 1959; two or more firing times at least 30 min apart were provided for each day. The earliest possible firing time was at approximately 2100 EST, 28 February; each subsequent day the earliest time was approximately 1 hr later.

Launching was first scheduled for the evening of 28 February. The timer, serial 24, was tested during the preflight countdown, and gave times of (a) 8.0, (b) 13.8, and (c) 16.5 sec as the three functions of (a) Stage 3, (b) initiate separation delay train, (c) Stage 4. The flight battery checked 23.7 volts under load.

The firing was originally scheduled for trajectory 10318, but was cancelled due to predicted low ceiling and low visibility. Mandatory requirements by Range Safety for any launching at the Cape are a 200-ft ceiling and a 4-mi visibility in order to provide for optical tracking to sufficient altitude for reliable S-band radar beacon tracking.

A. 1 March 1959

Rescheduled for trajectory 20416, preparations for the firing were proceeding smoothly except for C-band radar and weather. The initial radar problems were in the ground station and were apparently due to a power supply cable failure early in the countdown. Also, corrosion of the wave-guide joints had warped the guide and had produced RF loss and heating at the joints. The trouble was eventually repaired, and the radar operated properly during the tests at X-45 min.

The weather prediction indicated a mild frontal passage with rain squalls and gusty surface winds, subsequently clearing to good visibility and ceiling by firing time. The squalls passed with considerable rain around 1900 to 2100 EST, leaving gusty surface winds, but the weather was satisfactory for launching by firing time.

Much of the preparation of payload serial 4 had been completed the previous day, and the remainder was done earlier than scheduled so that the completed fourth stage could be transported to the pad and placed on the third platform at about 1400, prior to the predicted rain squalls. Checkout of the payload control wiring to the blockhouse was performed as scheduled, but the filament preheat current appeared to be low. The wiring was checked through all the connections from blockhouse panel to third stage and no fault was found. Later checking indicated that circuitry modification had changed the shunt across the panel meter giving an unexpected reading for the correct current.

Cluster work proceeded normally to completion. Several corrections were noted in the JPL countdown and its incorporation in the MFL countdown.

During igniter connection to Assembly 3, potting compound was found on the connector threads which required a few minutes for cleaning.

By X-25 min, satisfactory status reports on the tracking net and the payload had been received in preparation for firing the payload squib switch to transfer the payload permanently to internal power for flight. At X-20 min the COMMIT plug was inserted, and a short was seen on the meter instead of the normal momentary pulse. On turning the power switch to OFF the payload went off, indicating that the squitch had not fired. Additional attempts to commit were also unsatisfactory, and at about X-10 min it was decided to return the countdown to X-30, and to prepare for the second firing time on trajectory No. 20504.

The blockhouse payload panel connector was disassembled and found to have a poor connection on one lead and pinched insulation on another, but neither wire was involved in the circuits in question. The connections to the plug were remade properly.

Since the payload could not be turned on permanently, and the trouble could not be diagnosed as corrected without removing the payload, the firing was cancelled and rescheduled for trajectory 30511.

In reversing the cluster preparation, the second-stage ignition leads were disconnected and shorted, the ignition and timer battery shorting plugs were removed, and the igniters disconnected and shorted but not removed. The shroud was unbolted and lifted, but the surface winds made the bulky, light shroud virtually unmanageable. The shroud was set back in place, the shroud cone explosive bolts removed, and the cone taken off. Although working conditions through the RF windows and over the shroud were very poor, the fourth stage was finally removed, taken down in the elevator, and returned to the Spin Building.

Examination of the payload revealed that the squitch circuitry had been miswired, and that the additional attempts to fire the squitch had burned out several components in one of the power supply networks.

Those components which were accessible were replaced and retested, but some question existed regarding required repair and recalibration of damaged interior portions to which access was impossible in the time available. Serial 4 was unquestionably preferable to serial 3 in terms of better performance of the transmitter and the experiments, particularly since the RF power monitor in No. 3 had shifted calibration in Florida. However, additional testing proved that internal damage to No. 4 had resulted, and there was no choice but to fly payload No. 3. The heat-balance paint pattern was revised on both payloads.

B. 2 March 1959

Launching preparations began as scheduled at 1206 EST, 2 March, at X-540 min. The only changes required in the JPL countdown were to check off as completed those items concerning igniter installation and Jupiter fueling.

On countdown day, 2 March, the connection terminal on Stage 2 carrying channel 9 signal to the wire in the tension cone was found to be broken. The wire was resoldered.

Delivery of the payload to the pad was about 45 min late since payload preparation had been delayed by the additional trouble shooting, paint-pattern revision, etc. The delay was relatively unimportant since much of the MFL work normally done in the 2 hr scheduled hold at X-220 had already been accomplished. Since the delay had been anticipated, Stage 2 and 3 igniter connection was completed prior to Stage 4 insertion. The height of the fourth stage and fixture was reduced by adjusting the payload cover so that the transfer to the third level could be done on the elevator rather than by hoist. Stage 4 installation and payload checkout, up to the point of igniter connection, required 64 min, for which 20 min is allotted in the countdown preparation. Part of the 44-min difference is accounted for by poor access to the cluster with the shroud installed, and by the absence of the Stage 4 installation guides, but additional time should be allowed in the countdown for this work. The installation guides had to be removed from Stage 3 the previous evening as part of normal procedure and could not be reinstalled without a special adjustment fixture which was not available.

The payload timer was started at X-140.5 min or 1846:30 EST. Comparative readings during payload checkout between the Launch Doppler Station and the Gold Microlock Station indicated a malfunction in the Microlock Station counter. The trouble was found and bypassed prior to the second checkout at X-47 min. Good comparison was obtained from the latter readings.

The countdown procedure was slightly revised for the payload in that the payload was turned on at X-47 min following the second planned hold, and left on through the third planned hold of ½ hr at X-30. Just prior to picking up time at X-30, satisfactory status reports were obtained on the payload and tracking net, and the payload was committed to internal power. Satisfactory status reports were also obtained at X-16 and X-5 min. A short, planned hold was called at X-2 min to adjust the count for the desired lift-off time of 0010:50. Actual lift-off time was 0010:56.7 EST, 3 March, or 0510:56.7 GMT since the LOX vent valve and a fuel system valve were each about 3 sec slow in operation.

Booster flight was normal with cutoff occurring at 183.1 sec of flight compared to predicted 180.9 sec. Times for booster separation were 189.3 actual, and 187.0 predicted The second-stage ignition times were 242.6 actual, and 240 predicted. Booster cutoff velocity was very close to the predicted time. Operation of the high-speed stages was reported by the launch Doppler station, with the total Doppler shift being slightly less than predicted.

Weather conditions reported at 0016 EST at the Cape were as follows:

Temperature	8.6°C
Relative humidity	70%
Pressure	1018.2 millibars
Wind	5 knots at 310 deg
Visibility	10 mi

IX. PERFORMANCE

A. General

Boosted to escape velocity by a *Juno II* propulsion system, the 13.4-lb payload of *Pioneer IV* coasted to within roughly 37,000 mi of the Moon on the afternoon on March 4, and continued on, in heliocentric orbit. The new planet transmitted information back to Earth for a distance of 407,000 mi until its batteries were exhausted after about 82 hr of flight. At its closest approach to the Moon, the probe was 236,500 mi from Earth, and its velocity was 4,490 mi/hr radially away from the Earth.

At the time when signals failed, at 10:15 AM on 6 March 1959, the probe was traveling at a lower speed, due to the pull of gravitational force from the Earth: 3,880 mi/hr. On 17 March 1959, eleven days later, the probe was over 1.6 million miles away, having become subject to the gravity force of the Sun, around which it now assumed an elliptical orbit. Its speed of rotation around the Sun being compounded of the orbital speed of the Earth and its own residual escape velocity of about 3,000 mi/hr, the probe should be traveling now at an average of 64,800 mi/hr, requiring 395 days to complete its own elliptical orbit around the Sun.

B. Vehicle

In Table 12, the major incidents of the powered-flight history are indicated.

Table 12. *Pioneer IV* powered flight history

Event	GMT (3 March)	Time from liftoff, sec		Source
		Actual	Nominal	
Actual liftoff	05:10:56.7			
Nominal liftoff	05:10:50.0	—	—	*Jupiter* telemetering
Inflight spinup	05:13:09.8	133.1	135	*Jupiter* telemetering
First stage burnout	05:14:00.1	183	183	*Jupiter* telemetering
Booster-top separation	05:14:05.9	189.2	187	*Jupiter* telemetering
Shroud separation	05:14:18.5	201.8	200	*Jupiter* telemetering
Cluster ignition	05:14:59.2	242.5	238	*Jupiter* telemetering and doppler analog
Stage 2 burnout (approx)	05:15:04.9	248.2	—	Doppler analog
Stage 3 ignition	05:15:09.2	252.5	246	Doppler analog
Stage 4 ignition	05:15:19.0	262.3	255	Doppler analog
Stage 4 burnout (approx)	05:15:25.5	268.8	—	Doppler analog
Separation	05:15:33.3	276.6	268	Launch station signal strength

C. Probe

Data obtained from the transmitter indicated satisfactory operation of its components, with the exception of a transmitter power monitor and a photo-electric scanner. This device, also referred to as an optical shutter trigger, was intended to be actuated by light from the Moon at a much closer distance than was reached by the Moon probe. During the flight the mechanism was actuated and images were produced. It is conjectured that the scanner was actuated by light from the Earth. Below is a summary of the telemetry findings relative to this scanner and the other sensory devices.

Channel 1 was used to monitor the operation of the triggering of the despin device and the behavior of the optical trigger. Temperature data was also interpreted from the frequency of channel 1.

The actuation of the despin device was expected to occur approximately 10 hr after injection. At 16:32:34 GMT (approximately 11 hr and 20 min after injection), the actuation of the despin mechanism was indicated by channel 1. Simultaneously, the spin rate of the payload dropped from 415 to 11 rpm, a decrease by a factor of 37. The design decrease factor in spin rate was 50.

Prior to the actuation of the despin mechanism, changes of state had been observed in Channel 1 indicating optical intercepts and whether or not the shutter-trigger device was working properly. One such change occurred at 07:21 GMT, approximately 2 hr after injection. At the time of signal loss after the first tracking period at Goldstone, Channel 1 was observed to be in one of the lower states, as expected, since the memory circuit should not have been armed. When Goldstone acquired signal on the next pass (at approximately 12:30 GMT, March 4), channel 1 was observed to be in the highest state indicating that the memory circuit had been armed and that the shutter-trigger mechanism had responded to some illuminated object during the interval from shortly after leaving the vicinity of the Earth until this time. In fact, the only illuminated object capable of causing a coincidence in the optical system of the shutter-trigger mechanism during the whole flight of

Pioneer IV was the Earth, which could be seen by the optical system very shortly after injection. From that time on, no other known source was available. The point of closest approach to the Moon was too far for operation of the device.

At 18:37:58 GMT, a change of state was observed in channel 1 by Goldstone tracking. About a half hour later at 19:06:32 GMT, a reverse change of state was observed. These and other changes of state observed in channel 1 have as yet to be satisfactorily explained.

Weights of the payload components are noted in Table 13.

Channel 2 was used to monitor the radiation data from the Anton 213 Geiger-Mueller tube from time of launch until approximately 5½ hours after launch. The activity of channel 2 in making this measurement was quite satisfactory, and good radiation data is available. From 5½ hours after launch and throughout the rest of the flight, channel 2 was transferred to measure the output of the radio frequency power monitor of the transmitter. However, no such measurement was indicated by the data received on channel 2. Channel 3 gave indications of the output from the scalers which were being driven by the Anton 302 Geiger-Mueller tube. The behavior of channel 3 was excellent throughout the flight (although the highest speed scaler apparently failed to operate, since the data at the highest rates through the two radiation belts was not indicated in the channel 3 frequency changes). At lower levels of radiation, the behavior of channel 3 in the two lower scaling networks was good. Data on radiation from this channel is available until shortly before the last contact with the probe, some 83 hrs after launch. Only small regions near the peak of the true radiation belts are missing. The data did indicate, however, the dip in radiation level between the two belts, and were sufficient to provide a comparison on the length of the belt between this test and that of *Pioneer III*.

Table 13. Weight of payload components of *Juno II* Missiles

Component	Weight lb
Antenna assembly	0.50
Balancing weights	2.20
Batteries	7.17
Despinning device and damping weight	0.37
Power supply	0.97
Radiation counter circuitry, subcarrier oscillator	1.01
Shutter trigger	0.32
Separation device	0.81
Structure	2.07
Timer	0.50
Transmitter	1.35
Total	15.27

The temperature of the payload rose to about 43°C soon after the payload left the shadow of the Earth and entered into complete sunlight. Its temperature stayed at this level throughout the rest of the monitored flight.

Up until the time battery power began to fail, approximately 80 hrs after launch, the signal level at the Goldstone site was sufficiently high to indicate the capacity for checking this type of payload to a distance of more than one million kilometers, provided that adequate battery lifetime was available.

X. TRACKING SYSTEM PERFORMANCE

The times at which each of the three JPL stations (Cape Canaveral, Puerto Rico, and Goldstone) acquired and lost the signal and the ranges from the stations at those times are shown in Table 14. Similar data for Jodrell Bank are now available. During the early portion of the flight, Jodrell Bank was tracking for a 15-min period coincident with tracking by each of the three JPL stations. Thus, for 15 min after the first Goldstone acquisition, four stations were tracking simultaneously.

Angular position and frequency data from the Puerto Rico and Goldstone stations were automatically teletyped to the JPL computing center during the tracking period. The tracking data from Jodrell Bank was transmitted to the computing center at the Space Technology Laboratories (STL) in Inglewood, California, along with some of the data from the JPL stations. The two computing centers maintained continuous communications with each other throughout the tracking period. The trajectory information derived from the two computing processes was quite similar. This Report summarizes only the procedure and results obtained at the JPL computing center.

A. Launch Station

The receiver checkout and calibration proceeded satisfactorily during the final countdown. At X-47, the receiver was locked to the probe. Liftoff occurred at 05:10:56 GMT, 3 March 1959. The receiver maintained lock until 12 min after liftoff when the probe dropped below the horizon. At 08:14:00 the probe was again above the horizon and the receiver was again locked to the probe. Lock was maintained until 11:50:00, when lock became intermittent. Goldstone had acquired by this time and the launch station secured. The sampling-rate automatic change did not function properly during the flight. Telemetering channel 1 and 2 thresholds were −146 dbm, −3 db lower than the channel 3 threshold—for 90% lock. These discriminators were returned to Pasadena to be tested. The timing signal from AMR was cut off during a portion of the flight. All other launch station equipment functioned normally.

Figure 71 shows recorded signal level and the expected signal level recalculated with the altitude of the probe as obtained from the data of the optics experiment. This chart shows the period after the probe reappears over the horizon. During the initial flight, between Stage 4 separation and the disappearance of the probe over the horizon, elevation angles were less than 10 deg, and a good comparison between recorded and expected signal levels is not attainable.

Although a manually tracking antenna was used at the launch station, gain figures for the calculated signal level have been based on the maximum value of antenna gain.

Table 14. Periods of tracking for four stations

Station	Acquisition time, GMT	Range from station, km	Elevation above local horizon, deg	Loss time, GMT	Range from station, km	Elevation above local horizon, deg	Date
Launch	—	Liftoff	—	05:23:19	5,228	~0.4	3/3/59
	08:00:00	52,619	0.4	12:00:00	97,978	3.4	3/3/59
Downrange	05:15:41	1,308	6.0	05:56:11	18,091	1.6	3/3/59
	06:31:31	28,960	2.1	18:18:21	164,096	1.8	3/3/59
Goldstone	11:47:51	98,402	4.4	20:55:01	187,625	4.6	3/3/59
	12:34:01	314,676	5.8	21:14:01	379,326	4.0	3/4/59
	12:37:41	486,783	5.9	21:18:21	544,604	3.7	3/5/59
	12:50:21	643,797	8.1	15:15:11	656,978	27.3	3/6/59
Jodrell Bank	06:31[a]	27,538	16.5	12:23	105,722	−0.7	3/3/59
	07:42	276,404	11.4	12:54	317,941	−0.8	3/4/59
	05:39	439,590	0.4	12:58	489,773	−0.8	3/5/59
	05:41	599,197	0.8	12:59	645,736	−0.8	3/6/59

[a]Periodic tracking between 06:31 and 07:00 GMT.

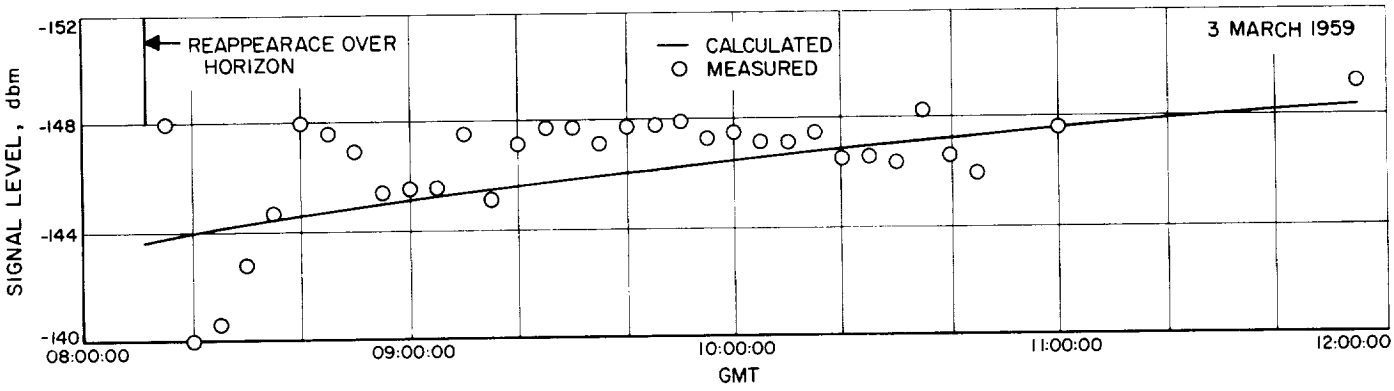

Figure 71. Launch station signal level for Pioneer IV

The gain correction for the pointing error and polarization of the receiving antenna has been applied to the recorded signal levels. Because of this correction, the recorded signal level as shown in Fig. 71 is actually as much as 2.5 db less at the receiver input.

The accuracy of the measured signal levels is based upon the possible errors in the calibration of the receiver and the resolution of the recorded signal. The calculated value accuracies are primarily a function of errors in receiver antenna gain and the probe radiated power. For the tolerances of absolute value accuracy, all the listed uncertainties listed below must be considered.

Signal level accuracies:

Measured signal level AGC vs signal level, calculated	±1.75 db
Recorder resolution	±0.50 db
Total	±2.25 db

Calculated signal level:

Probe output power	±0.50 db
Probe antenna gain	±1.00 db
Receiver antenna gain	±0.50 db
Total	±2.00 db

B. Downrange Station

The first countdown on March 1, 1959, was entirely satisfactory.

The final countdown began at 22:21:00 on March 2, 1959. A 5-min hold was called during the first antenna boresight due to an error in setting the receiver bandwidth. This time was picked up when the receiver calibrations were completed early.

At X-60, the hours and minutes failed to read out correctly. The associated transistor boards were changed but the trouble persisted. Operation continued with the hours and minutes reading out in improper sequence but at accurate 30-sec intervals. WWV was recorded on Ampex track 3 (playback servo reference signal) to reference the time encoder pulses. Also, the Sanborn traces were time labelled at 30-min intervals.

The calibration oscillator channels 2 and 3 shifted frequency randomly and were too unsteady for discriminator calibration. The discriminator band-edge frequencies were calibrated using the audio oscillator.

The downrange receiver acquired at 05:15:37 GMT, some 5 min after liftoff, followed immediately by telemetering a few seconds later by the servo system. Tracking was smooth. Loss of lock occurred at 06:05:01 GMT, when the probe went below the 1.4 elevation mask at 100 deg azimuth. Reacquisition occurred at 06:25:26 GMT, at 2.0 deg elevation and 103.2 deg azimuth. Track was then continuous, except for short dropouts (15 to 30 sec)[1] until 17:27:00 GMT. At this time, the range power-station power for the 400 cycle converter failed. The standby 400-cps gas turbine was started and the receiver reacquired at 17:30:00 GMT. Final loss of lock occurred at 18:30:00 GMT when the probe disappeared over the horizon at 0 deg elevation and 247.0 deg azimuth.

At L+10 hr, the doppler frequency reference malfunctioned. This unit was immediately replaced with the spare. A postfiring check showed the unit to be functioning normally and the failure cannot be explained.

Angle and doppler data were taken and transmitted at a rate of 6 samples per min throughout the operation.

The variable-bandpass filter installed in the telemetering spin modulation circuit was unsatisfactory because of its high Q and subsequent ringing. This filter was

[1]Believed to have been caused by the 30.455-Mc reference oscillator, which shifted frequency.

bypassed in the last part of the mission. During the flight it appeared that the threshold of the channel 2 subcarrier discriminator was degraded by 2 to 3 db. However, postflight tests showed its performance to be unchanged and that the actual channel 2 sideband power was considerably lower than expected.

Valid telemetry data was recovered in real time at the downrange station for approximately 8 hr.

Figure 72 shows the received signal strength.

C. Goldstone Station

Both countdowns were normal with no malfunctions. Complete preflight calibrations required approximately 4 hr. Spot calibrations before and following each acquisition were extended, requiring additional time (70 min).

Boresight checks were made throughout the operation.

At approximately 1 hr prior to the first acquisition, the receiver VCO was changed from one with a natural frequency of 31.001650 to one with a natural frequency of 31.00125 Mc. Radio frequency acquisition was normal at 11:47:00 GMT 3 March 1959. Telemetry locked on immediately afterwards and servo was placed in the automatic mode a few seconds later. Tracking appeared normal until loss of lock at 21:15:00 GMT. The Ampex direct-record amplifier for track 5 of machine B failed but was immediately replaced with a spare.

The second acquisition occurred without difficulty at 12:34: GMT, 4 March 1959. The VCO reading at acquisition was 31.001248. Shortly after 13:00 GMT, it was noticed that the 30/31 loop was not in lock. The frequency control was adjusted and this loop was locked at 13:22. The new VCO reading was 31.001244 Mc. The Hallamore DC amplifier driving the channel 5 VCO overloaded intermittently during this second track. The same problem occurred with the DC amplifier in the dynamic phase error and spin modulation channels. Overloading occurred only 5 to 10 times, lasting for periods of 1 to 10 sec. It seems to be characteristic of the Hallamore amplifiers and is being investigated. Loss of lock occurred at 21:16 GMT.

After turning equipment on prior to the third acquisition, the receiver 30/31 could not be locked until the crystal frequency control was adjusted. Then the 30.455 loop was found to be out of lock. This was caused by a loose BNC connector. This lead was the connection between the output of the tracking filter and the 30.455 VCO. It is impossible to know when this BNC came loose enough to cause loss of 30.455 control. It is very possible that this happened during the second tracking period resulting in the doppler bias later discovered for that time.

The third acquisition occurred without difficulty at 12:37 GMT, 5 March 1959. Tracking was normal until loss of lock at 21:19 GMT.

The fourth acquisition occurred with difficulty at 12:50 GMT, March 6. Actual acquisition had occurred several minutes previously but the receiving system would not stay in lock when the acquisition switch was changed from the acquisition mode to the normal mode. From 12:50 until loss of lock at 15:15, tracking was normal although signal strength was approximately −150 dbm

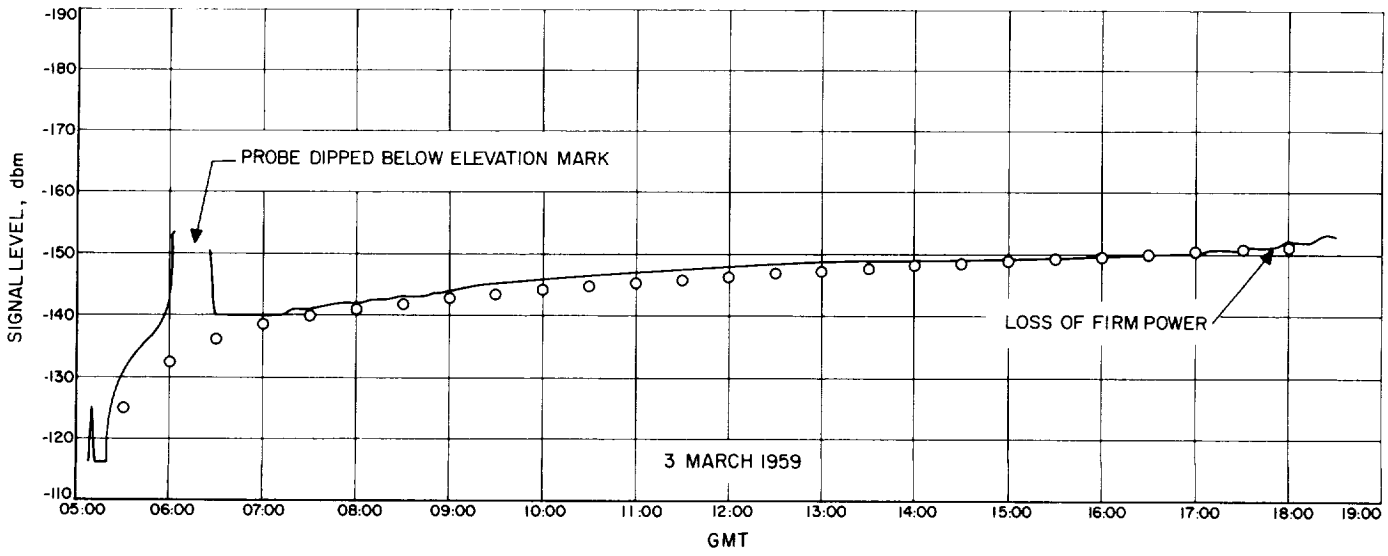

Figure 72. Downrange station signal level for Pioneer IV

and lower. After loss of lock, a 5-cps tracking filter was installed in the receiver main loop and acquisition was attempted. Some indications pointed to a reacquisition of the signal for a few minutes (although never in the normal mode). Extrapolations of the AGC curve and VCO frequency shift leave doubt about this acquisition.

The servo system performed without malfunction throughout the entire tracking operation. Computer predictions placed the main lobe on the probe. Therefore, acquisitions on the four tracking periods were accomplished without difficulties. The servo continued to track the probe until the receiver lost lock. The integrators were operated with the 0.025 cps bandwidth throughout the operation. This reduced bandwidth proved very successful on the last day of tracking when the signal strength dropped off as the batteries failed.

The data-handling system performed without malfunction throughout the operation. Clock errors were ± 0.5 millisec as referenced to transmitted WWV.

Telemetering subcarrier discriminators performed within 1 db of the value predicted during all tracking periods. Excessive drift in the signal strength recording on magnetic tape was noted between pre- and post-shoot calibrations on all four operating days. Absolute calibration of the recording equipment during this period showed the drift to be a result of slight changes in the operation of the isolation amplifier located in the receiver racks.

D. Jodrell Bank

The radio telescope at Jodrell Bank independently tracked *PIONEER IV* through four periods. Data from these tracking periods were made available through the Space Technology Laboratory's computing center. Fortunately, this backup system and information were not needed, since the primary system operated successfully.

E. Network Performance

Using the first 15 min of data after last-stage burnout, pointing predictions were made for the Puerto Rico station for a time 1 hr later than the last data point used. These predictions and all later predictions for Puerto Rico were subsequently found to agree with the observations to within less than 0.2 deg. The initial conditions obtained with 15 min of data differ from the present best estimate by 12 km in injection altitude and 30 m/sec in velocity.

With 3½ hr of data from Puerto Rico, an acquisition prediction was transmitted to the Goldstone station which agreed with subsequent observations to within 0.1 deg. The initial conditions obtained at that time differ from the present best estimates by 2 km in altitude, 0.05 deg in latitude and longitude, 5 m/sec in velocity, and 0.1 deg in the velocity angles. All predictions made after the first day of tracking for periods one day later were found to agree with the observations to within 0.05 deg.

The Goldstone antenna was evaluated using in part the tracking-computing program described above. The data were found to have a standard deviation of about 1 min of arc which, because of the large quantities of data obtained, resulted in errors of the mean smaller by 1 or 2 orders of magnitude from the source. The uncertainty in the determination of biases appears to be 1 min of arc with the data reduction procedures used.

At the distance of the Moon, the accuracy of the probe position as determined by the tracking and computation network is estimated to have been 100 km. The Goldstone station tracked and received useable telemetry through the life of the payload transmitter batteries. The payload was 650,000 km distant when the batteries were depleted after their nominal flight lifetime of more than 80 hr.

REFERENCES

1. *Space Research Summary No. 1* (for the period 15 May 1958 to 15 July 1958), Jet Propulsion Laboratory, Pasadena, 1 August 1958 (SECRET).

2. *Space Research Summary No. 2* (for the period 15 July 1958 to 15 September 1958), Jet Propulsion Laboratory, Pasadena, 1 October 1958 (SECRET).

3. *Space Research Summary No. 3* (for the period 15 September 1958 to 15 November 1958), Jet Propulsion Laboratory, Pasadena, 1 December 1958 (SECRET).

4. *Space Programs Summary No. 1*, Jet Propulsion Laboratory, Pasadena, 1 February 1959 (SECRET).

BIBLIOGRAPHY

A complete bibliography of the *Juno* program, with appropriate background information, is included in Vol. I of this Report. The following documents relate to the space probes, *Pioneer III* and *IV*.

Pioneer III and IV (Juno II)

1. Martin, Benn D., *A Coherent Minimum-Power Lunar-Probe Telemetry System,* External Publication No. 610, Jet Propulsion Laboratory, Pasadena, May 12, 1959.
2. Martin, Benn D., *A Coherent Minimum-Power Lunar-Probe Telemetry System,* External Publication No. 610 (Revision 1), Jet Propulsion Laboratory, Pasadena, August 12, 1959.
3. Richter, Henry L., Jr., and Stevens, Robertson, *The Elements of a Deep-Space Tracking System: The Tracking of PIONEER IV,* External Publication No. 685, Jet Propulsion Laboratory, Pasadena, August 13, 1959.
4. Carr, Russell E., *The Jet Propulsion Laboratory Method of Tracking Lunar Probes,* External Publication No. 793, Jet Propulsion Laboratory, Pasadena.
5. Eimer, Manfred, and Stevens, Robertson, *Tracking and Data Handling for the PIONEER III and PIONEER IV Firing,* External Publication No. 701, Jet Propulsion Laboratory, Pasadena, August 14, 1959.
6. Curtis, Henry, and Schneiderman, Dan, *PIONEER III and IV Space Probes,* Technical Release 34-11, Jet Propulsion Laboratory, Pasadena, January 29, 1960.
7. Snyder, Conway W., *The Radiation Dose in PIONEER IV and Shielding Requirements for Future Space Probes,* Section 22-6, Jet Propulsion Laboratory, Pasadena, July 6, 1959.
8. Eimer, Manfred, and Stevens, Robertson, *Tracking and Data Handling for the PIONEER III and PIONEER IV Firings,* External Publication No. 701, Jet Propulsion Laboratory, Pasadena, August 14, 1959.
9. *Firing Test Report,* No. 59950, ABMA, Huntsville, Ala., January 14, 1959 (SECRET).
10. *Atlantic Missile Range Operations Directive No. 104 JUNO IIA Launch (AM11),* No. 1641, AFMTC, November 20, 1958 (SECRET).
11. Brandner, F., *Revised Data (10-23-58) Missile No. 11,* No. 58667, ABMA, Huntsville, Ala., October 27, 1958 (CONFIDENTIAL).
12. *JUNO II—Lunar Probe Flight AM-11, Flight Dynamics and Trajectory Outlay,* No. 58806, ABMA, Huntsville, Ala., November 17, 1958 (CONFIDENTIAL).
13. *Operations Requirements No. 104, Detailed Test Requirements for JUNO II Launch,* No. 1644, AFMTC, October 21, 1958 (SECRET).
14. *JUNO II—Missile AM-11 Flight Safety Analysis,* No. 14080, ABMA, Huntsville, Ala., November 17, 1958 (SECRET).
15. *Revised Control Factors for JUPITER Missile AM-11 (JUNO II),* No. 58986, ABMA, Huntsville, Ala., November 26, 1958 (SECRET).
16. Weyler, G. M., *Preliminary Evaluation of JUPITER Missile AM-14 Test Flight,* No. C-135319, ABMA, Huntsville, Ala., July 23, 1959 (SECRET).
17. Baylis, James R., *Instrumentation Operation Analysis Part IIIb of the Firing Test Report JUPITER Missile* AM-14, No. 16429, ABMA, Huntsville, Ala., April 24, 1959 (SECRET).
18. *Index and Test Results Part I of the Firing Test Report JUPITER Missile AM-14,* No. C-199070, ABMA, Huntsville, Ala., March 31, 1959 (SECRET).
19. *Consolidated Data Summary Missile NR AM-14 AFMTC Test NR 250,* No. 15627, ABMA, Huntsville, Ala., April 3, 1959 (SECRET).